Dissertation

submitted to the
Combined Faculty of Natural Sciences and Mathematics
of the Ruperto Carola University Heidelberg, Germany
for the degree of
Doctor of Natural Sciences

Presented by

M.Sc. Sara Ben Ayed

Born in: Berlin, Germany

Oral examination: 30.09.2019

Ca^{2+} signalling and its consequences in the mouse spinal cord dorsal horn under chronic pain

Referees:

Prof. Dr. Hilmar Bading

Prof. Dr. Rohini Kuner

Prof. Dr. Gudrun Rappold

Prof. Dr. Christoph Schuster

Abstract

Chronic pain represents one major health problem of today's global society. Some treatments fail and still many aspects of chronic pain development and maintenance are unknown. Here, we present new insights into the Ca^{2+} signalling behaviour of acute slices of murine spinal cord dorsal horn astrocytes and parvalbumin(PV)-positive neurons. To our knowledge we showed here for the first time that stimulation of preferred fibre classes from the dorsal root evokes Ca^{2+} signalling in the cytosol and nucleus of astrocytes and the cytosol of PV-neurons. In addition, we detected a decrease of these evoked Ca^{2+} signals under neuropathic pain conditions when stimulated with Aβ- or Aδ-fibre preferred frequencies. We did not observe differences under chronic inflammatory pain conditions, neither in astrocytes nor in PV-positive neurons. Further investigation showed that the Ca^{2+} signalling dependent immediate early gene *Npas4* was reduced 3 days after neuropathic pain induction and that overexpression of NPAS4 in spinal dorsal horn neurons *in vivo,* leads to a rescue of mechanical but not thermal hypersensitivity. These findings suggest an important role of the Ca^{2+} signalling behaviour of astrocytes in response to Aβ- and Aδ-fibre stimulation under neuropathic pain under the tested conditions. Especially because of the occurrence of Ca^{2+} signalling in the astrocytic nucleus, we propose a similar gene regulation function as in neurons, which probably induce plasticity changes in astrocytes. This might be due to adaption to the neuronal activity required to transmit signals from the periphery to the brain, which is possibly disturbed under chronic pain conditions. Thus, the purpose of astrocytes to support those changes in pain conditions would also require changes in signalling behaviour. In addition we hypothesize an important role of NPAS4 regulation in the spinal cord dorsal horn under neuropathic pain conditions, primarily to control the inhibition of pain stimuli.

Zusammenfassung

Chronische Schmerzen sind ein großes Gesundheitsproblem der Weltgesellschaft. Einige Behandlungen scheitern und viele Aspekte der chronischen Schmerzentwicklung und -erhaltung sind immer noch unbekannt. Hier präsentieren wir neue Einblicke in das Ca^{2+} -Signalverhalten von Astrozyten und Parvalbumin (PV) -positiven Neuronen im spinalen dorsalen Horn in akuten Schnitten von Mäusen. Unseres Wissens nach zeigen wir hier zum ersten Mal, dass die Stimulierung bevorzugter Nervenfaserklassen aus den sensiblen Nervenwurzeln Ca^{2+} -Signale im Zytosol und im Zellkern von Astrozyten und im Zytosol von PV-Neuronen hervorruft. Zusätzlich haben wir eine Abnahme dieser hervorgerufenen Ca^{2+} -Signale unter neuropathischen Schmerzbedingungen festgestellt, wenn sie mit Frequenzen, die bevorzugt diese Fasern Aβ- oder Aδ-Fasern anregen, stimuliert wurden. Wir haben keine Unterschiede unter chronischem Entzündungsschmerz beobachtet, weder in Astrozyten, noch in PV-positiven Neuronen. Weitere Untersuchungen zeigten, dass die Expression des Ca^{2+} -Signal-abhängigen unmittelbare frühe Gen Npas4 an drei Tagen nach neuropathischer Schmerzinduktion reduziert war und dass eine Überexpression von NPAS4 in Neuronen des Hinterhorns *in vivo* zu einer Rettung der mechanischen, aber nicht thermischen Überempfindlichkeit führt. Diese Ergebnisse legen eine wichtige Rolle des Ca^{2+} -Signalverhaltens von Astrozyten als Reaktion auf Aβ- und Aδ-Faserstimulation unter neuropathischen Schmerzen, abhängig von den getesteten Bedingungen, nahe. Insbesondere aufgrund des Auftretens von Ca^{2+} -Signalen im Zellkern von Astrocyten schlagen wir eine ähnliche Genregulationsfunktion wie in Neuronen vor, welche wahrscheinlich Plastizitätsänderungen in den Astrozyten zur Folge hat. Dies könnte auf die Anpassung an die neuronale Aktivität zurückzuführen sein, die zur Übertragung von Signalen von der Peripherie zum Gehirn erforderlich und die unter chronischen Schmerzbedingungen möglicherweise gestört ist. Daher würde der Zweck von Astrozyten, diese Veränderungen der Schmerzzustände zu unterstützen, auch Veränderungen des Signalverhaltens erfordern. Zusätzlich nehmen wir an, dass die NPAS4-Regulation im Hinterhorn des Rückenmarks unter neuropathischen Schmerzzuständen eine wichtige Rolle spielt, vor allem, um die Inhibition der Schmerzsignale zu kontrollieren.

Acknowledgement

I would like to thank Prof. Dr. Hilmar Bading for his great supervision, support and stimulating discussions during the whole PhD process. I also want to thank Prof. Dr. Rohini Kuner for accepting to become my second supervisor of this thesis and member of my thesis advisory committee (TAC). Furthermore, I would like to thank Dr. Rolf Sprengel and Prof. Dr. Martin Schmelz for becoming part of my TAC as well and contributing with guidance, ideas and supporting me. Thanks also to Dr. Richard Carr who helped to developed the stimulation protocol.

I also thank Dr. Anna Hertle, who taught, supervised and supported me during my whole PhD. I thank her for all the patient she had with me and for the discussions that helped me to manage that project.

I want to thank the following institutions for funding my PhD position and research: the “Sonderforschungsbereich” (SFB) 1158 and the Deutsche Forschungsgemeinschaft (DFG), the Heidelberg Biosciences International Graduate School (HBIGS) and the Interdisciplinary Center for Neuroscience (IZN).

For their great support, advice, discussions and nice atmosphere, I would like to thank the friends and colleagues from the Neurobiology department.

Last but not least, I would like to thank my family and friends, especially my parents, for teaching and supporting me throughout my whole life. I want to thank my husband for giving me strength and reassurance. I love you all!

Heidelberg, July 2019

Sara Ben Ayed

Table of Contents

List of Abbreviations

AAV	adeno-associated virus
AMPA	amino-3-hydroxy-5-methyl-4-isoxazole propionate
ANOVA	analysis of variance
ATP	adenosine triphosphate
BDNF	brain-derived neurotrophic factor
bp	basepair
CFA	complete Freund's adjuvant
CNS	central nervous system
Cre	cyclization recombination
d	day
DAPI	4',6-Diamidin-2-phenylindol
dn	dominant-negative
DNA	desoxyribonucleinacid
DR	dorsal root
DRG	dorsal root ganglion
EDTA	ethylendiaminetetraacetic acid
ER	endoplasmic reticulum
FLEX	flip-excision
GABA	gamma aminobutyric acid
GFAP	glial fibrillary acidic protein
GFP	green fluorescent protein
HA	Human influenza hemagglutinin
IEG	immediate early gene
IL-β	interleukin-β
IP3	inositol 1,4,5-triphosphate-3
loxP	locus of crossing-over of bacteriophage P1
MAPK	mitogen-activated protein kinase
NeuN	neuronal nuclei
NGF	neuronal growth factor

NMDA	N-methyl-D-aspartate
Npas4	neuronal PAS domain protein 4
OE	overexpression
o/n	over night
PBS	phosphate buffered saline
PBST	Phosphate buffered saline with Tween-20
PCR	polymerase chain reaction
PFA	paraformaldehyde
PI3K	phosphoinositide 3-kinase
PKC	proteinkinase C
PLC	proteinlipase C
PNS	peripheral nervous system
PV	parvalbumin
ROI	region of interest
Rpm	round per minute
SNI	spared nerve injury
TRIS	tris(hydroxymethyl)aminomethan
WT	wild type

List of Figures

List of Tables

1. Introduction

“When you get to the end of your rope, tie a knot and hang on.” This quote, originally said by Theodor Roosevelt, reflects what many chronic pain patients suffer from every day. Chronic pain is a severe symptom of known or sometimes unknown reasons. It costs patients and their relatives and friends, who often suffer with their beloved ones, much strength and power of endurance. Many patients suffer from the fact that they are often misunderstood, because chronic pain is something one cannot see, something other people cannot understand or feel. If people see someone who has a broken leg, they feel sympathy for that person. But an apparently healthy person, without any visible disability might be confronted with disbelief or even ignorance. On top of that, the frustration of not being able to treat the chronic pain and not being able to escape leads to depression, altered concentration or addiction (Boersma et al. 2019).

For society chronic pain and other diseases caused by chronic pain, for example depression or opioid-addiction, lead to many other problems as well. Money is only one of those reasons. For example in the United States of America in 2010 the estimated costs were at $560 to $635 billion (Gaskin and Richard 2012). And unfortunately there are no good long-term treatments at the moment. Scientists put a huge amount of effort into investigating causes, development and maintenance of chronic pain in order to find possible treatments. Sometimes it is possible to heal the original cause, the injury, but the pain remains. Why is that? What drives the development of chronic pain? Why do some patients do not even respond to analgesic treatment? And when patients react positively to analgesics, they face the long-term problem of addiction or insensitivity to the drug. Also mental problems like depression itself or post-traumatic stress can cause chronic pain. Both, stress and chronic pain seem to share similar mechanisms (Abdallah and Geha 2017). We still need to understand many different aspects of how the central nervous system (CNS) works and why it develops chronic pain. Pathways still have to be unravelled.

1.1. The mechanism of pain – from skin to brain

Pain is supposed to be a protective mechanism, acting as a warning system in case of tissue damage and the immediate reaction to avoid more damage to the body. Even

inflammation, which seems to be an annoying status of pain, ensures that we reduce movements or stress onto the inflamed body part so that we give the tissue time to recover. Responsible for the sensation of pain are so called nociceptors, thinly myelinated Aδ-fibres and unmyelinated C-fibres**,** transmitting the stimuli from the periphery into the dorsal horn of the spinal cord, forming synapses with neurons and glia cells. The approximate diameter of Aδ-fibres lies between 1 - 5 µm and the signal transmission speed of their action potentials at 5 – 35 m/s. For C-fibres, which are not myelinated, the diameter is very thin, between 0.2 and 1.5 µm. Their action potentials travel at a speed around 0.5 – 2 m/s. These fibres can detect different stimuli through a huge variety of receptors, expressed in their peripheral terminal ends. For example, some of their many receptors react to ATP, prostaglandin, serotonin or capsaicin. After detecting painful stimuli through those receptors, the signal can be transmitted into the cell body, located in the dorsal root ganglion, where it can initiate gene expression. This gene expression might increase the synthesis of neuropeptides that will be released in the central terminal of the fibres which build synapses in the spinal cord dorsal horn. Here the signal is transmitted to neurons in different dorsal horn layers via diverse neurotransmitters, chemokines, cytokines and neuropeptides, but mainly through glutamate, substance P and brain-derived growth factor (BDNF) (Gangadharan and Kuner 2013). In the dorsal horn itself, the received signal from the periphery might or might not be transmitted directly or indirectly to projection neurons in the superficial layer of the dorsal horn and then forwarded to the brain. For the sensitisation of pain in the brain, there is not one single brain region responsible, but several which fulfil different aspects of how one feels pain. Under acute pain or physiological pain conditions these signals are further transmitted to the thalamus and then ending in the pariental lobe of the cerebal cortex. Further involved brain regions are, for example, limbic regions and the amygdala, involving emotions into the sensation of pain. The hippocampus seems to be involved as well, in the context of pain and memory, for example in the context of aversive conditioning (Basbaum and Woolf 1999). But under specific conditions this acute pain can develop into a chronic pain. Even peripheral terminals that are responsible for light touch-sensation, Aβ-fibres, can develop from non-noxious into noxious fibres. Those large diameter (about 6 – 12 µm), thick-myelinated fibres are responsible for light-touch sensations that are transmitted very fast to the dorsal horn (35 – 75 m/s) but can, for example after inflammation, start to express substance P, which will be transmitted to dorsal horn

neurons and thus send a signal which will be understood and transmitted as pain instead of “light-touch”.

The different fibres from the periphery innervate the spinal cord dorsal horn in different layers. Aδ nociceptors project for example to lamina I and the deeper lamina V into the dorsal horn. The touch-fibre Aβ on the other hand forms synapses in laminae III-V. Finally, C-fibres project into the superficial laminae I and II (Basbaum and Braz 2010) (Fig. 1). But this is not an exclusive structure. As reviewed for example by Gangadharan and Kuner (Gangadharan and Kuner 2015), the spinal pain circuits are not yet clearly described. Just parts of it get unravelled bit by bit. For example Duan and colleagues (Duan et al. 2014) show that excitatory somatostatin positive interneurons in lamina II receive input from Aβ-fibers. Those neurons are then connected to projection neurons in lamina I. Also in lamina III, where Aβ-fibres build synapses with glutamatergic neurons, these signals are then transmitted into more superficial layers to excitatory as well as to inhibitory neurons (Peirs et al. 2015).

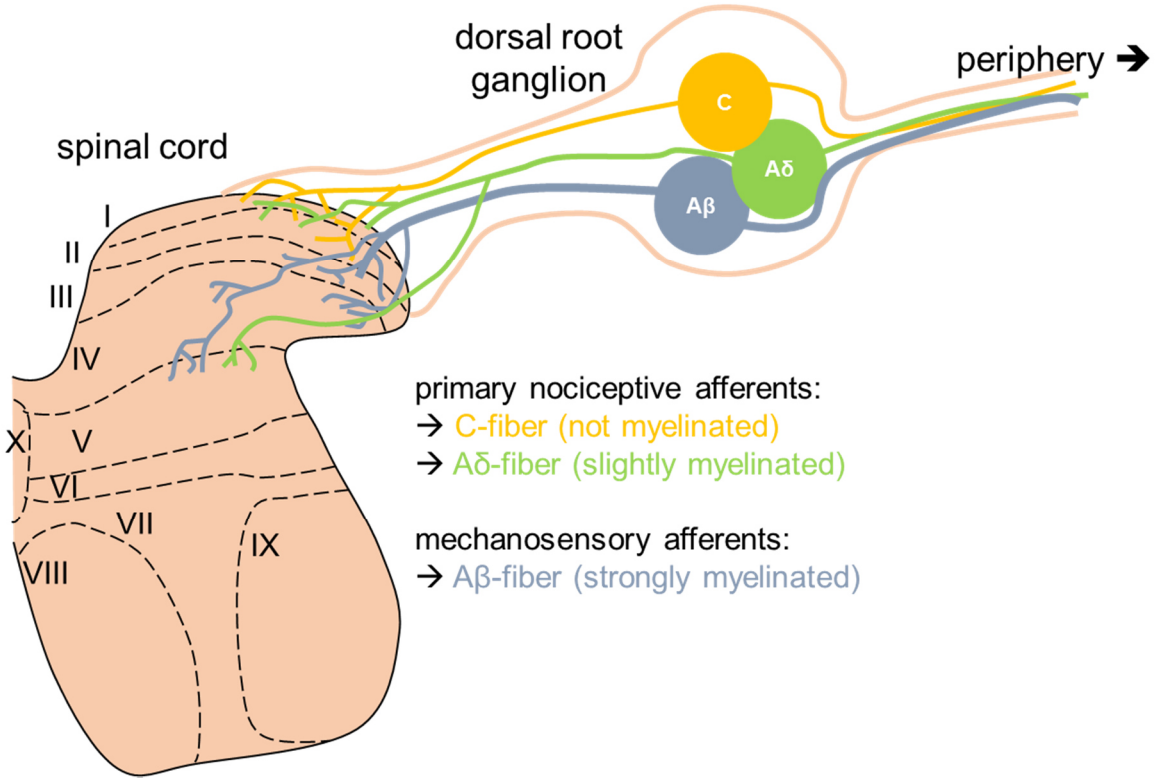

Figure 1: Afferent fibres innervating spinal dorsal horn. Graphical scheme represents one hemisphere of the spinal cord from the lumbar area 3 – 5. Peripheral fibres, Aβ-fibres (blue), Aδ-fibres (green) and C-fibres (yellow), with cell bodies in the dorsal root ganglion, entering and forming synapses in the different laminae of the dorsal root of the spinal cord.

For a patient pain is defined as chronic when the symptoms endure longer than six months (Merskey 1994; Treede et al. 2015) . In this case the pain persists for a long and undefined period of time of suffering, even when the initial caise of the pain (like dysfunction or damaged tissue of the periphery, inflammation, tumour invasion or due to diabetic consequences) is solved or healed. An increased sensation to painful stimuli is called **hyperalgesia** and a pain sensation to normally non-painful stimuli is defined as **allodynia**. This maladaptation to pain is caused by a dynamic development of neural and glial plasticity in the periphery and the CNS, thus also inside of the dorsal horn of the spinal cord.

This chronic pathological condition can be divided into two groups. On the one hand, there is inflammatory pain which is often induced by tissue damage. On the other hand, there is neuropathic pain where the somatosensory nervous system is altered by a lesion or disease. Both types of chronic pain conditions show the characteristics of the mentioned hyperalgesia, allodynia or both (Woolf and Salter 2000).

1.1.1 The spinal cord dorsal horn and its cells

To understand the changes in the mechanisms of the development and the maintenance of chronic pain, it is important to have a look at all the different key players. Chronic pain can unfortunately not be decreased by treatment of peripheral nociceptors only. This is because of the central sensitisation which happens in the dorsal horn of the spinal cord. This central sensitisation is similar yet not equal to activity dependent changes of synaptic transmission, described ad long-term potentiation (LTP) or long-term depression, in the higher brain regions like plasticity changes for example in learning and memory processes in the hippocampus (see section 1.2.2 Ca^{2+} induced synaptic plasticity). Yet the central sensitisation also consists of plasticity changes of synapses and the increased expression of transmitters, eventually adaptions or even loss of functions. Those changes are often coupled to Ca^{2+} signalling changes, similar to LTP in the hippocampus. More information about Ca^{2+} is provided in a later section (see 1.2 Ca^{2+} - An universal messenger).

In the spinal cord dorsal horn, the largest group of neurons are glutamatergic neurons, which actively transmit the sensory signal from the periphery to the brain. These

excitatory neurons are controlled by inhibitory interneurons, the second type of neurons in the spinal cord dorsal horn that use gamma aminobutyric acid (GABA) or glycine as neurotransmitters (Todd 2010, 2017). These interneurons silence the glutamatergic neurons to make sure that not every spontaneous signal is transmitted as painful (Basbaum and Braz 2016). Here might already lie a hint for a destructive system when the inhibitory interneurons become dysfunctional. In fact, it has already been discussed, that impairment of the inhibitory system, like a loss of function of GABAergic neurons, would cause a so-called disinhibition. This would finally result in increased pain (Melzack and Wall 1965; Basbaum et al. 2009; Takazawa and MacDermott 2010b, 2010a) as the excitatory signals would not be under control anymore.

Other cells present in the spinal cord are glia cells such as astrocytes and microglia. Astrocytes became of increasing importance in the last two decades as their assumed simple supportive role for neurons turned out to be an underestimation. Microglia are known to be activated under pain conditions (Tsuda 2016). Moreover, microglia are believed to have a major role in the mechanism of chronic pain as within hours after injury, microglia accumulate and release gliotransmitters like BDNF or cytokines like interleukin-6 (Basbaum and Braz 2010; Tawfik et al. 2007). Furthermore, microglia express receptor channels such as transient receptor potential (TRP) channels that, when stimulated, lead to Ca^{2+} influx into the cells (Echeverry, Rodriguez, and Torres 2016). Those channels are known to be involved into neuropathic pain development. In addition, it is also known, that microglia can respond to neuronal activity and neurotransmitter with mitogen-activated protein kinases (MAPK) pathway (Ji and Strichartz 2004), which in return induces gene expression, responsible for plasticity changes. Thus, microglia can be activated and change plasticity under pain conditions.

1.1.1.1 Glutamatergic neurons

Glutamatergic neurons represent the largest population of neurons in the CNS. As their name already indicates, this type of neurons release glutamate. As major neurotransmitter glutamate activates predominantly postsynaptic amino-3-hydroxy-5-methyl-4-isoxazole propionate (AMPA), kainite, metabotrobic glutamate receptors and NMDA receptors. For the fast neurotransmission the ionotropic AMPA receptor

channel are the major key players. After glutamate binding the AMPAR channels are opened and the postsynaptic cell is depolarized by the Na+ influx. If the depolarisation is strong enough an action potential is evoked and the postsynaptic cell in turn is transmitting the signal to connected neurons. The glutamate activation of NMDA, kanaite, metabotrobic receptors and some AMPA receptor subtype are used to modify the response of the postsynapse to presynaptically released glutamate. Here the influx of Ca^{2+} ions through NDMA and AMAPR subtypes and the release of intracellular Ca^{2+} ions has a dominating function.

In the context of chronic pain it has been shown that excitatory neurons react with increased Ca^{2+} signalling under chronic pain conditions when the dorsal root is stimulated in acute spinal cord slices (Simonetti et al. 2013) . This goes into the direction of central sensitisation of dorsal horn neurons, referring to hyperexcitability which results in enhanced pain sensitisation ((Woolf 1983), (Basbaum et al. 2009), (Sandkuhler 2009)). Also the involvement of AMPA receptors was already shown (Gangadharan et al. 2011) to be involved in inflammatory pain in mice. The authors showed that deletion of AMPA receptors in nociceptors as well as blocking AMPA receptors with antagonists led to decreased hypersensitisation under acute and chronic inflammatory pain. The excitatory signal from the periphery was therefore not transmitted to other excitatory neurons in the spinal cord dorsal horn. This result shows that excitatory transmission of signals in the pain circuits is important for the sensitisation of pain. As already mentioned, this signal is normally controlled by inhibitory neurons, silencing for example spontaneous activity of excitatory neurons.

For the so-called central sensitisation in the spinal cord dorsal horn caused by stimulation of C-fibres also NMDA receptors have been shown to be involved ((Woolf and Salter 2000) (Drdla and Sandkuhler 2008) (Basbaum et al. 2009)). The activation of the NMDA receptors increased the glutamatergic signal transmission- memory in the hippocampus. This seemed to be more important for chronic pain than for acute pain (Liu et al. 2008) . There LTP induces through NMDA receptors permanent plasticity changes. This is comparable to the central sensitisation in the dorsal horn. Furthermore, it was shown that blocking NMDA receptors in the spinal cord lead to decreased pain sensitisation.

1.1.1.2 GABAergic neurons

Activated neurons that inhibit action potentials of other cells by hyperpolarisation are called inhibitory neurons. In contrast to glutamatergic neurons, they release GABA or glycine, a transmitter responsible for the formation of hyperpolarisation of the postsynaptic cell and thus contributing to their silencing. Those inhibitory neurons are therefore called GABAergic neurons. In general these kinds of neurons are important for controlling and preventing the excitability of a cell system.

Overall, the inhibitory system plays a key role in the context of chronic pain. It is believed, that neuropathic pain is established because of an impaired inhibitory network. Thus, it seems to be of even more interest in the spinal cord. Here the excitatory signal is already “filtered” by inhibition through the dorsal horn cell circuit before the signal is transmitted to the brain. Therefore, investigating inhibitory neurons specifically in the spinal cord dorsal horn provide with important details about the sensory regulation system before any information is passed to the brain.

The loss of inhibitory function in the context of chronic pain is called “disinhibition”. This loss of function of inhibitory interneurons was already shown very early to increase pain sensitisation (Melzack and Wall 1965; Basbaum and Braz 2010).

Alan Basbaum and Joao Braz showed described in their review (Basbaum and Braz 2016), that transplanting inhibitory precursor cells from cell culture into the spinal cord dorsal horn can reduce pain sensitisation. Transplanting embryonic medial ganglionic eminence (MGE) cells, from GABAergic interneurons are derived, into cerebral cortex and spinal cord showed that inhibitory neurons, tested positive for GABA for example, developed axons and dendrites and also migrated successfully into the tissue. The studies are an example that the altered inhibition of the tissue, either seizure- or peripheral nerve injury-dependent, can be restored by MGE cell transplants. The cells showed good survival and built functional connections to other neurons within the tissue.

In vivo tests even showed that mice recovered from spared nerve injury (SNI) to baseline mechanical sensitivity when transplanted with MGE cells after SNI surgery, compared to the control group which received only medium injection and developed hypersensitivity. The level of GAD expression, which is a marker for inhibitory neurons and normally altered after SNI induction, also reaches baseline levels again after the

MGE cell transplant. Interestingly, it only reached baseline, so a functional recovery and did not developed uncontrolled inhibition.

Thus, in central sensitisation, an increase of excitatory activity, combined with a disinhibition, seems to play a central role in the development and possible the maintenance of maladaptive pain sensitisation.

This thesis will concentrate on parvalbumin (PV), a calcium-binding protein, positive inhibitory neurons. These GABAergic neurons are represented in the spinal dorsal horn. They distribute mainly in laminae II – III (Zacharova and Palecek 2009; Zacharova, Sojka, and Palecek 2009; Antal, Freund, and Polgar 1990; Ren and Ruda 1994; Yamamoto et al. 1989) . Zacharova et al. already showed that there was a reduction of PV-positive GABAergic neurons in the superficial dorsal horn laminae under peripheral inflammatory conditions. Other groups suggested no role of GABAergic neurons from the spinal dorsal horn in neuropathic pain models. For example, Gassner and colleagues (Gassner et al. 2013) found no changes in the excitability of GABAergic neurons in spinal laminae III between naïve and neuropathic pain induced animals.

That this area is still under debate makes it even more important for further investigation into the role of GABAergic cells in the spinal dorsal horn and the development and maintenance of different pain conditions.

1.1.1.3 Astrocytes – more than just “the glue”

Among neurons, we find glia cells in the spinal dorsal horn. The biggest group of glia cells are the astrocytes. Although glia-derived mediators were described to be powerful modulators of excitatory and inhibitory signal transmission and are described to be involved in the central modifications underlying pain the exact role in pain sensation is not resolved (Gosselin et al. 2010; Ji, Berta, and Nedergaard 2013). In the 1990s, the discovery of cytoplasmic Ca^{2+} signals in astrocytes that were induced by released neurotransmitters that would activate G protein-coupled receptors (GPCRs), changed the estimated role of astrocytes in the CNS for the first time. Before, glial cells, including astrocytes, were believed to be a simple supportive cell type for neurons. Astrocytes were there to transport nutrients from the blood vessels to neurons and to stabilize the tissue. Due to the discovery of GPCRs in the astrocytic

membrane, it was discovered that there was more to astrocytes. Apparently, they were able to react to Ca^{2+} signals released from the inner calcium store of the endoplasmic reticulum (ER). When, for example, ATP would bind the GPCR and lead to inositol 1,4,5-triphosphate-3 (IP_3) activation, which would then bind to IP3 receptors in the ER membrane, that would lead to a Ca^{2+} release from the ER into the cytoplasm of the astrocyte. Those Ca^{2+} signals were described as calcium waves through the astrocytes. Still, the importance of Ca^{2+} in astrocytes and its effect on neurons is very controversial. Some groups see differences in early stages of learning and memory, when astrocytic Ca^{2+} signalling is altered (Semyanov 2019), while others do not. For example, Agulhon and colleagues (Agulhon, Fiacco, and McCarthy 2010; Fiacco et al. 2007; Agulhon et al. 2008) tested the impact of astrocytic Ca^{2+} signalling on pyramidal neurons in the CA1 region of the hippocampus. They did not see an effect on the behaviour or dynamics of neuronal Ca^{2+} signals when astrocytic Ca^{2+} was blocked.

Furthermore, it has been shown that the fine processes of astrocytes have Ca^{2+} signals that do not always reach the soma of the astrocyte and that the Ca^{2+} signalling dynamics in the processes can be very different from the ones in the soma. This was for example shown in $Itpr2^{-/-}$ mice (mice with disturbed Ca^{2+} release from internal stores), where there were no alteration of Ca^{2+} signals in the processes but in the astrocytic soma (Srinivasan et al. 2015) . Other studies have even shown that the Ca^{2+} driven communication between neurons and astrocytes can be independent from astrocytic soma Ca^{2+} signalling but involve only Ca^{2+} communication of astrocytic endfeet and processes (Szokol et al. 2015; Panatier et al. 2011) . These findings already indicate how diverse the Ca^{2+} signalling in astrocytes can be and how the different types of signalling might serve different purposes.

The amount of other receptors expressed in the astrocytic membrane made clear that there is much more to astrocytes than only being “the glue” of CNS tissue. The fact that astrocytes can, through different receptors, sense GABA, glutamate, TRPA1 and even cannabinoids, shows that they definitely contribute to the signalling pathways in the CNS. Guerra-Gomes and colleagues (Guerra-Gomas et al. 2018) nicely reviewed the many different inputs that would cause inner Ca^{2+} rises in astrocytes and the output following that stimulation. The review was mainly based on data from the hippocampus. Inhibitory and excitatory input from neurons onto astrocytes would lead to a Ca^{2+} rise in the astrocytic cytoplasm and then lead to the release of

gliotransmitters, like BDNF, glutamate, ATP, or D-serine, among others. This release can in turn influence the synaptic activity of neurons and thus the signalling cascade. This is why in the past years the term “tripartite synapse” has been established (Araque et al. 1999). This term refers to the astrocytes as a third part of the classical pre- and post-synapse formation, surrounding the synaptic cleft of neurons.

One tool to label astrocytes is through the glial fibrillary acidic protein (GFAP), which is an intermediate filament protein that is mainly expressed in the cytoplasm of astrocytes in the CNS (Brenner et al. 1994). GFAP immunostaining is commonly used to identify astrocytes. For example astrogliosis, a reactive state of astrocytes, was measured by an increase of number of GFAP positive cells as well as astrocytes after brain injury, peripheral injury, plaque formation in Alzheimer’s disease, genetic disorders or chemical insult (Eng, Ghirnikar, and Lee 2000). The activation of astrocytes is also called reactivation and astrogliosis, which both refers to an increase of the cell body volume, thicker processes and strong proliferation.

This activation is directly connected to an increase in GFAP positive cells. An upregulation of GFAP and a hypertrophy of astrocytes has already been shown under some pain conditions. Normally, a certain gliosis is beneficial for recovery after brain injury but excessive gliosis and its associated neuroinflammatory responses will have a negative impact on the structural and functional recovery of affected brain tissue (Sofroniew 2009). This effect of astrogliosis can also be caused, for example, by spared nerve injury (SNI) or intraplantar injection of complete Freund’s adjuvant (CFA). Activation of astrocytes is also linked to ATP-dependent chronic pain (Chessell et al. 2005) , suggesting that Ca^{2+} signalling in astrocytes plays a major role in the establishment and maintenance of chronic neuropathic and inflammatory pain.

One form of how reactive astrocytes involved in gliosis can influence chronic pain modifications in the spinal cord circuits, is through increasing release of gliotransmitters like chemokines, which then enhances the excitatory synaptic transmission (Zhang, Jiang, and Gao 2017) . As the process of astrogliosis and transmitter release might be Ca^{2+} -dependent, it is worth investigating the role of Ca^{2+} signalling in astrocytes under chronic pain conditions. Surprisingly little is known about nuclear Ca^{2+} signalling in astrocytes, even though it might be obvious that it happens and leads to altered gene transcription, just like in neurons. Gene transcription and

protein expression would then lead to the increased growth of astrocytic processes. There are only very few published studies that investigate whether the Ca^{2+} signalling in astrocytes functions in the same way as it does in neurons. It has been shown that, for example, Ca^{2+}/calmodulin-dependent protein kinase IV (CaMKIV) (see section 1.2.1 Ca^{2+} from induction to other cell compartments) is expressed in astrocytes and increased when they are stimulated, which then leads to expression of BDNF (Liu, Zhang, et al. 2017). This indicates a similar reaction pathway of astrocytic Ca^{2+} signals just like in neurons, where Ca^{2+} signalling into the nucleus leads to gene transcription.

To summarize, not much is known about the Ca^{2+} signalling of astrocytes in the spinal cord, especially under chronic pain conditions. Even less is known about nuclear Ca^{2+} signalling. However a recent study showed that spinal cord dorsal horn astrocytes release GABA in response to synaptic activation (Christensen et al. 2018), which might promote astrocytes are potential therapeutic targets in pain control.

Thus, the role of astrocytes needs further investigation in order to understand the neuron-glia interaction in the spinal circuits and its central sensitisation under chronic pain conditions.

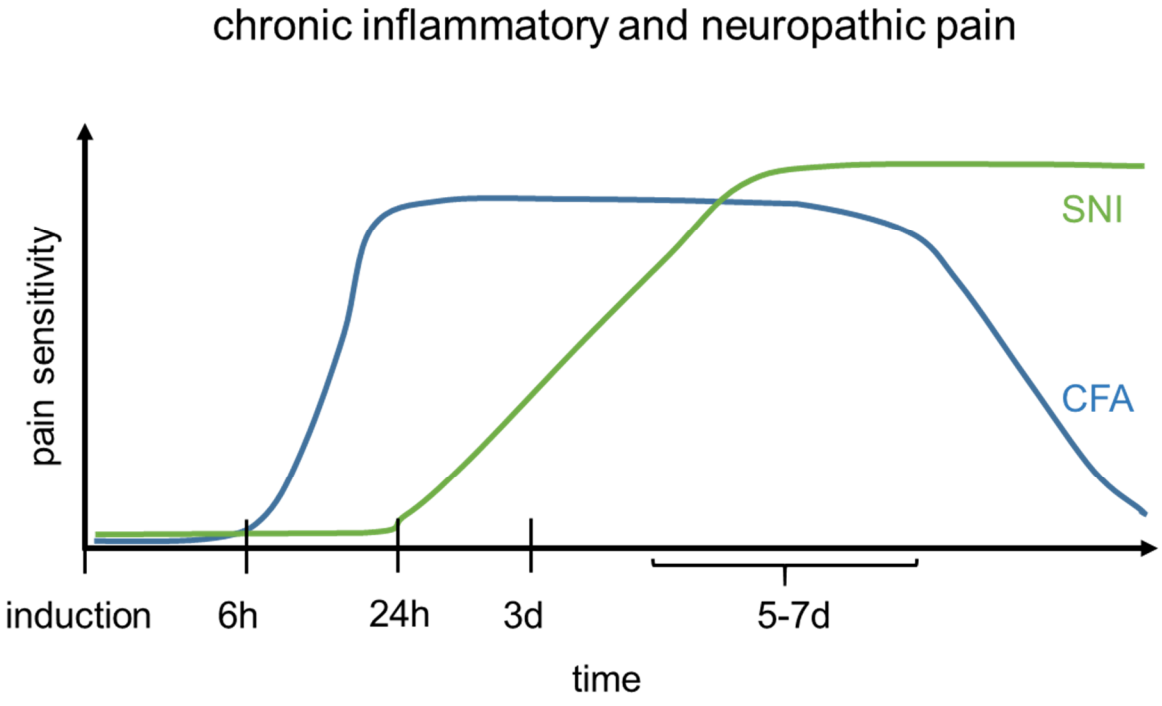

Figure 2: Chronic pain models and their development. Graphical scheme represents the time course of pain sensitivity development of SNI surgery, causing neuropathic pain (green) and CFA injection, responsible for chronic inflammatory pain (blue).

1.1.2 Animal pain models

To investigate chronic pain, it is not always possible to work with patients. Especially discovering the underlying molecular and cellular pathways requires animal models. There are a few established models that demonstrate different chronic pain conditions.

For neuropathic pain, one model has been shown to be quite reproducible: spared nerve injury (SNI). This model comes with different modifications and names. In principle, nerve branches from the periphery of the hind paw, leading to the lumbar part 3 – 5, are damaged in a way that remaining branches develop a hypersensitivity. The developing neuropathic pain increases over the first few days, reaching a peak and plateau at day 7, and lasts for many weeks (Fig. 2). The mice then avoid stressing the neuropathic paw too much and the paw appears to be cramped.

Chronic inflammatory pain is often represented in animal models with complete Freund's adjuvant (CFA). The heat-shocked Mycobacteria tuberculosis cause the release of cytokines and other inflammatory signals in the periphery and thus lead to inflamed tissue. The paw appears swollen, red and warm. The chronic inflammatory pain after CFA injection is already established several hours after injection and increases until reaching a peak of hypersensitivity at 24 h after injection (Fig. 2).

1.2 Ca^{2+} signalling – An universal second messenger

The occurrence of Ca^{2+} ions as second messengers is transversal in nature. Due to its chemical and physical characteristics, this cation can form complexes with many proteins, inducing activity changes in many signalling pathways (Clapham 2007). One of the most important ways to transmit information from cell to cell and to induce structural changes via gene transcription is through Ca^{2+} signalling, as will be explained in detail in the next subsections.

In order to sensibly interact with their environment, living beings must sense stimuli. Furthermore, they have to transmit and analyse every stimulus to make favourable decisions. They can even store and recall these events as information when they are useful to face new situations. The central nervous system (CNS) plays a major role in all those vital functions. Different parts of the CNS are responsible for processing

different inputs and producing specific outputs, establishing communications within their own tissue as well as with many other regions.

The neurons in the CNS convey information through action potentials, and these action potentials always initiate the activation of different Ca^{2+} signalling pathways, including those responsible for the release of neurotransmitters. For example, glutamate can bind to N-methyl-D-aspartate (NMDA) or amino-3-hydroxy-5-methyl-4-isoxazole propionate (AMPA) receptors and induce a Ca^{2+} influx from the extracellular matrix into the cytoplasm of the neuron. Ca^{2+} can easily enter the nucleus of cells through nuclear pore complexes and act upon gene transcription. In the following section, I will go into more detail concerning how gene transcription is induced and what role different cell compartments play in Ca^{2+} signalling.

1.2.1 Ca^{2+} from induction to other cell compartments

The cytoplasmic concentration of Ca^{2+} in resting cells lies at ~100 nM and the cell keeps that level by actively exporting Ca^{2+} ions from the intra- to the extracellular space via plasma membrane calcium ATPases and sodium-calcium exchangers (NCXs). Another way to keep the Ca^{2+} concentration in the cytosol at a steady level is through take-up into the endoplasmatic reticulum (ER), which is a major intracellular calcium store. Through sarcoendoplasmic reticulum calcium ATPase (SERCA) pumps, which are located in the membrane of the ER, Ca^{2+} is actively transported form the cytosol into the ER.

Action potentials can induce an influx of Ca^{2+} ions from the extracellular space into the neuron, through voltage-gated calcium channels (VGCCs). Other ligand binding receptor-channels, like AMPA and NMDA receptors, drive Ca^{2+} entry causing a dramatic local rise of Ca^{2+} concentration up to ~1 - 2 mM and thus mirror the activity state of the cell. After Ca^{2+} has entered the intracellular space, it binds to calmodulin. The Ca^{2+}/calmodulin complex can then bind and activate Ca^{2+}/calmodulin-dependent protein kinase kinase (CaMKK). The activated CaMKK can then bind and phosphorylate, among others, Ca^{2+}/calmodulin-dependent protein kinase IV (CaMKIV) which can freely enter the nucleus through nuclear pore complexes (as well as Ca^{2+}/calmodulin itself) and phosphorylates cyclic AMP response element binding protein (CREB) through the histone acetyltransferase CREB binding protein (CBP).

This complex can finally induce transcription of specific genes (Bading 2013; Hagenston and Bading 2011).

To shortly summarize, activity-dependent Ca^{2+} signalling in the neurons induces a cascade of events, leading to the formation of complexes that can freely enter the nucleus of the cells and induce gene transcription by binding transcription factors. The resting Ca^{2+} concentration in the nucleus is the same as in the cytosol, as the nuclear envelope does not represent a barrier for Ca^{2+} ions and the ions can freely pass the nuclear envelope through the nuclear pore complexes.

As already mentioned, the ER represents an internal store for Ca^{2+} and can release it when ER-resident Ca^{2+} channels like IP3 receptors or ryanodine receptors (RyR) are activated. Inositol triphosphate 3 (IP3) production is activated by stimulation of the G protein-coupled receptors (GPCRs), which then activates phospholipase C (PLC) which in turn cleaves phosphatidylinositol-4,5-biphsphate to IP3, the second messenger responsible for activating IP3 receptors. Through these mechanisms and the SERCA pumps, the ER contributes to buffer and shape the Ca^{2+} signalling inside a cell (Berridge 1998). As the ER distributes throughout the whole cell, from dendrite to active zones in the axon, it is a key player in the transmission of Ca^{2+} signals from the periphery of the cell to the soma, where the nucleus is. Through Ca^{2+} “waves” that go the whole way via the ER, synapse stimulation can then cause nuclear Ca^{2+} signalling (Watanabe et al. 2006).

Mitochondria also play an important role in neuronal Ca^{2+} signalling. Not only are they important for the energy support that is needed near the synapses, but they can also store Ca^{2+} ions. Ca^{2+} ions are imported and exported through uniporters and mitochondrial Na-Ca-exchangers (mNCXs). Thus, mitochondria can buffer the cytosolic Ca^{2+} concentration. Furthermore, Ca^{2+} stimulates mitochondrial ATP synthesis by activating the tricarboxylic acids cycle (Marchi et al. 2018). But if the function of mitochondrial Ca^{2+} buffering is disturbed and too much Ca^{2+} ions are transported into sand accumulated in the mitochondria, this can induce apoptosis.

Thus, one of the most important roles of Ca^{2+} signalling in neurons is to regulate gene transcription in the nucleus. But what is the function of gene transcription in neurons?

1.2.2 Ca^{2+} induced synaptic plasticity

One major function of nuclear calcium signalling is neuroprotection. For example, the activation of NMDA receptors in the hippocampus leads to expression of neuroprotective genes (Papadia et al. 2005). Papadia and colleagues transferred hippocampal cell cultures from growth medium into basal medium to induce cell death. This effect was rescued by blocking $GABA_A$ receptors with bicuculline to indirectly activate synaptic NMDA receptors. They showed compelling evidence that long-lasting neuroprotection is nuclear Ca^{2+} signalling- and CREB activation-dependent.

Nuclear Ca^{2+} signalling is involved in learning and memory formation processes. For example, the blockade of CaMKIV in the forebrain causes impaired memory consolidation in mice (Limback-Stokin et al. 2004; Kang et al. 2001). One gene, whose expression is induced by nuclear Ca^{2+} signalling, is for example vascular endothelial growth factor D (VEGFD). This growth factor appeared to be crucial for contextual fear conditioning (Mauceri et al. 2011). In learning and memory, the development of plasticity changes such as increased spine density are crucial, and many genes needed for these processes are Ca^{2+} signalling-dependent. Long-term potentiation (LTP) is a phenomenon caused by frequent neuronal activation, which induces NMDA receptor stimulation and results in boosted Ca^{2+} signalling. It is known that LTP is crucial for learning and memory processes. LTP induces expression of genes through frequent Ca^{2+} influx and thus nuclear Ca^{2+} signalling, which leads to persistent plasticity changes (Bengtson et al. 2010). Bengtson and colleagues evoked nuclear Ca^{2+} signals by stimulating CA1 pyramidal neurons from hippocampus in acute mouse brain slices with established transcription-dependent late LTP-inducing stimulation protocols.

1.2.3 Maladaptation of Ca^{2+} signals in pathogenesis and pain

Even though Ca^{2+} signalling is a major messenger in the CNS, responsible for crucial plasticity changes in memory formation and neuroprotection, it can also become a problem.

Drug addiction is one example, for when memory formation, LTP and thus initially Ca^{2+} signalling becomes a problem instead of a supportive system in the CNS. It has been shown that addiction is a malfunction of the reward system, involving persistent

structural and functional changes in regions involved in addiction (Bading 2013; Hyman, Malenka, and Nestler 2006).

It is also suggested that Ca^{2+} signalling driven plasticity changes occur also in chronic pain, just as they do in memory formation (Ji et al. 2003). In addition, it has been shown that Ca^{2+} signalling is increased in, for example, excitatory neurons (Bading 2013; Simonetti et al. 2013). But in general, research concentrated mostly on Ca^{2+} signalling in learning and memory formation and, related to that, drug addiction and its involvement plasticity changes. Very little is known about the role of Ca^{2+} signalling in chronic pain development and maintenance.

1.2.4 How to investigate Ca^{2+} signals

All these studies have been achieved by using tools to detect Ca^{2+} signalling in cells. One good and reliable tool is the use of genetically encoded calcium indicators (GECIs). GECIs can be expressed specifically in different cell types, depending under which promoter the GECI is inserted. By binding calcium/calmodulin to the M11 motif of the GECI, the protein changes its conformation, which leads to an increased fluorescence of the bound GFP construct. Bengtson et al. 2010 showed for the first time the expression of GECI in the nucleus of neurons by combining the Ca^{2+} sensor GCaMP with three copies of a nuclear localisation signal (NLS). They showed that action potentials cause Ca^{2+} signalling in the nucleus of pyramidal neurons in the CA1 of the murine hippocampus.

Other localisation signals can be used in combination with these indicators, in order to investigate different cellular compartments. For example, by adding a nuclear export signal (NES), the localisation of the indicator can be ensured to be outside the nucleus and in the cytosol of the cell only. Another way would be to bind the indicator to the membrane in order to investigate processes or axons in their Ca^{2+} signalling behaviour, as the cytoplasm localised indicator would be mainly visible in the soma of the cell due to the high volume-to-surface ratio. The binding to the membrane can be done by expressing the indicator fused to a lymphocyte-specific protein tyrosine kinase (Lck), which is a membrane bound kinase.

1.3 Npas4

Neuronal PAS Domain Protein 4 (NPAS4) is an immediate early gene (IEG) and transcription factor (TF). It belongs to the basic-helix-loop-helix (bHLH)-PER-ARNT-SIM (PAS) family of transcription factors, which contain a bHLH domain for DNA binding and tandem PAS domains for dimerization and protein-protein interactions.

NPAS4 is expressed in excitatory neurons and diverse types of inhibitory neurons, like somatostatin-, parvalbumin- or 5HT3a-positive cells. In both cell types, *Npas4* is induced by neuronal activity, specifically via nuclear Ca^{2+} signalling (Zhang et al. 2009) . In all these cell types, NPAS4 regulates the expression of other IEGs in response to stimulation and neuronal activity. Spiegel and colleagues (Spiegel et al. 2014) showed that *Npas4* is expressed in cortical cultures after stimulation with high potassium levels. NPAS4 induction in all cell types leads to *Npas4*-dependent induction of other IEGs like *FosB*, another transcription factor which regulates other genes in order to induce plasticity changes in neurons (Nestler, Kelz, and Chen 1999). Similar results were achieved *in vivo* with sensory input through light stimulation to mice that were kept for a certain time in the dark. Unlike the IEGs, only about 25 % of expressed late-response genes happen to be in both cell types (excitatory and inhibitory neurons), for example: *Nptx2* and *Gpr* that are involved in the synthesis of AMPA and GPCRs (Fig. 3 A) (Spiegel et al. 2014). Strikingly, many other late-response genes were regulated by NPAS4 in a cell type-specific manner. For example, in excitatory neurons, NPAS4 regulates the induction of *Bdnf* which then promotes synaptic growth and is known to be involved in synaptic plasticity changes (De Vincenti et al. 2019). In inhibitory neurons, on the other hand, NPAS4 induces the expression of genes like *Frmpd3* and *Rerg* which are involved in synaptic density and signal transduction (Lee, Tsang, and Birch 2008).

As Bloodgood and colleagues (Bloodgood et al. 2013) showed in their previous work that the number of inhibitory synapses onto the soma of pyramidal neurons is regulated and increased by NPAS4 expression *in vivo* and that a knockout of NPAS4 in mice decreases the number of inhibitory synapses onto excitatory neurons in the hippocampus, Spiegel et al. determined the different synaptic inputs onto the distinct cell types. To investigate the distribution of different synapses onto the distinct cell types, they labelled inhibitory synapses with the specific marker Gad65/GABAARβ2/3 and Synapsin 1/PSD 95 for excitatory synapses. They counted the amount of

synapses and discovered an increased number of inhibitory synapses onto excitatory neurons, confirming Bloodgood and colleagues' results, and an increase of excitatory synapses onto inhibitory neurons when NPAS4 was increased in those cell specific cultures or their decrease, when NPAS4 was knocked down (Spiegel et al. 2014).

The conclusion from this work is that through expression of distinct genes in excitatory and inhibitory neurons leads to a change in plasticity and synaptic dynamics in those cells. They showed that in cortical tissue, activity-induced NPAS4 regulates the number of inhibitory synapses on excitatory neurons and excitatory synapses onto inhibitory neurons. Thus, activity-induced NPAS4 promotes the inhibitory influence in the neuronal circuit. Spiegel and colleagues suggest a homeostatic influence of NPAS4 in cortical and hippocampal regions.

As already mentioned for the work of Bloodgood and colleagues, NPAS4 plays an important role in the hippocampus. Here, normal house kept mice didn't show detectable NPAS4 expression, but when housed in environmental enrichment cages, the mice showed an increase of NPAS4 expression. Further, NPAS4 knockout mice showed reduced inhibitory postsynaptic currents compared to the controls. This indicated the role of neuronal activity induced NPAS4 in the balance of inhibitory input onto excitatory neurons in the hippocampus. Other groups have also shown that NPAS4 is important, for example, in contextual memory formation (Sun and Lin 2016; Ramamoorthi et al. 2011).

Another study showed that in the hippocampus NPAS4 is induced in pyramidal neurons by sensory experience, which then selectively enhances somatic inhibition through recruiting inhibitory synapses from cholecystokinin-expressing basket cells (Hartzell et al. 2018). Activity-induced NPAS4 regulates an increase of basket cell synapses onto the soma of pyramidal cell in the CA1 of the hippocampus.

This means that in the context of learning, memory and experience-driven neuronal activity, NPAS4 is important in the regulation of inhibitory input onto pyramidal cells. This together with the study in the cortical regions by Spiegel et al., indicates that NPAS4 represents an important key player in the regulation and control of neuronal circuits, balancing the system in an inhibitory manner in different brain regions (Fig. 3 B).

In the context of its important role in promoting inhibitory input onto the CNS, when activated, it might well be possible that impaired NPAS4 expression is involved in cognitive disorders. In some cognitive disorders like schizophrenia and autism (Ung et al. 2018) the inhibitory system of the CNS is dysfunctional, meaning less inhibitory neurons and synapses or expression of GAD65 and GAD67. In schizophrenia for example, the expression of the number of parvalbumin positive neurons is altered in the prefrontal cortex. It was just recently shown that NPAS4 is decreased in parvalbumin positive interneurons in a model of schizophrenia, where neonatal mice were treated with the NMDA receptor antagonist ketamine (Shepard et al. 2019). In this study, schizophrenia-like behaviour in mice, such as hyperactivity and social deficits, were caused by a knockdown of NPAS4.

The role of Npas4 is not yet well described. In fact, one study examined the function of NPAS4 in environmental enrichment-mediated responses in the hippocampus under neuropathic pain. Wang and colleagues demonstrated, for instance, that neuropathic pain, caused by chronic constriction injury (CCI), a ligation of the sciatic nerve, leads to a dysfunction of NPAS4 expression in the hippocampus (Wang et al. 2019).

As mentioned above, chronic pain can also cause depression and memory impairment. Wang and colleagues investigated not only the expression of NPAS4 in the hippocampus under neuropathic pain, but also the involvement of environmental enrichment. It is already known that environmental enrichment decreases hypersensitivity under neuropathic pain and thus represents a possibility for therapeutic intervention. When *Npas4* expression was decreased under neuropathic pain, environmental enrichment was no longer able to “rescue” the positive effect onto pain sensitivity, depression-like behaviour or memory deficit under neuropathic pain. Furthermore, the expression of tumour necrosis factor (TNF)-α under neuropathic pain indicates inflamed brain tissue. In addition, increased Npas4 also decreased the expression of TNF-α on protein levels.

In conclusion, the exact role of *Npas4* in chronic pain is not yet clear. Especially in the spinal cord tissue, which, in contrast to the hippocampus, plays a more central part in the pain circuit, nothing specific is known so far about how Npas4 regulates the neuronal circuit or how it might be involved in the transmission of painful sensory input.

In total, there are not many published studies about *Npas4* in the context of chronic pain or the spinal cord but as it is responsible for promoting inhibitory balance in neurons in the CNS, like the cortex or the hippocampus, it becomes more and more worth to investigate.

As mentioned above (see section 1.1.2.2 GABAergic neurons), GABAergic synapses and thus inhibitory neurons of different types are already shown to be impaired in their function or reduced in their number under chronic pain also in the spinal cord. Recently, it was discovered that a preoperative stress leads to reduced NPAS4 expression and might be linked to postoperative hyperalgesia in the spinal cord of rats (Wu et al. 2019). In this study, the authors measured postoperative hyperalgesia after the implementation of preoperative stress. Here, increase of glucocorticoid under hyperalgesia also comes along with synaptic plasticity changes, like decreased GABAAα-1, GABAAγ-2, GAD65 and GAD67. These are known to be regulated by NPAS4 and support the inhibitory circuit in the CNS, as they are markers for inhibitory synapses. By reducing corticosterone with antagonists, Wu and colleagues were able

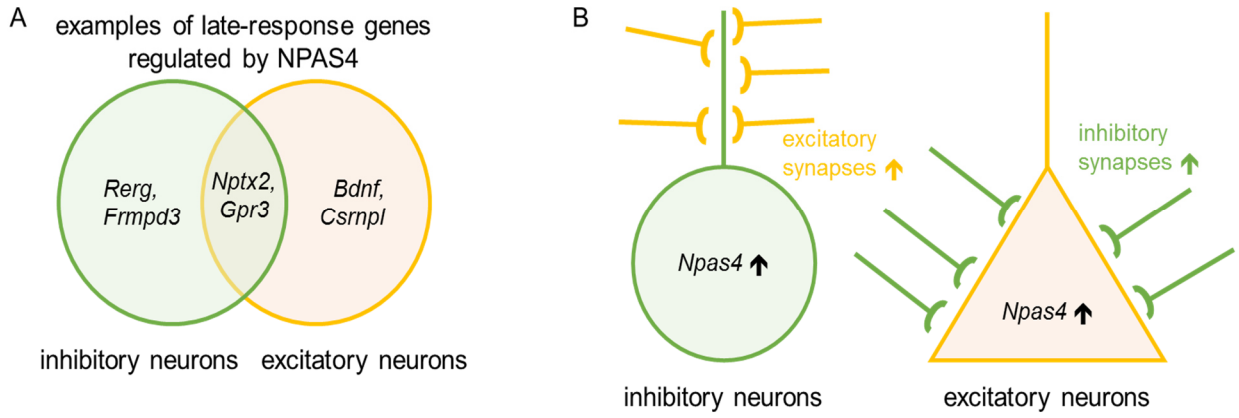

Figure 3: Npas4 regulates gene expression and plasticity changes. (**A)** Schematic example of late-response genes that are regulated by NPAS4. Inhibitory neurons (green) express for example *Rerg* and *Frmpd3* in an NPAS4-dependent manner. Excitatory neurons (orange) express for example *Bdnf* and *Csmpl* in a NPAS4-dependent manner. Both cell types express genes like *Nptx2* and *Gpr3* in a NPAS4-dependent manner. All those genes promote synaptic dynamics and plasticity. (**B)** An increase of NPAS4 in inhibitory neurons (green) results in increase of excitatory synapses onto the inhibitory neuron and an increase of NPAS4 in excitatory neurons (orange) leads to an increased amount of inhibitory synapses onto the excitatory neuron.

to rescue the expression of NPAS4 and GABAergic markers after stress induced postoperative hyperalgesia. They further showed that overexpression or knock down of NPAS4 through intrathecal rAAV injection either reduced hyperalgesia (for overexpression) or increased hyperalgesia sensation (for knock down of NPAS4 with rAAV-Npas4 RNAi). Their constructs for manipulating NPAS4 expression also influenced expression of GABAergic markers. Overexpression of NPAS4 led to increased GABAergic markers, whereas injection with the NPAS4 RNAi led to reduced GABAergic markers.

Thus, *Npas4* represents an interesting target for further research, as it regulates genes that are important for inhibitory input onto excitatory neurons and the excitatory input onto inhibitory neurons, resulting in an increase of inhibitory function in the CNS (Fig. 3). As the inhibitory system is reduced or impaired in its function under chronic pain conditions (see section 1.1.2.2 GABAergic neurons) it is necessary to investigate NPAS4 in the context of the mechanisms of chronic and acute pain. The question of whether chronic pain is linked to impaired NPAS4 expression is still unsolved. It might be, as other authors already suggested, that Npas4 represents a possible target for pain treatment.

Aims of this thesis

As presented in the introduction, the spinal cord dorsal horn has many different cell types, neurons as well as glial cells that respond with Ca^{2+} signalling to synaptic activity. Chronic pain has been shown to include Ca^{2+} signalling in excitatory neurons in the laminae I-II of the spinal cord dorsal horn. As shown above, glial cells as well as inhibitory neurons have already been shown to be altered by increased or decreased activity under chronic pain models. Thus, it makes sense to ask for the role of Ca^{2+} signals in those cells and their different cellular compartments. Figure 1 shows the different main cell types in the dorsal horn of the spinal cord. Mechanisms and functions are all about communication between different cell types and their alterations in case one player changes its behaviour. So how does Ca^{2+} signalling change, for example, in astrocytes and inhibitory neurons (Fig. 4)? This thesis will therefore concentrate on the following goals:

1. As astrocytes are known to react to different transmitters with Ca^{2+} signalling and as it is also known that astrocytes react with gliosis under chronic pain, do these two things change together? Does chronic inflammatory as well as neuropathic pain have an influence on Ca^{2+} signalling in different cellular compartments? In this thesis, I concentrated on astrocytic Ca^{2+} signals, evoked by electrical stimulation of the dorsal root in acute slices. I used GECIs to investigate the signal in the cytoplasm, the membrane and the nucleus. I further investigated the signal changes under different chronic pain conditions.

2. Another interesting target would be Ca^{2+} signalling in inhibitory neurons. As shown above, inhibitory neurons like parvalbumin positive cells, play already an important role under chronic pain conditions. Excitatory neurons respond with increased Ca^{2+} signalling under chronic pain conditions. What about parvalbumin positive neurons? Electrically evoked Ca^{2+} responses in parvalbumin neurons were so far not described in spinal cord dorsal horn. In addition, would the Ca^{2+} signalling be altered under chronic pain?

3. As already mentioned in the introduction, one gene draws our attention, as it is induced by synaptic activity and Ca^{2+} signalling: Npas4. It is responsible for an excitatory-inhibitory balance in the CNS, favouring inhibition and some studies indicate that increased pain is coupled to decreased Npas4 and decreased GABAergic synapses. So in the last part of the thesis I will investigate the role of Npas4 in the spinal cord dorsal horn under chronic and acute pain conditions.

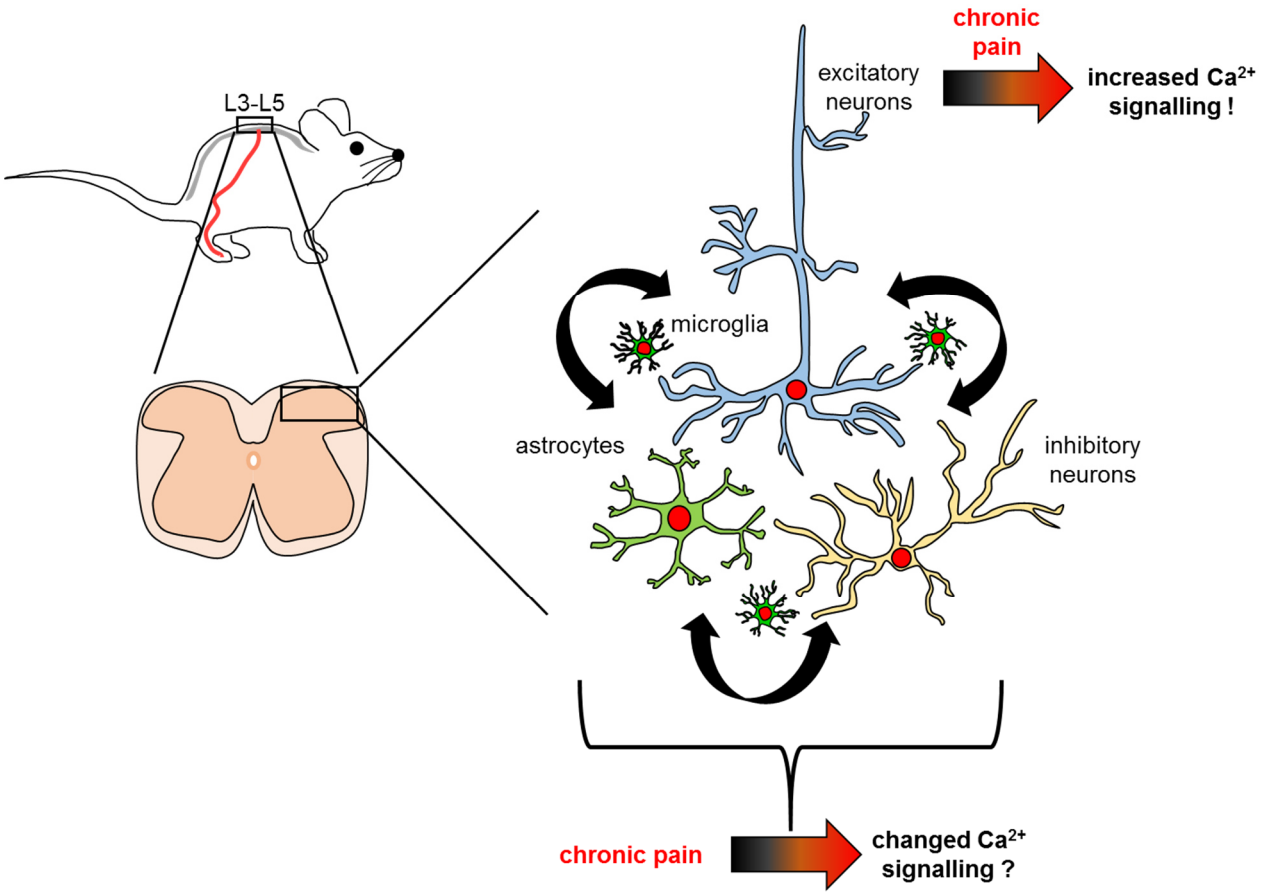

Figure 4: Involvement of different cell types and their Ca^{2+} signalling in the spinal dorsal horn under chronic pain conditions. Schematic drawing represents introduction of chronic pain conditions concerning the lumbar part L3 – L5 of mice spinal cord dorsal horn and major classes of different cells: excitatory, inhibitory neurons as well as glia cells like astrocytes and microglia. Under chronic pain conditions, excitatory neurons already showed to have increased Ca^{2+} signalling.

Hypothesis

We hypothesise in this thesis that Ca^{2+} signals can be evoked by fibre stimulation from the dorsal root in different cell types of the spinal dorsal horn and that the Ca^{2+} signalling in astrocytes will change under different chronic pain conditions. In this context, we investigated the Ca^{2+} signalling behaviour of different cell compartments of astrocytes in acute spinal cord slices of mice under chronic inflammatory pain and neuropathic pain.

We further hypothesise that Ca^{2+} signals in parvalbumin-positive neurons change under chronic pain conditions. As a consequence of this, we think that Ca^{2+} signalling-dependent expression of genes like *Npas4* then plays a crucial role in the development of chronic pain conditions and that its changes have an input on the development of chronic pain.

2 Materials and Methods:

2.1 Molecular biological methods

Plasmids and cloning plans of used constructs in this project were kindly provided by colleagues from the department Neurobiology, Heidelberg University, Heidelberg Germany.

2.1.1 rAAV production

For this study we used recombinant serotype 1/2 adeno-associated viral vectors (rAAV). In order to express in astrocytes different calcium indicators for calcium imaging, the rAAV included a plasmid with a human GFAP promotor (Brenner et al. 1994) to control the green fluorescent GCaMP based genetically-encoded calcium indicators (GECIs) which were targeted to the cytoplasm (GCaMP5E), the plasma membrane (Lck.GCaMP5E) (Tang et al. 2015) and the nucleus (GCaMP3.NLS) (Bengtson et al. 2010). For the CRE-mouse line to target parvalbumin positive cells, which was kindly provided from the working group of Prof. Dr. Rohini Kuner, the created rAAV included a floxed EF1a:GCaMP5NES for the cytoplasm expression. For the CRE-mouse line to target astrocytes under Aldh1l1 promoter, we created and used rAAV with a EF1a:GCamP3.NLS expressing plasmid.

For the behaviour experiments the rAAV constructs were supposed to increase or decrease the expression of NPAS4. To increase the basal NPAS4 expression we used an over expression plasmid under the human Synapsin promoter coupled to an HA-tag and a tDimer for fluorescent expression (hSyn:Npas4.HA_hSyn:tdimer) and its control construct (hSyn:MCS.HA_hSyn:tDimer). To decrease the basal expression and also the induced expression of *Npas4*, we used a sh-binding function under the U6 promoter and GFP under CMV enhancer, chicken beta-Actin (CAG) promoter, for green fluorescent expression (U6:shNpas4_CAG:GFP) and its control which consisted of a scrambled version for the sh-construct (U6:shUNC_CAG:GFP) or the dominant negative construct which consisted of a sequence that would bind to the functional expressed protein and would therefore block its function (hSyn:dnNpas4.HA_hSyn.tDimer) and the control construct from the overexpression (see above).

For the production of the virus particles, carrying the announced constructs, HEK cells were grown in complete Dublbecco's Modified eagle Medium (DMEM, Life Technologies Limited, Paisley, UK) (Table 1) on 14 cm plates and incubated at 37°C, 95 % relative humidity and 5 % CO_2. Two to three hours prior to virus transfection the medium from the HEK cells was completely changed to complete Iscove's Modified Dulbecco's Medium (IMDM, Life Technologies Limited, Paisley, UK) (Table 2). The plasmids were mixed in a concentration of 65 µg with 1 M $CaCl_2$ and sterile H_2O and helper plasmids for viral capsid expression (125 µg pFD6, 31.25 µg pRV1 and 31.25 µg pH21) and finally filter sterilized. Filter sterilized 2xHEBS with a pH of 8.0 (Table 3) was added and the solution was vortexed for 15 s. The substrate rested for more than 90 s, building a fine participitate and then 5 ml per plate from the mix was added dropwise to the prepared HEK cell plates with a growth confluency of about 70-75 %. During this procedure the plate had to be swirled gently. 16-20 h post to transfection the medium was changed to fresh and pre-warmed (37°C) complete DMEM. 60-65 h post-transfection the medium was taken from the HEK cells, the cells were washed with pre-warmed (37°C) 1x PBS and harvested in 25 ml pre-warmed 1x PBS. The cell suspension was centrifuged at 2100 rpm for 5 min, supernatant discarded and the cells re-suspended in pre-warmed and filter sterilized NaCl (150 mM)/ Tris (20 mM) and frozen at -20°C. At least 24 h later the cell suspension was thawed at RT in a water-bath, then fresh sodium deoxycholate (Sigma, 10 % in sterile H_2O) for a final concentration of 0.5 % and 5.1 µl Benzonase DNAse (Sigma-Aldrich Chemie GmbH, Munich, Germany) for final concentration of 50 U/ml were added, mixed thoroughly and incubated at 37°C in a water-bath for 1 h and mixed from time to time. Then the cell suspension was frozen at -20°C again for at least 24 h. Finally the virus was purified from the cells by thawing, centrifuging and loading the supernatant onto Heparin columns (HiTrap Heparin HP, GE Healthcare Bio-Sciences AB, Uppsala, Sweden). Loading was followed by washing and then elution with increasing salt concentrations of NaCl/Tris (100 mM, 200 mM and 300 mM for washing, 400 mM, 450 mM and 500 mM for elution). The virus solution was finally filtered and concentrated (Amicon Ultra – 4, Darmstadt, Germany) and washed with 1x sterile PBS. To confirm and evaluate the success of the virus production two experiments were done afterwards: SDS gel (Table 11) analysis to detect rAAV capsid proteins and extraction of viral DNA to determine the titre. For the capsid protein detection, 5 µl of the virus sample were taken and mixed with 15 µl 2x sample buffer with 1:1000 DTT and

incubated for 5 min at 95°C. The probes were then run on a 10 % SDS gel at 30 mA for ~1.5 h. Afterwards, the gel was stained with coomassie for 30 min at RT on a rocker and destained o/n at 4°C on a rocker with a paper towel tissue to take up the blue colour from the coomassie. For the records a photo was taken from the gel showing a successful virus production.

For extraction of viral DNA, 2 µl of the viral stock is mixed with 10 µl of 10x ABI buffer (Table 4), 86 µl sterile H_2O and 1 µl DNAseI to digest all remaining non-viral DNA. This mix was incubated for 30 min at 37°C in a water bath and the DNAseI was then inactivated by incubation at 70°C for 10 min. To digest the viral capsid, 1 µl proteinase K was added and incubated for 1 h at 50°C and finally inactivated at 95°C for 20 min. 1 µl of each single-stranded viral DNA was then used for PCR reaction prepared with 10 µM sense and 10 µM antisense primer, SYBR Green PCR master mix (2x) (ThermoFischer Scientific) as well as RNAse-, DNAse-free H_2O. The probes were pipetted on a 96-well-plate, together with standards from 10^4-10^9 plasmid DNA molecules/µl and a negative control only consisting additional H_2O. The PCR program was run with a thermal cycler C1000TM (Bio-Rad, Hercules, USA) (Table 13) and the mean quantity was taken to determine the viral titre.

Table 1: Complete DMEM

Name	Stock concentration	Final concentration	Weight or Volume
DMEM[1]			500 ml
Heat-inactivated FBS[1] (Fetal Bovine Serum)			50 ml
Non-essential amino acids (NEAA)[1]	100x	1x	5 ml
Sodium pyruvate[2]	100x	1x	5 ml
Penicillin/Streptomycin[2]	200x	1x	2.5 ml
[1]Life Technologies Limited, Paisley, UK [2]Sigma-Aldrich Chemie GmbH, Munich, Germany			

Table 2: Complete IMDM

Name	Weight or Volume
IMDM[1]	500 ml
Heat-inactivated FBS[1]	25 ml
[1]Life Technologies Limited, Paisley, UK	

Table 3: HEBS 2x

Name	Stock concentration	Final concentration	Weight or Volume
HEPES	1 M	50 mM	25 ml
NaCl	5 M	280 mM	28 ml
Na_2HPO_4	1 M	1.5 mM	750 µl
NaOH	1 M	1M	
ddH_2O			(up to) 500 ml
All chemicals are from Sigma-Aldrich Chemie GmbH, Munich, Germany.			

Table 4: 10x ABI

Name	Stock concentration	Final concentration	Weight or Volume
KCl	3 M	0.5 M	3.33 ml
Tris-HCl, pH 8.0	1 M	0.1 M	2.0 ml
$MgCl_2$	1.9 M	50 mM	526 µl
ddH_2O			(up to) 20 ml
All chemicals are from sigma-Aldrich Chemie GmbH, Munich, Germany.			

2.1.2 Primary hippocampal cell culture

For testing if the constructs were efficient in expression and their function, the different viruses were tested *in vitro* before injecting them into mice. The cells were freshly prepared hippocampal primary cultures either with or without glass coverslips. The culture dishes were coated with 200 µl Poly-D-Lysin (PDL)/ 90 µl Laminin mix in 15 ml H_2O (Sigma-Aldrich Chemie GmbH, Munich, Germany) O/N in the cell culture incubator and washed with sterile H_2O 24 h later and prepared with L-glitamine neurobasal medium (gibco life Technologies, Thermo Fisher Scientific, MA, USA). The cells were kept in an incubator with 37°C and 95 % relative humidity and 5 % CO_2. At DIV 3 the culture was treated with 1:1000 cytosine arabinoside (AraC) in the morning to reduce the amount and growth of glia cells and infected with the previously prepared viral constructs in the evening. The medium was changed completely to transfection medium (TM) (Table 10) on DIV 8. The treatment with BIC or without BIC as control for 2 h, to determine the activity and the function of the tested virus, was done on DIV 10. The cells were then ready for harvesting to check for protein levels, mRNA expression or to mount the coverslips with primary infected neurons with Hoechst/Mowiol to make example pictures of the expression in the cells due to the construct.

2.1.3 Primary spinal cord culture

As we wanted to test the constructs in mouse spinal cord, we also considered testing several constructs in spinal cord cell culture. For that, the pups that were sacrificed for hippocampal cell culture, were after beheading taken for spinal cord isolation. After isolation, the dura mater was removed from spinal cord tissue and the spinal cord tissue was cropped into two to three pieces. The tissue was then transferred into enzyme solution (Ky/Mg in dissociation medium + 22.5 mg L-cysteine, Sigma-Aldrich Chemie GmbH, Munich, Germany + 500 units papain, CellSystems GmbH, St. Katharinen, Germany) (Table 6-7), incubated for 20 min at 37°C in a water bath with a magnetic fish to slowly but continuously swirl the solution and in addition carefully swirled by hand every 5 min. Then the solution was carefully removed and the step was repeated. Afterwards, the tissue was washed three times for 1 min each with 2 ml dissociation medium and then incubated two times for 5 min each in inhibitory solution (Ky/Mg in dissociation medium + 1 g trypsin inhibitor, Sigma-Aldrich Chemie GmbH

Munich, Germany + 0.2 M NaOH) (Table 6 -7) at 37°C in a water bath. The tissue was washed three times for 1 min with 2 ml NBA/growth medium (Table 8) and then dissociated 50 times by pipetting up and down in 2 ml NBA medium and the cell suspension was then allowed to rest for 5 min. The suspension was carefully removed and transferred to a 15 ml falcon tube. This step was repeated three times. In the end a total cell suspension volume of ~ 10 ml was determined for its cell concentration and calculated for different diameters of culture dishes (Table 5).

Table 5: Cell distribution according to plate.

Plate	~ Area (cm^2)	Cells	Volume (with 0.5 x 10^6 cells/ml)
35 mm	9.6	1 x 10^6	2 ml
6-well	9.6	1 x 10^6	2 ml
12-well	3.8	0.75 x 10^6	1 ml (1.5 ml 2.5 h medium change)
24-well	1.9	0.25 x 10^6	0.5 ml (1.5 ml 2.5 h medium change)
4-well	1.9	0.25 x 10^6	0.5 ml (1 ml 2.5 h medium change)
48-well	0.95	0.125 x 10^6	0.25 ml (0.5 ml 2.5 h medium change)

2.5 h after cells were pipetted into culture dishes, the medium was changed to fresh NBA. Cells were checked upon every day. AraC treatment was done at DIV 4 in the morning, viral transfection in the evening. Medium change to transfection medium ™ (Table 9-10) was done at DIV 8 or 9, experiment was done at DIV 10 or 11.

Table 6: Ky/mg solution.

Component	Final concentration	Stock concentration	For 80 ml
Kynurenic acid	10 mM	Powder	158.56 g
$MgCl_2$	100 mM	2 M	4 ml
HEPES	5 mM	1 M	0.4 ml
Phenol red	0.5 % v/v	100 %	0.4 ml
NaOH	12.5 mM	1 M	1 ml
H_2O			up to 80 ml
All chemicals are from Sigma-Aldrich Chemie GmbH, Munich, Germany.			

Table 7: Dissociation Medium (DM).

Component	Final concentration	Stock concentration	For 80 ml
Na_2SO_4	81.1 mM	1 M	20.45 ml
$MgCl_2$	5.85 mM	1.9 M	0.77 ml
K2SO4	30 mM	0.25 M	30 ml
$CaCl_2$	0.25 mM	1 M	0.063 ml
HEPES	1 mM	1 M	0.25 ml
Glucose	20 mM	2.5 M	2 ml
Phenole red	0.2 % v/v	100 %	0.5 ml
H_2O			up to 250 ml
All chemicals are from Sigma-Aldrich Chemie GmbH, Munich, Germany.			

Table 8: NB-A/Growth Medium (GM).

Component	For 100 ml
Neurobasal A-medium	97 ml
B 27	2 ml
Rat serum	1 ml
Glutamin (200 mM)	0.25 ml
Penicillin/Strepomycin	0.5 ml
H_2O	Up to 100 ml
All chemicals are from Sigma-Aldrich Chemie GmbH, Munich, Germany. Sterile filtered through 0.22 m Millipore filter and stored at + 4°C.	

Table 9: Salt Glucose Glycine Solution (SGG).

Component	Final concentration	Stock concentration	For 80 ml
NaCl	114 mM	5 M	11.4 ml
$NaHCO_3$	0.22 % v/V	7.5 % m/v	14.6 ml
KCl	5.29 mM	3 M	0.882 ml
$MgCl_2$	1 mM	1.9 M	0.264 ml
$CaCl_2$	2 mM	1 M	1 ml
HEPES	10 mM	1 M	5 ml
Glycine	1 mM	1 M	0.5 ml
Glucose	0.54 % v/v	45 % m/v	6 ml
Sodium pyruvate	0.5 mM	0.1 M	2.5 ml
Phenole red	0.2 % v/v	100 %	0.5 ml
H_2O			up to 500 ml
All chemicals are from Sigma-Aldrich Chemie GmbH, Munich, Germany. Sterile filtered through 0.22 m Millipore filter and stored at + 4°C.			

Table 10: Transfection Medium (TM).

Component	For 100 ml
SGG	88 ml
MEM (without glutamine)	10 ml
ITS	1.5 ml
Penicillin/Strepomycin	0.5 ml
H_2O	Up to 100 ml
All chemicals are from Sigma-Aldrich Chemie GmbH, Munich, Germany. Sterile filtered through 0.22 m Millipore filter and stored at + 4°C.	

2.1.4 Protein expression (SDS Page)

For examination of the targeted protein levels in the cell culture with or without BIC treatment, the cells were cultured in 35mm dishes and treated as described above. At DIV 10 the cells were harvested with 2xsample buffer (30 % glycerol, 4 % SDS, 169 mM Tris-HCl 1 M pH 6.8, 0.02 % bromophenol blue, ddH_2O) with 1:1000 DTT and incubated at 95°C for 5 min on a heating block to break the sulfate bridges between the proteins in order to unfold them for a separation on a SDS gel. The samples were then loaded on a 10 % SDS gel, containing of a stacking gel and a separation gel (Table 11). After ~ 70 min at 30 mA the gel was taken out of the chamber to blot it onto a nitrocellulose membrane (Waterman) for 2h with constant voltage of 20 V (Transferring buffer: 150 mM glycine, 20 mM Tris, 0.1 % SDS and 20 % Methanol). The membrane was marked to not lose orientation and then stained with ponceau (SERVA Elecotrophoresis, Heidelberg, Germany) for 10-15 min on a rocker at RT to check the quality of the blot. When no bubbles were disturbing the blot, then the membrane was rinsed with H_2O and blocked with 5% milk (frema Reform, Instant-Magermilchpulver, Radolfzell, Germany) in Phosphate buffered saline with Tween-20 (PBST) for 30 min, washed 3x10 min with PBST and then incubated in the first antibody (1:400 000 for α-Tubulin and 1:5000 for the other antibodies, see table X) in 5 % milk PBST or 5 % BSA (albumin fraction V, Roth) in PBST (for Npas4 antibody) for 2 h at RT on a rocker or o/n at 4°C, washed with PBST 3x10 min and finally incubated on a rocker at RT with secondary antibodies in 5 % milk PBST for 30 min (Table 19) at RT. The membrane was washed with PBST and incubated for 5 min with ECL detection solution (Bio-Rad, Hercules, USA) and the pictures were taken with the ChemiDoc™ imaging system (Bio-Rad, Hercules, USA).

Table 11: SDS-PAGE.

Solution	Stacking gel (3.7%) 10ml	Seperation gel (10%) 20ml
H_2O	6.25 ml	8.2 ml
4x Buffer [1]	2.5 ml	5 ml
Rotiphorese Gel 30 [2]	1.25 ml	6.7 ml
10% APSc [3]	100 µl	100 µl
TEMED [4]	10 µl	10 µl

[1] 4x stacking gel buffer: 0.5 M Tris-HCl, pH 6.8 and 0.4% (w/v) SDs;
4x separation gel buffer: 1.5 M Tris-HCl, pH 8.8 and 0.4% (w/v) SDS.
[2] 30% Acrylamid solution with 0.8% Bisacrylamid from Carl Roth (Karlsruhe, Germany)
[3] 10% (w/v) ammonium persulfate (APS) H2O.
[4] N,N,N',N'-Tetramethyl-ethylenediamine from SERVA Electrophoresis (Heidelberg, Germany).

2.1.5 Gene expression analysis

2.1.5.1 cDNA synthesis

All RNA related work was conducted under RNase-free conditions. The cells were collected with freshly prepared 1% β-Mercaptoethanol (ME) in lysis buffer (RLT) and scratched off the surface of the dishes (3.8 cm^2 12-well plate, each with 300 µl RLT/ME mix). Additional 300 µl 70% ethanol was added and mixed well to be put onto a RNeasy Mini Kit column (Qiagen, Venlo, Netherlands) placed in a 2 ml collection tube and RNA was purified as described in their provided protocol, including the optional steps by using on-column DNaseI digestion (RNase-free DNase Set Qiagen). After elution concentration was measured and a master mix (Table 12) was prepared. For each sample, 6.3 µl of master mix was mixed with 1.0 µg of RNA to produce cDNA in a PCR reaction (Table 13).

Table 12: cDNA synthesis mixture.

Solution[1]	Volume for total 20 µl
(10x) RT buffer	2 µl
(100 nM, 10x) dNTPs	0.8 µl
(10x) Random primers	2 µl
(50 U/µl) Reverse transcriptase	1 µl
(40 U/µl) RNase inhibitor	0.5 µl
RNase-free H_2O	3.7 µl
[1] All chemicals are provided by Applied Biosystems, Waltham, USA. + 20 µl diluted RNA (1.0 µg) for each reaction	

Table 13: cDNA synthesis program.

Procedure step	Temperature	Duration
1. Annealing	25°C	5 min
2. Annealing/Elongation	37°C	120 min
3. Denaturation	85°C	5 s
4. Storage	4°C	for ever
PCR reaction was performed in thermal cycler C1000TM (Bio-Rad, Hercules, USA)		

2.1.5.2 Real-time quantitative PCR

PCR product, cDNA, was then filled up with 100 µl sterile and RNAse and DNAse free H_2O. For real-time (RT) quantitative (q) PCR, a master mix for each gene was prepared (Table 14-15) from TaqMan^R (Applied Biosystems^R, Waltham, USA). 5.5 µl of TaqMan master mix was mixed with 4.5 µl of cDNA and then run with a StepOnePlus^R real time PCR system (Applied Biosystems^R) with a temperature program presented in table 16 to determine the expression levels of the targeted genes. Target mRNA expression level was normalized to the relative ratio of the expression of *Gusb* mRNA.

Table 14: RT-qPCR taqman probes.

Acronym	Gene name	Assay ID
Arc	Activity regulated cytoskeletal-associated protein	Mm00479619_g1
Bdnf	Brain derived neurotrophic factor	Mm00432069_m1
cFos	FBJ osteosarcoma oncogene	Mm00487425_m1
Gusb	Glucuronidase, beta	Mm00446953_m1
Inhba	Inhibin beta-A	Mm00434338_m1
Npas4	Neuronal PAS domain protein 4	Mm00463644_m1
Nptx2	Neuronal pentraxin 2	Mm00479438_m1
All probes are designed by Applied Biosystems^{R} (Waltham, USA)		

Table 15: RT-qPCR reaction mix per well.

Solution	For 10 µl
(2x) Master mix	5 µl
(20x) Probes	0.5 µl
(diluted) cDNA	4.5 µl

Table 16: RT-qPCR temperature program.

Procedure step	Temperature	Duration
1	50°C	2 min
2	95°C	10 min
3	95°C	15 s
4	60°C	1 min
5	Go to step 3	50 cycles
6	Stop	For ever

2.2 Animal work

This study was approved by the local animal care and use committee (Regierungspräsidium Karlsruhe, Referat 35, Karlsruhe, Germany), project G-272/14. All animal experiments were designed and carried out in accordance with ARRIVE guidelines and the EU Directive 2010/63/EU for animal experiments.

2.2.1 Mouse lines

Aldh1l1-Cre/ERT2 treatment with tamoxifen. The Cre/ERT2 toolbox is reduced in its cre activity in the absence of tamoxifen. To induce cre recombination, adult male mice that were injected with EF1a:FLEX(GCaMP3.3xNLS.myc) rAAV received tamoxifen injection i.p. for five days, one week after viral injection.

Parvalbumin CRE-mouse line was used for specific viral transported Ca^{2+} indicators in parvalbumin positive cells in the spinal cord of the mice.

For most of the studies, either for astrocyte Ca^{2+} imaging analysis or for investigation of the early immediate gene Npas4, C57BL/6N wild-type mice (Charles River, Sulzfeld, Germany) were used for the experiments.

Mice were either housed in the facility of Heidelberg University (Interfakultäre Biomedizinische Forschungseinrichtung (IBF)), the behavioural facility Interdisciplinary Neurobehavioral Core (INBC, Heidelberg Universit) or the neurobiology department (Heidelberg University, Germany). Mice were group-housed on a 12 h light/dark cycle with ad libidum access to water and food. Surgeries and behavioural tests were performed during light phases. Behavioural tests were performed in the morning hours.

2.2.2 Virus injection

In order to express the different rAAVs, the virus construct was injected into the mice spinal cord. The virus was prepared in a dilution 2:1 with Manitol or undiluted and filled into a 1ml Hamilton needle. Sleep mix (table) was prepared freshly and injected IP (1 g = 10 µl) according to the weight of the mouse. Mice's backs were shaved above the spinal cord, the back was disinfected and to protect the eyes from drying out during the surgery, some salve (Bepanthen, Bayer) was put on the mice eyes, then Carprofen

(table) (1 g = 10 µl) as analgesia was injected sub-cutaneously in order to prevent the mouse from suffering post-surgery pain. The mouse was placed down on a warming plate (39°C) and the back was supposed to be slightly bent into a hunchback to identify L3-L5 position of the spinal cord. Skin and muscles were opened carefully. Spinal cord was revealed and the dura opened. As soon as the needle (35 G bevelled needle (WPI; NANOFIL, NF35BV) was in place to be inserted into spinal cord tissue, left or right of the dorsal blood vessel, it was tested if it was clogged or if viral solution would come out as mannitol tends to build crystals at RT. When the needle was not clogged, it was inserted into spinal cord tissue until the opening of the needle was not visible anymore. Before injection, the needle had to rest in position for 5 min then injection started: 500 nl / injection, speed: 50 nl / min. In addition the injected liquid was allowed to distribute in the tissue for another 5 min before removing the needle from the spinal cord dorsal horn. To close the wound a piece of gelatine sponge was put directly onto the open wound and the cut was closed with 3:1:2 stiches. For local anaesthesia lidocaine (Aspen Pharma Trading Limited, Dublin, Ireland) was sprayed directly onto the closed wound. Wake-mix was injected sub-cutaneously and after awaken the mouse was tested for hind-limp function to exclude any possible damage due to surgery. To prevent post-surgical pain, 1 h after wake-mix application, Buprenorphine was injected. Mice were kept on a warming plate (39°C) O/N to recover from surgery and got wet and soft food pellets.

Table 17: Mice injection solutions.

Mix	Company	Component and amount	Concentration
Sleep Mix (for 1 ml)		0.9% NaCl 750µl	
	Sedin	Medetomidinhydrochlorid 50µl	stock: 1 mg/ml
	Midazola m-hameln	Midazolamhydrochlorid 100µl	stock: 5 mg/ml
	Fentanyl-Piramal, Critical Care	Fentanylcitrat 100µl	stock: 0.05 mg/ml
Carprofen Analgesia (for 5 ml)		0.9% NaCl 4.95ml	
	Carprieve, Norbrook	Carprofen 50µl	stock: 50 mg/ml
		0.9% NaCl 750µl	

Wake Mix (for 5 ml)	Atipazole	Atipamezolehydrochlorid 250µl	stock: 5 mg/ml	
		Flumazenil Kabi Fresenius	Flumazenil 2.5ml	stock: 0.1 mg/ml
		Naloxon Inresa	Naloxonhydrochlorid 1.5ml	stock: 0.4 mg/ml
Buprenorphine Analgesia (for 5 ml)		0.9% NaCl 4.88ml		
		Buprenorphine 120µl	stock: 0.324 mg/ml	

2.2.3 Acute spinal cord slices

Three weeks after virus injection and after treatment with one of the pain protocols (see below) the mouse was prepared for acute slicing. Needed solutions (Table 18) were prepared and slicing solution was cooled down to ~4°C. Mice were injected with Narcoren and as soon as they were not responding to foot pinches, the thorax was opened and perfused with ice cold carboxylated slicing solution. Spinal cord was then taken out and dura removed from the spinal cord. The spinal cord with dorsal roots attached to the infected hemisphere was then mounted into a groove within a block of 1.5 % agarose in PBS and secured with cyanoacrylate adhesive to the stage of a Microm HM650V (Thermo Scientific) vibratome containing NMDG slicing solution bubbled with 95 % O2/5 % CO2 and cooled to 1-4 °C. Slices (~330 µm) were prepared using double edge coated blades (Science Services, washed version, #7200-WA) and then placed into NMDG slicing solution bubbled with 95 % O2/5 % CO2 and warmed to 34 °C for ten minutes. Slices were subsequently transferred to extracellular recording solution (Table 18) adjusted to a final osmolarity of 300-305 mOsm and pH 7.35, bubbled with 95 % O2/5 % CO2 and warmed to 34 °C, and then allowed to cool to room temperature for a recovery period of ≥ 1 hour

Table 18: Slicing and imaging solutions.

	Name	Stock MW or concentration	Final concentration	Weight or Volume
NMDG/HEPES slicing solution (500 ml, pH 7.35, final osmolarity: 300-305 mOsm) Fresh on the day of use!	NMDG (N-methyl-D-glucamine)	195.22 g/mol	93 mM	9.07773 g
	HCl	37 %	93 mM	~3.2 ml
	KCl	3 M	2.5 mM	416.7 µl
	NaH_2PO_4	1 M	1.2 mM	600 µl
	sodium pyruvate	500 mM	3 mM	3 ml
	HEPES	1 M	20 mM	10 ml
	$NaHCO_3$	1 M	30 mM	15 ml
	D-glucose	1.25 M	25 mM	10 ml
	L+ ascorbic acid	176.12 g/mol	5 mM	0.4403 g
	N-acetyl-L-cysteine	163.19 g/mol	10 mM	0.81595 g
	thiourea	76.12 g/mol	2 mM	0.07612 g
	$MgSO_4$	2 M	10 mM	2.5 ml
	$CaCl_2$	2 M	0.5 mM	125 µl
	ddH_2O			(up to) 500 ml
Recording solution (2l, pH 7.35, final osmolarity: 300-305 mOsm) Storage at 4°C	NaCl	58.4 g/mol	125 mM	14.6 g
	D-glucose	180.16 g/mol	10 mM	3.6 g
	$NaHCO_3$	84.01 g/mol	25 mM	4.2 g
	KCl	3 M	2.5 mM	1.67 ml
	NaH_2PO_4	1 M	1.25 mM	2.5 ml
	$MgSO_4$	2 M	1.2 mM	1.2 ml
	$CaCl_2$	2 M	2.0 mM	2.0 ml
	ddH_2O			(up to) 2 l

2.2.4 *In vivo* imaging and recording

Single spinal cord acute slices were placed to a recording chamber (PM-1, Warner Instruments, Hamden, CT, USA or PC-R, Siskiyou, OR, USA) perfused (~3 ml/min) with 95 % O2/5 % CO2-bubbled extracellular recording solution warmed with an in-line heater to 34 °C. The slices were secured with a platinum harp ring with nylon strings. Dorsal roots were sucked into a glass stimulation electrode, the tip of which had been dipped into Vaseline to improve the electrical seal around the root. We regularly controlled the electrode resistance to ensure that it was greater than 20 kθ. The stimulation was controlled by a stimulus isolator (World Precision Instruments, A365) controlled by Clampex10.3 Software (Molecular Devices) or a stimulus isolator (STG 4002, Multichannel Systems) controlled by MC Stimulus II software (Multichannel Systems) (Fig. 5 D).

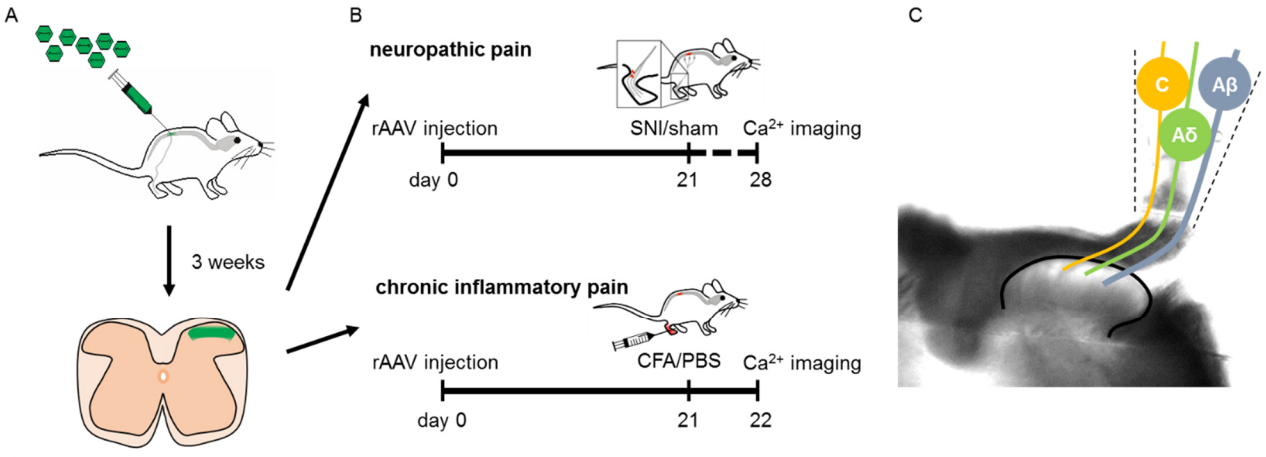

D

preferred fiber class	frequency	pulse duration	train duration
Aβ-fibers (thickly myelinated) → touch	100 Hz	0.1 ms	1 s
Aδ-fibers (thinly myelinated) → nociceptive	20 Hz	0.1 ms	1 s or 10 s
C-fibers (non-myelinated) → nociceptive	4 Hz (sinusoidal)	1.0 ms	1 s

Figure 5: Experimental procedure rAAV injection, pain protocols and stimulation of acute slices. (A) Schematic drawing of rAAV introducing Ca^{2+} indicator into mice spinal cord dorsal horn. **(B)** Two different pain models: 1. Neuropathic pain model with SNI or sham surgery 3 weeks after rAAV injection and performance of acute slicing and Ca^{2+} imaging at day 28 (7 days after SNI/sham surgery). **(C)** Example picture of acute slice under imaging set-up and suction of dorsal root. In the dorsal root there are periphery fibres represented like Aβ-, Aδ- and C-fibres, forming synapses in the spinal dorsal horn. **(D)** Stimulation protocol for the preferred fibre classes, their stimulation frequency, pulse duration and train duration of the single stimulations. Stimulation intensities started at 0.01 mA followed by 0.05, 0.1, 0.2, 0.5, 0.8 and finally 1 mA.

At the end of the stimulation protocol, the slice was exposed to a high concentration of potassium to cause a strong increase in intracellular Ca^{2+}. GCaMP constructs were excited using a CooLed light source (480±10 nm), and fluorescence emission (530±20 nm) acquired at a rate of 2 Hz with a cooled camera (Photometrics Coolsnap HQ, Roper Scientific) with 2x2 binning through a 20x water-immersion objective (XLM PlanFluor 0.95W, Olympus) on an upright microscope (Olympus BX51WI) connected through a software interface (Metafluor, Universal Imaging Systems and Molecular Devices). Overview images were taken with a 4x air objective (PlanCN, Olympus). After recording, the electrode was removed from the dorsal root and the slice was stored for further immunohistochemistry analysis in 4% formalin for ~2 h and then stored in 30% sucrose at 4°C for cryo-protection.

2.2.5 Cryo slices

Whole spinal cords or fixed former acute slices were used for cryo slicing for further immunohistochemistry staining. For whole spinal cord slicing, Narcoren injected mice were perfused with PBS first and then with 4% formalin on ice. Spinal cord was extracted and post-fixed in 4% formalin for additional 2 h and afterwards incubated in 30% sucrose at 4°C at least O/N. Fixed spinal cord with placed in cryo-cutting medium and then placed anterior side down on a cryostat holder and slicing was performed at a Leica-Cm1950 cryostat. Spinal cord or spinal cord slices were cut at -15°C into 20 µm and secured on superfrost coated glass slides. For storage the slides were kept in a cryo box at -20°C.

2.2.6 Fresh tissue harvest

To determine the amount of certain gene or protein expression *in vivo*, fresh spinal cord tissue was taken of narcotised beheaded mice. The tissue was rinsed in cold 1x PBS, shock frozen with dry ice pieces and the dorsal horn from the area L3-L5 was separated from the rest of the spinal cord. Tissue was then incubated and homogenised in RIPA buffer (5 M NaCL, 1 % Triton X-100, 0.5 % sodium deoxycholate, 0.1 % SDS, 50 mM Tris 1 M pH 8.0, ddH_2O) with protein inhibitor. For protein concentration measurement, BCA Kit was used after centrifugation of the

probes. Probes were then used for gene expression (PCR & qPCR) or protein expression (SDS Page), see methods above.

2.2.7 Immunohistochemistry and immunocytochemistry

To stain the spinal cord cryo slices they were dried at 50°C for 20 mins. With a pap-pen a circle was drawn around the slices and they were incubated for 1 h 30 mins with GDB 2x + 10 % normal goat serum (NGS) or normal donkey serum (NDS), depending on the host of the secondary antibody. The blocking solution was removed and the slices were washed three times for 10 min with 1% Triton X-100 in 1 x PBS. Then slices were incubated with the first antibody at RT O/N in a moist chamber to prevent the slices to dry out O/N. Next day the first antibody was removed and slices were washed again as mentioned before. Then the slices were incubated for 1 h 30 min at RT with the secondary antibody in GDB 2x + 10% serum medium. After incubation the slices were washed like described above and then optionally treated with 0.01% Sudan Black B in 70% ethanol for 15 min to reduce background binding from antibodies and then washed again as indicated. Finally the slices were mounted by addition of a mix of Hoechst in Mowiol (1:5000) and covering with a glass coverslip.

Table 19: List of antibodies.

1. Antibody	Host species	Company	Dilution
GFAP (clone G5)	mouse IgG1	Cell Signaling Technologie, 3670	1:300
GFP	rabbit polyclonal	Molecular Probes, A-6455	1:300 - 1:500
NeuN	mouse clone A60	Millipore, Merck, MAB377	1:1000
Npas4	rabbit monoclonal	ActivitySignaling.com	1:5000
Alpha Tubulin	mouse monoclonal	Sigma, 9026	1:400000
Isolectin B4	Biotin-conjugate	Sigma, L2140	1:250
HA.11	mouse 16B12 IgG1	BioLegend, MMS-101R	1:5000
2. Antibodies			Concentration
Alexa 594	goat anti mouse	Invitrogen, A11005	1:500 - 1:1000
Alexa 488	goat anti rabbit	Invitrogen, A11008	1:500 - 1:1000
Alexa 594	donkey anti rabbit	Dianova, 711-585-152	1:500
Mouse	goat IgG, HRP	DIanova 115-035-003	1:5000
Rabbit	goat IgG, HRP	Dianova, 115-035-144	1:5000

Pictures from the fixed and stained slices were made with a wide field microscope (Leica DM IRBE, camera: Monochrome w/o IP, Diagnostic instruments, inc., USA, software: Visiview, Visitron Systems, Puchheim, Germany).

2.3 Animal pain model – protocols and behavioural tests

2.3.1 Complete Freund's Adjuvant (CFA)

For chronic inflammatory pain we used CFA (Sigma F5881-10ml, St. Louis, MO, USA) which is a heat killed *Mycobacterium tuberculosis* (strain H37Ra, ATCC 25177) which attracts macrophages and thus causes inflammatory chronic pain. Mice were anaesthetized with Isofulrane in CO_2 (5% at the start and during injection at 2%, EZ-Anesthesia EZ 702). 20 µl of CFA was injected under the skin, parallel to the surface, on the ventral side of the left hind paw of the animal, directly behind the walking pads. The injection needle had to be inside the paw for 1 min to let the CFA distribute inside the tissue. After rejecting the needle, the mouse was released from the Isoflurane and woke up after 30s – 1min and was then placed back into its home-cage. Animals for Ca^{2+} imaging were tested 24 h after injection. Mice which were included into pain behaviour von Frey and Hargreaves testing (see below) were tested 6 h, 24 h, 72 h, 5 d, 7 d and 10 d after injection.

2.3.2 Spared Nerve Injury (SNI)

One common used neuropathic chronic pain model is SNI surgery (Decosterd and Woolf 2000). Mice were anesthetized with an IP injection of sleep mix (10µl/g, see table 17). As soon as mice were asleep, the skin and the muscle from the left hind limb was opened to get access to the peroneal, tibial and sural nerve. The common peroneal nerve, the tibial nerve and the sural nerve were carefully freed from muscle. Then common peroneal and tibial nerve were ligated by a sural branch, whereas the sural nerve must stay intact and unharmed. About 1 mm of the ligated nerve was cut away after ligation to ensure that the endings of the separated nerves would not recover by ligating to their cut-off ends. Muscles were carefully placed back into position to cover the nerves. This surgery triggers neuropathic hypersensitivity. After the cut was closed, wake mix was injected subcutaneously and lidocaine spray was

applied to decrease post-surgical stress for the animals. The mouse was put back into its cage with wet food pellets and the cage was placed onto a heating plate o/n for the mouse to recover. After 7days the mouse was sacrificed for the final experiment.

2.3.3 Pain behaviour

Observers were blinded to the identity of the animal groups in all behavioural tests.

2.3.3.1 Catwalk

Mice were analysed for their locomotor and walk behaviour before spinal cord injection, before and after chronic pain induction, by testing in a catwalk (CatWalkXT, Noldus). Mice were habituated to the catwalk in the dark for 10-15 min 24h before testing. While testing, three runs were taken where the mice were continuously running and not stopping during recording to generate an average of walk behaviour. Animals were not habituated again to the catwalk when tested in it at later time point. Mice that showed impaired walking behaviour after spinal cord injections, for example limping, were excluded from further experiments.

2.3.3.2 Mechanical sensitivity (von Frey test)

Animals were acclimatized to the experiment room and the test boxes 3-4 days prior to experiments and baseline measurements were taken 2 days before pain protocol application. Mice were then placed on an elevated wire grid and mechanical sensitivity determined upon paw withdrawal to either application of graded force via a dynamic aethesiometer (Ugo Basile Inc.) or to manual application of graded von Frey hairs (0.07 – 4 g) to the plantar surface. Response frequency was calculated as the mean number of withdrawals out of five applications of the respective filament in 2-4 min intervals. Withdrawal threshold was determined as the filament at which the animal withdraws its paw at least two times out of five applications (40% threshold) or three times out of five applications (60% threshold).

2.3.3.3 Thermal sensitivity (Hargreaves test)

All experiments for von Frey and Hargreaves tests were obtained in the Interdisciplinary Neurobehavioral Core (INBC), Heidelberg, Germany.

Paw withdrawal latency to a ramp of infrared heat was measured using a plantar test apparatus (Ugo Basile Inc.). Animals were acclimatized to the experiment room and experiment boxes for 3-4 days and baseline measurement was taken 2 days before pain protocol application. Light was pointed to the left hind paw five times in 2-5 min intervals. Measurements were only valid when the mice were not busy with grooming or exploring their environment. Time was measured from the starting of the light application until withdraw of the hind paw. Withdrawal threshold was determined as mean of the withdrawal times in one session.

2.3.3.4 Cold plate

Animals were tested for cold hypersensitivity before spinal cord injection, after spinal cord injection and after pain protocol induction. Testing was always done directly after von Frey testing. The cold plate (Ugo Basile Inc.) was cooled down to 4°C and mice were tested one by one by placing on the plate and time was recorded until the first reaction, like paw lifting, licking or shaking.

After experiments, the animals were placed back into their home cages.

2.4 Data Analysis

Graphs for this thesis were made with Prism (GraphPad Software, La Jolla, USA, version 6.0). Images were processed with Adobe Photoshop (Adobe Systems Inc., San Jose, USA, version 2015) or ImageJ. All graphs were finalised with Power Point (Microsoft Corporation, Redmond, WA, USA) or Adobe Illustrator (Adobe Systems Inc., San Jose, USA, version 2015). All references were managed through Endnote (Clarivate Analytics, Phildadelphia, USA, version X8). Statistical analysis for graphs was done as well with Prism. All figures presented in the result section include the used statistical tests in their legends. For most of the tests one-way ANOVA for multiple comparison was used. In general, the following definition for significance was made: not significant (n.s.): $p > 0.05$; *: $p < 0.05$; **: $p < 0.005$; ***: $p < 0.001$.

3. Results

3.1 Ca^{2+} indicator-injection into the mouse spinal cord dorsal horn

In previous studies it was shown that Ca^{2+} signalling in spinal dorsal horn excitatory neurons plays a role in the development and maintenance of chronic pain conditions

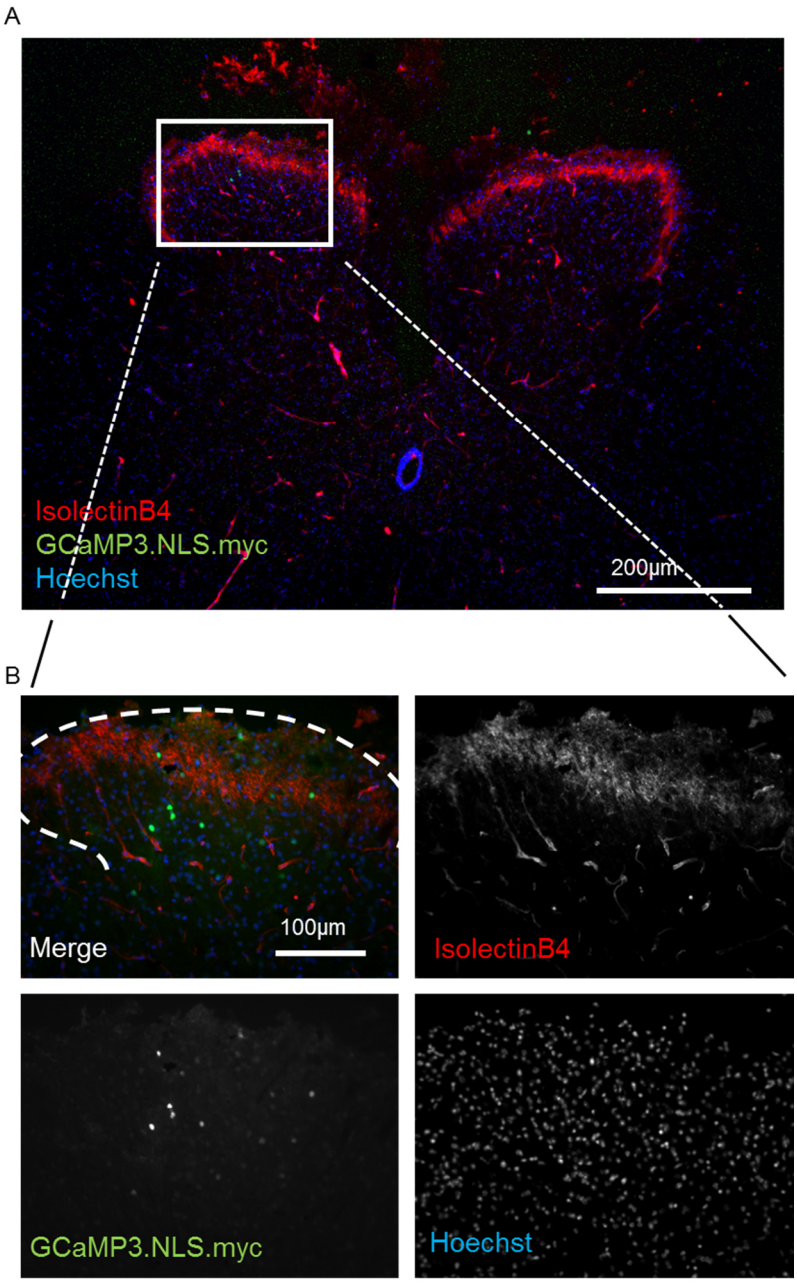

Figure 6: Verification of spinal cord dorsal horn injections. GFAP:GCaMP3NLS.myc Ca^{2+} indicator expression in spinal cord dorsal horn laminae I-III. **(A)** and **(B)** showing immunohistochemistry staining of fixed slices expressing Ca^{2+} indicator (GFP in green) and Isolectin B4 expression (red) on fibres membrane. Scale bar = (A) 200 µm and (B) 100 µm.

(Simonetti et al. 2013) as it is necessary for signal transmission from in the responsible circuits. In addition nuclear Ca^{2+} signalling induces gene transcription which is necessary to lead to structural and functional changes of the neuron. However, many questions remain unsolved and our knowledge about the involvement of Ca^{2+} signals and its possible changes in chronic pain conditions or its role in the actual development of chronic pain are limited.

In order to investigate the role of Ca^{2+} signalling in different cell compartments of different cell types in the spinal dorsal horn, Ca^{2+} indicators were injected for analysis of acute slices under dorsal root stimulation.

To first verify the injection method and quality, wild-type mice were injected with a Ca^{2+} indicator which is located in the nucleus of astrocytes (GFAP:GCaMP3NLS.myc). Further results on this Ca^{2+} indicator will be presented in section 3.1.1.3 Nuclear Ca^{2+} signalling in GFAP-positive cells. After 2-3 weeks of incubation time for expression of the indicator, the mice were sacrificed and perfused with 4 % PFA. Following the extraction of the spinal cord, the tissue was post fixed for another 1 h in 4 % PFA and cryo-preserved in 30 % sucrose. Then the spinal cord was cut at the cryostat into 20 µm thick slices and probed with a GFP antibody and for visualisation with Alexa 488 in order to amplify the GFP signal from the Ca^{2+} indicator and Isolectin B4-594 for marking the superficial lamina of the dorsal horn. Isolectin B4 is one common way to label unmyelinated and small diameter (thus C-fibers) sensory neurons as these afferent neurons from the periphery express on their membrane carbohydrates where the plant lectin isolectin B4 from *Griffonia simplicifolia* can bind to. The fluorescent pictures (Fig. 6) show that the GFP expressing indicators were close to the Isolectin B4 expressing cells in laminae I-III. Laminae I-III was the target area to investigate fibre induced Ca^{2+} signalling in the dorsal horn as a first contact side from the periphery to the CNS. GFP expression from inside the nucleus was visible in close proximity of Isolectin B4 positive signals. Further experiments were planned due to the confirmation of this experiment.

3.1.1 Ca^{2+} signalling behaviour in spinal cord dorsal horn astrocytes under chronic pain conditions

It was shown that astrocytes react with astrogliosis under chronic pain conditions but still many aspects of astrocytes and especially their Ca^{2+} signalling in the spinal dorsal horn under chronic pain conditions remain unresolved and are poorly understood. Particularly the role of different astrocytic cell compartments and their role in Ca^{2+} signalling. Thus, the investigation and characterisation of dorsal root evoked Ca^{2+} signals in astrocytes also under chronic inflammatory pain and neuropathic pain were the first aim of this project.

3.1.1.1 Cytoplasmic Ca^{2+} signalling in GFAP-positive cells

It has already been shown that astrocytes can react with Ca^{2+} signals to stimuli like neurotransmitters from synaptic clefts. Right now, little is known about the role of Ca^{2+} signals in astrocytes in the dorsal horn under chronic pain conditions. Here, we used a Ca^{2+} indicator which expresses GFP when bound to Ca^{2+}/calmodulin. This indicator is not able to enter the nucleus, as it is too big to cross the nuclear membrane through nuclear pore complexes. Hence, the indicator is located in the cytosol and mainly visible in the soma of the astrocytes due to the surface-to-volume ratio which is higher for the volume in the soma compared to the higher amount of surface of fine processes. In Fig. 7 A the used rAAV introduced construct for Ca^{2+} imaging is presented. The construct contained the Ca^{2+}/calmodulin detector GCaMP5 after a GFAP, an astrocytic specific, promoter. Acute slices were made from wild-type mice, 2 – 3 weeks after the rAAV construct was injected into the spinal cord dorsal horn. A representative expression of the used construct is shown in Fig. 7 B. This picture arrived from an acute slice, which was fixed and stained after the Ca^{2+} imaging experiment. It shows that the amplified GFP expression (green) from the Ca^{2+} indicator overlaid with GFAP positive (red) stained astrocytic constructs (white arrow heads).

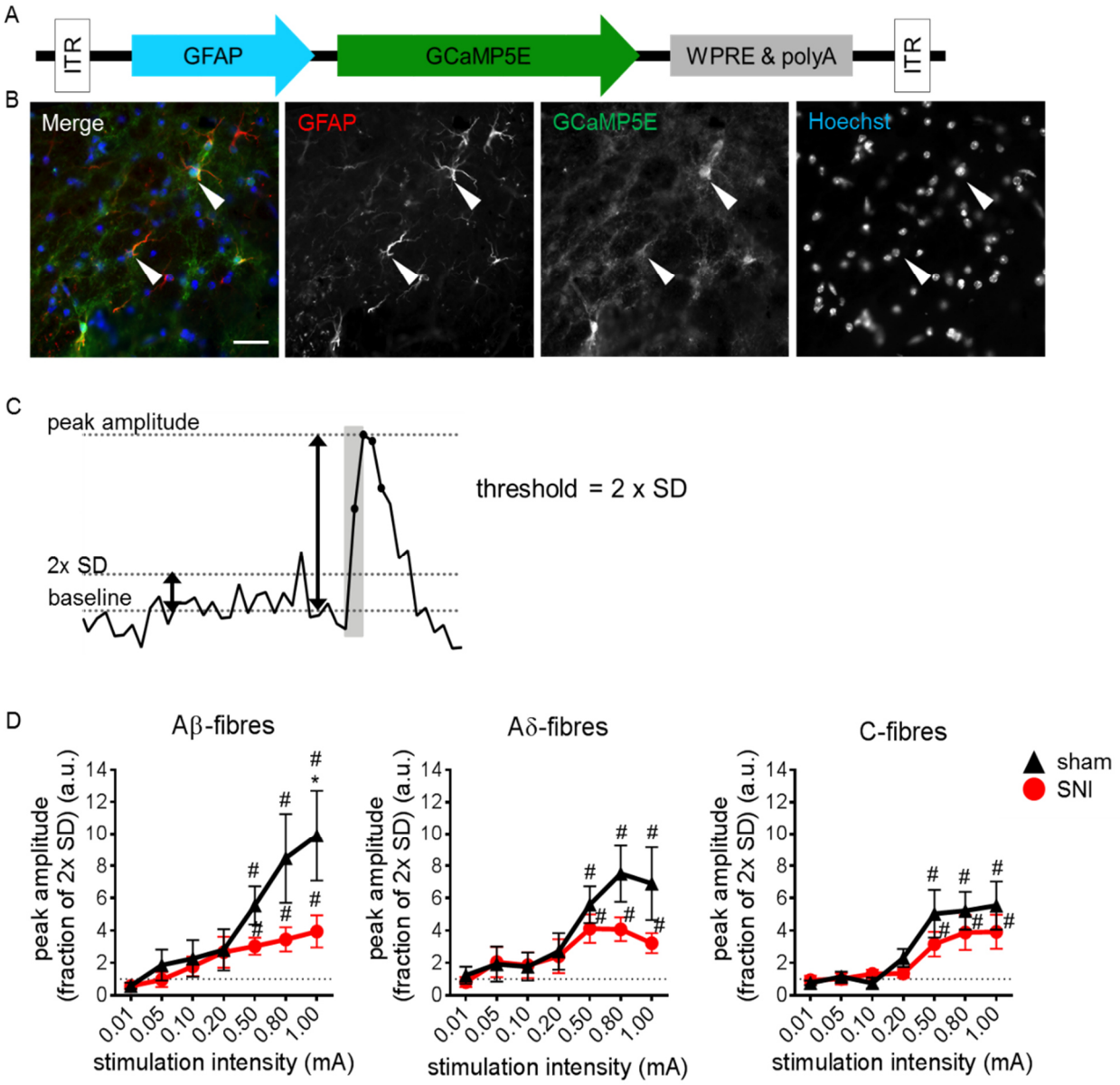

Figure 7: Ca^{2+} signalling changes in cytoplasm of spinal cord dorsal horn astrocytes under neuropathic pain conditions. (A) Injected construct to express cytoplasmic localised Ca^{2+} indicator under GFAP promoter. **(B)** Immunohistochemistry staining of fixed slices expressing indicator (GFP in green) and stained against GFAP (red). Picture shows overlay expression of GFAP positive and indicator expressing cells, indicated through white arrow heads. **(C)** Representative stimulation response. Response was defined as peak amplitude when higher than 2 x SD of baseline before stimulation. **(D)** Peak amplitude as the fraction of 2x SD of 100 Hz for Aβ-, 20 Hz for Aδ- and 4 Hz for C-fibre stimulation under SNI conditions (red) and sham/control conditions (black). n = 6 slices for SNI, n = 6 slices for control (from 4 mice per group) mean ± SEM; two-way ANOVA Bonferonni's multiple comparison post-hoc test for differences between the two tested condition groups, ns > 0.05, * < 0.05 and # = one-sample t-test for suprathreshold significance for a hypothetical value of 1. Scale bar = 50 µm.

In order to further investigate the Ca^{2+} signals characteristics, induced by electrical dorsal root stimulation, the change of GFP fluorescence (Appendix Figure 1) was detected from spinal cord acute slices. To shortly describe the process: the indicator construct was injected into the spinal dorsal horn and after 2 – 3 weeks incubation time, neuropathic pain through SNI or a sham surgery as control, was induced to the mice. According to the literature, 7 days after SNI neuropathic pain is established and reached a plateau, which would last for several weeks. At day 7 after SNI or sham surgery, acute slices were made and the dorsal root was stimulated like explained in the Material and Method section: 20 Hz square pulsed stimulation for 1 s to induce stimulation of preferably Aδ-fibres (Sandkuhler et al. 1997), 100 Hz square pulsed stimulation for 1 s to evoke signals through Aβ-fibres (Daniele and MacDermott 2009) and 4 Hz square pulses or sinusoidal pulses to mainly evoke responses through C-fibres (Jonas et al. 2018). Fig. 7 C represents an example response and how the measured signals were calculated in order to determine if a signal was defined as a peak amplitude and if it was a response over the defined threshold of a hypothetical value of 1 and therefore defined then as suprathreshold. The baseline was measured ~10 s before each stimulation and an amplitude was defined as peak amplitude when it was bigger than 2x the standard deviation (SD) of the before measured baseline. The suprathreshold was calculated when two data points before and after the peak were as well bigger than the 2x SD and significantly higher than a hypothetical value of 1.

The stimulation of the dorsal root of acute slices under neuropathic pain as well as under control conditions showed that astrocytes responded to all the stimulated fibre classes. With an increased stimulation intensity, the peak amplitude responses also increased. Fig. 7 D shows that under Aβ-fibre stimulation, responsible for innocuous touch sensation, both groups, the neuropathic pain SNI group (red) and the sham group (black) had a significant suprathreshold for 0.5, 0.8 and 1 mA stimulation intensity. Furthermore, the SNI group showed a trend of decrease in its peak amplitude and thus the Ca^{2+} signalling intensity, compared to the control group, from 0.5 mA stimulation intensity on. The neuropathic pain group is for Aβ-fibre stimulation even significantly decreased at 1 mA stimulation intensity compared to the sham group.

Aδ-fibre stimulation resulted in a similar dynamic of Ca^{2+} signalling in the cytoplasm of spinal dorsal horn astrocytes. Both groups, the neuropathic pain and the control group

were increased for their peak amplitude and had a significant suprathreshold for 0.5, 0.8 and 1 mA stimulation intensity. In addition, the SNI group showed a trend towards a decrease in its peak amplitude during increased stimulation intensities compared to the sham group.

The last stimulation type, the C-fibre stimulation of 4 Hz, showed as well an increased peak amplitude of the Ca^{2+} signals in the cytoplasm of astrocytes over increasing stimulation intensity, with a significant suprathreshold for 0.5, 0.8 and 1 mA for both groups, the neuropathic pain treated and the sham treated group. There was no detectable difference though between the two groups, thus no observed difference between neuropathic pain and sham group when stimulated for C-fibre preferred signal transmission into the spinal dorsal horn.

3.1.1.2 Membrane Ca^{2+} signalling in GFAP-positive cells

It has been shown, that many Ca^{2+} signals are happen to be localised at the fine processes and endfeet of astrocytes induced by glutamate release from neurons and binding to astrocytic receptors (Haydon and Carmignoto 2006; Anderson and Nedergaard 2003). This indicates an interesting and possible from soma Ca^{2+} signalling independent role of Ca^{2+} signalling in astrocytes. To investigate this in further detail, the Ca^{2+} indicator was cloned in combination with a lymphocyte-specific protein tyrosine kinase (Lck), which is a membrane bound kinase, so that the indicator would be close to the membrane in order to investigate evoked signals at astrocytic processes. This membrane bound indicator was expressed under the GFAP promoter for astrocytic specific expression (Fig. 8 A). Such an indicator would show in a better surface-to-volume ratio the membrane of the astrocytes and thus their processes as well as the soma. In comparison, the cytoplasmic localised indicator is mainly present in the soma of astrocytes, due to the already mentioned surface-to-volume ratio. Immunohistochemistry pictures showed that the expressed indicator (green) overlapped with GFAP positive stained (red) constructions, meaning a successful expression of the indicator in astrocytes (arrow heads Fig. 8 B). Dorsal root stimulation with 20 Hz (preferably resulting in evoked signals transmitted from Aδ-fibres) for

duration of 1 s resulted in Ca^{2+} signals. The response amplitude was higher for increased stimulation amplitude. Surprisingly even when the responses seemed to be strong for the stimulation, there was no significant suprathreshold detectable (Fig. 8 C and D). Only stimulation 0.8 and 2 mA were close to significance as the other

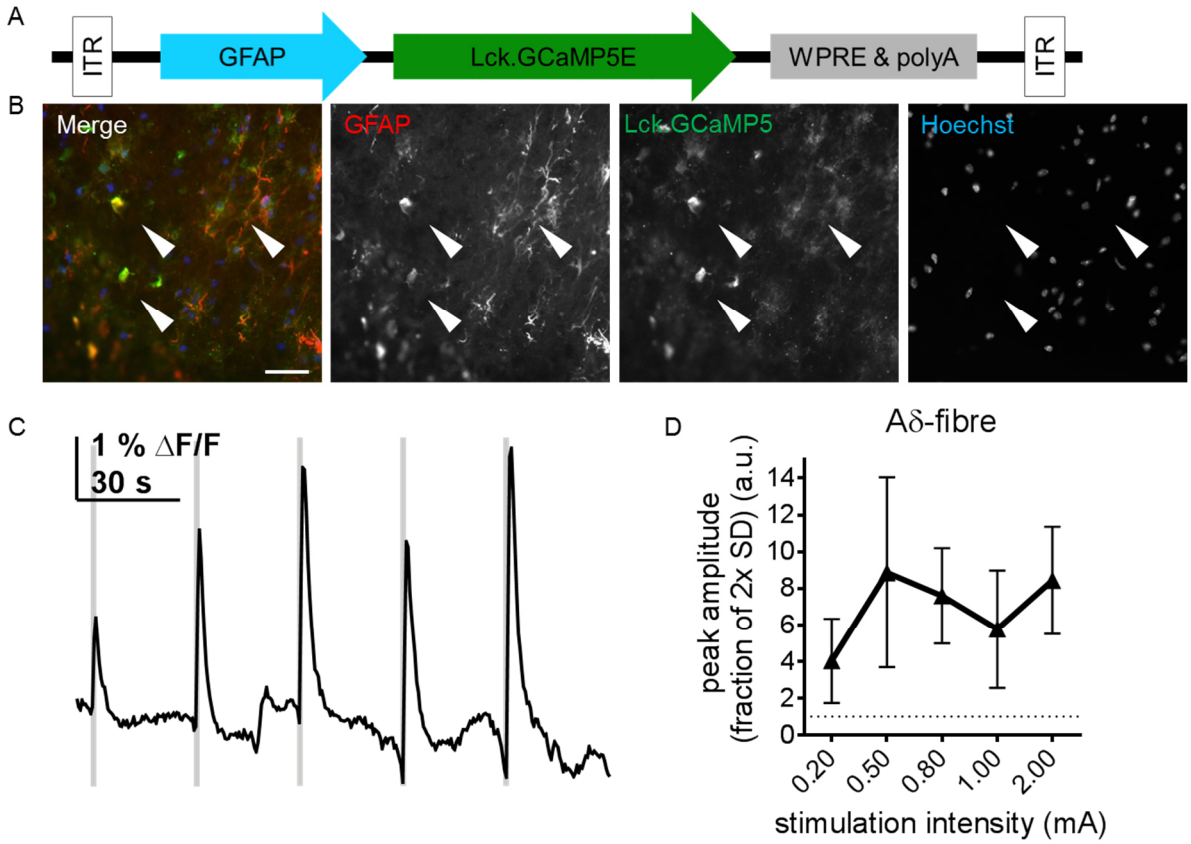

Figure 8: Evoked Ca^{2+} responses at the membrane of spinal cord dorsal horn astrocytes. (A) Injected construct to express Ca^{2+} indicator under GFAP promoter, bound to the membrane. **(B)** Immunohistochemistry staining of fixed slices expressing indicator (GFP in green) and stained against GFAP (red). Picture shows overlay expression of GFAP positive and indicator expressing cells. **(C)** Representative stimulation response here for 20 Hz 1 s stimulation with stimulation intensities from 0.2 – 2 mA. **(D)** Response for stimulation train of 20 Hz square pulses for 1 s for Aδ-fibre stimulation represented as peak amplitude as fraction of 2x SD. n = 5 slices (3 mice) mean ± SEM; # = one-sample t-test for suprathreshold significance for a hypothetical value of 1. Scale bar = 50 µm.

measured values had to high error bars. Fig. 8 C shows a representative stimulation response of Ca^{2+} signals under 20 Hz stimulation in astrocytes. The behaviour of this stimulation evoked responses occurred quite immediately and showed similar peak amplitudes compared to the cytoplasmic localised indicator.

Even when the investigation of Ca^{2+} signals in fine processes and endfeet of astrocytes would have been very interesting, we figured out that our set-up was not suitable for further experiments in this context, as we were not able to focus on single endfeet. A confocal microscope with high resolution would have been more suitable. For that reason, further planned experiments with this construct were not pursued as there would be any kind of specific outcome or added value which could not be investigated with the cytoplasmic localised indicator.

As not all Ca^{2+} signals, evoked in the processes of astrocytes, would result in Ca^{2+} rises in the cytoplasm (Volterra, Liaudet, and Savtchouk 2014), the cytoplasmic indicator represented a stronger way to investigate Ca^{2+} relevant signals for potential gene transcription activation. Nevertheless, here it was shown for the first time that dorsal root stimulation of acute slices at a frequency of 20 Hz would result in membrane bound Ca^{2+} indicator activation in astrocytes of the spinal dorsal horn.

Concerning the Ca^{2+} signals that only occur in processes but would not reach the soma, nothing is known about their purpose or function. This topic will be further discussed in later sections.

3.1.1.3 Nuclear Ca^{2+} signalling in GFAP-positive cells

Until now there are, to our knowledge, no publications about evoked nuclear Ca^{2+} signals in astrocytes, especially in the dorsal horn of the spinal cord. Only a few groups investigated nuclear Ca^{2+} signals in for example embryonic cortical astrocytes (Zhao and Brinton 2003). They showed that for example the G-protein coupled receptor type vasopressin receptor (GPCR) causes Ca^{2+} signalling in astrocytes which induces a pathway that includes PKC, CaMKII and ERK1/2 for CREB activation. This leads to the suggestion of nuclear calcium driven gene regulation as it was demonstrated in neurons (Bading 2013).

A first indication for potential stimulation driven gene regulation through Ca^{2+} signalling was presented in the previous section where it was shown that dorsal root stimulation of all tested preferred fibres would evoke cytoplasmic Ca^{2+} signals. As Ca^{2+}/calmodulin is free to traffic through the nuclear envelope, it is possible that dorsal root evoked Ca^{2+} signals in astrocytes would also cause nuclear Ca^{2+} signalling and induce activity dependent gene transcription, similar to neurons.

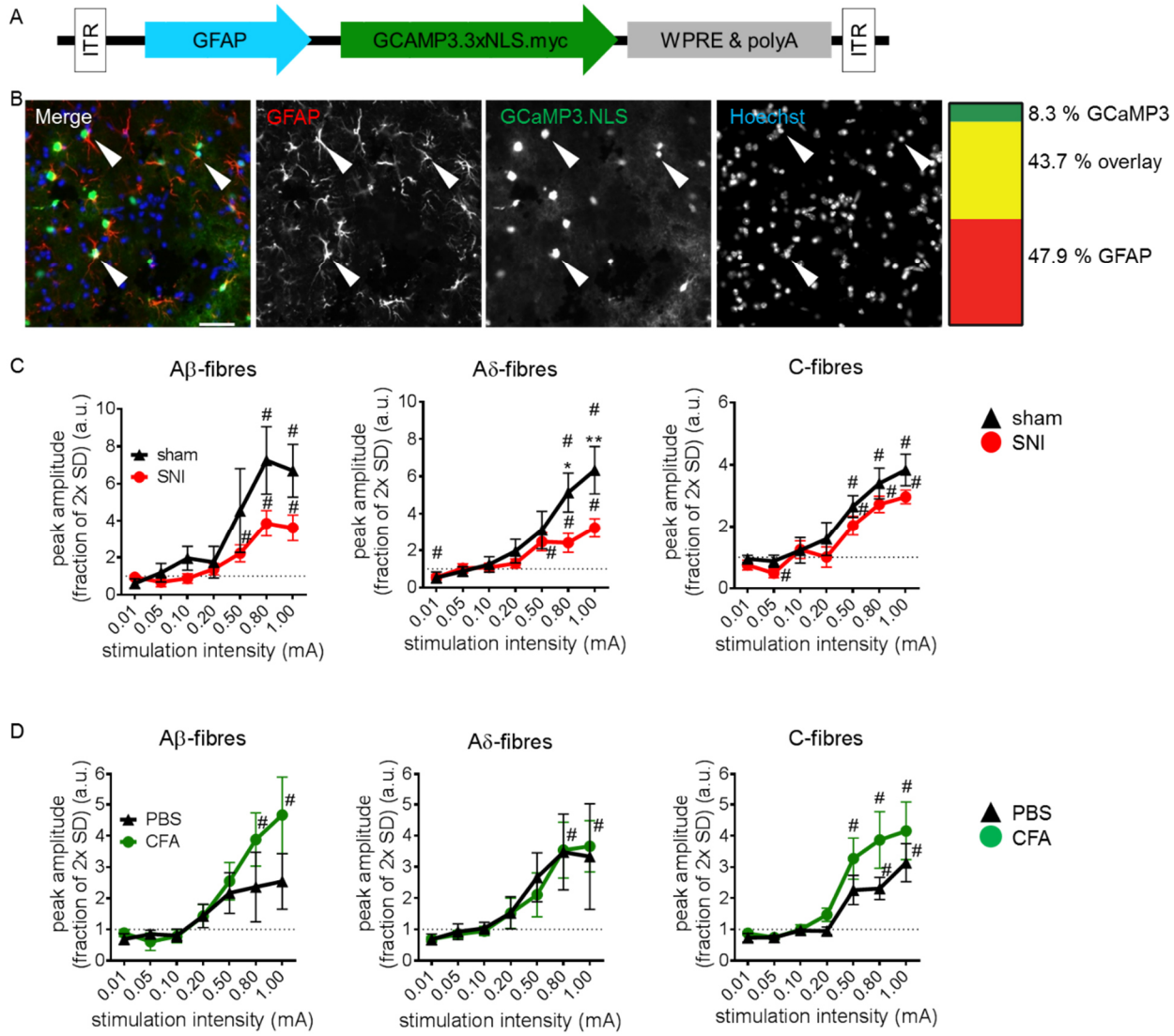

Figure 9: Ca^{2+} signalling changes in the nucleus of spinal cord dorsal horn astrocytes under chronic pain conditions. (A) Injected construct to express nuclear localised Ca^{2+} indicator under GFAP promoter. **(B)** Immunohistochemistry staining of fixed slices expressing indicator (GFP in green) and stained against GFAP (red). Picture shows overlay expression of GFAP positive and indicator expressing cells. Amount of cells expressing GFP (green) or GFAP (red) only are represented in the colour bar on the right. Overlay of GFP expressing and GFAP staining is shown in yellow. **(C)** Stimulation response showed as peak amplitude as fraction of 2xSD for 100 Hz Aβ-, 20 Hz Aδ- and 4 Hz C-fibre stimulation under neuropathic pain conditions induced through SNI surgery (red) and control conditions (black). n = 6 slices (3 mice) for SNI, n = 5 slices (3 mice) for control. **(D)** Stimulation response showed as peak amplitude as fraction of 2x SD for 100 Hz Aβ-, 20 Hz Aδ- and 4 Hz C-fibre stimulation under chronic inflammatory pain conditions induced by CFA injection into the hind-paw (green) and its PBS control (black). n = 5 (4 mice) for CFA, n = 5 (5mice) for PBS mean ± SEM; two-way ANOVA Bonferonni's multiple comparison post-hoc test for differences between the two tested condition groups, ns > 0.05, * < 0.05, ** < 0.005 and # = one-sample t-test for suprathreshold significance for a hypothetical value of 1. Scale bar = 50 µm.

To investigate this issue, the nuclear localised Ca^{2+} indicator GCaMP3.NLS (Bengtson et al. 2010) was cloned into a rAAV construct under the promoter control of GFAP, to be expressed in astrocytes only (Fig. 9 A). The nuclear localisation signal NLS ensures that the Ca^{2+} indicator stayed inside the astrocytic nucleus.

The immunohistochemistry of spinal cord tissue, injected with this construct, showed overlay of cells, expressing the nuclear localised Ca^{2+} indicator in nuclei with cells positive for GFAP staining (Fig. 9 B). The infection rate was detected in about 44 % of all identified astrocytes in these staining (Fig. B). This ratio was also representative and estimated for all other indicators, as it was only possible to make such a specific quantification with the nuclear localised indicator due to the fact of certain localisation when stained anti GFAP structures. Still about ~ 8 % were GFP expressing cells but with no GFAP positive structure surrounding. This problem of undefined GFP expression will be addressed in the next section.

The stimulation of the dorsal root showed surprising new results. First of all, for all the tested fibre stimulations, astrocytes responded with nuclear Ca^{2+} signalling. Under neuropathic pain conditions (Fig. 9 C, red), Aβ-fibres had a significant suprathreshold at 0.5 mA stimulation intensity and increased with higher intensities. Compared to the sham group (black), there was already a trend towards decreased Ca^{2+} signalling intensities of the response amplitude. The suprathreshold of the sham group was significant for 0.8 mA though. Aδ-fibres, thus the first tested nociceptive fibre, showed a suprathreshold for 0.5 mA and increasing stimulation intensities under neuropathic pain and was significantly decreased compared to the sham group, which showed a higher peak amplitude for 0.8 and 1 mA stimulations. The defined suprathreshold for those fibres in the control group started, just like the Aβ-fibres with 0.8 mA stimulation.

For unmyelinated C-fibre stimulation the Ca^{2+} peak amplitude was for both groups, the neuropathic pain and the sham operated group, the same. There was no significant difference nor a trend detectable. Both groups had a significant suprathreshold at 0.5, 0.8 and 1 mA stimulation intensities.

The investigation of chronic inflammatory pain (Fig. 9 D) showed for all stimulations responses but no significant changes between the peak amplitude of the CFA injected group (green) and the PBS injected control group (black). Because of the huge error bars from the PBS injected group, there was no significant suprathreshold detected

for Aβ- and Aδ-fibres, though there is a trend to increased peak amplitude when the stimulation intensity is increased. For the PBS group under C-fibre stimulation the significant suprathreshold is shown at 0.8 and 1 mA. The CFA group on the other hand showed significant suprathreshold for Aβ- and Aδ-fibres for 0.8 and 1 mA stimulation intensity and for C-fibre stimulation even at 0.5 mA.

3.1.1.4 Expression of Ca^{2+} indicator in neurons under GFAP control and evoked Ca^{2+} signals in *Aldh1l1* mice

In the previous section, we showed that we detected GFP expression which were not surrounded by positive GFAP stained structures. The question came up what kind of cells expressed the indicator under GFAP promoter and did this influence in some way the previous recorded Ca^{2+} signals from astrocytes.

To approach this question, GFAP:GCaMP3.NLS expressing slices were staining with the neuron specific antibody NeuN. That resulted in some overlay of GFP positive cells with NeuN positive cells of about ~ 3 % of total cell amount (Fig. 10). Even when those cells had a weaker expression (yellow arrow heads) compared to GFP signals from non-NeuN positive cells (white arrow heads), the problem had to be approached as it was possible that the so far recorded signals from the previous experiments were all contaminated in their measured Ca^{2+} signals with stimulated neurons that expressed the Ca^{2+} indicator as well.

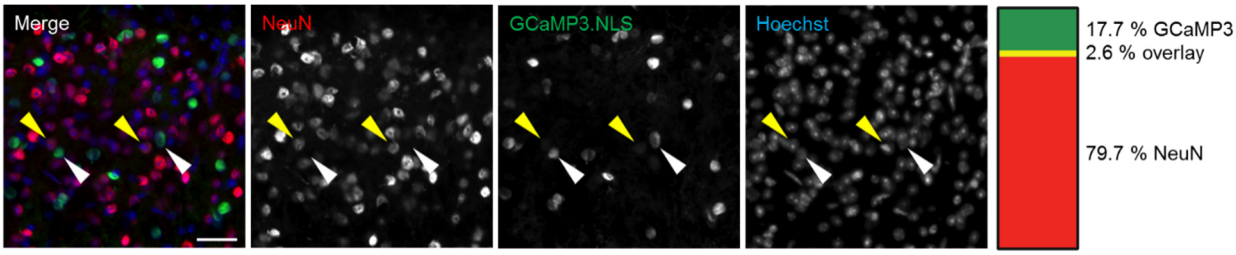

Figure 10: Astrocytic Ca^{2+} indicator expression in neurons. GFAP:GCaMP3.NLS GFP signal (green) in NeuN positive cells (red). Right bar represents the amount of all detected cells, in green showing only GFP positive cells, yellow an overlay of green and red expressing or stained cells and red all NeuN positive cells. Yellow arrow heads represent weak expressing GFP cells that overlay with NeuN cells, white arrow heads show example of strong GFP only expressing cells. Scale bar = 50 µm

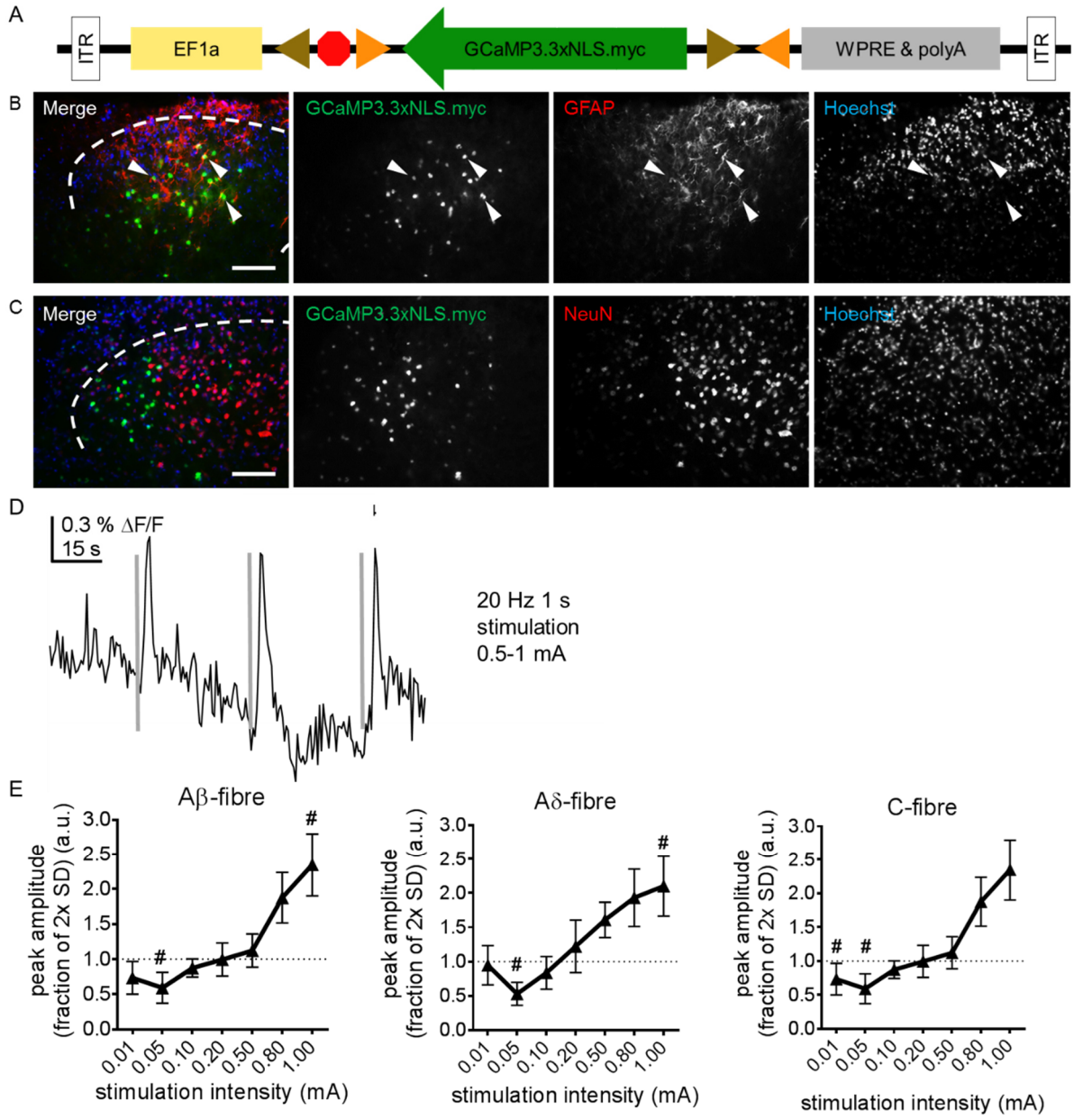

Figure 11: Ca^{2+} signalling changes in the nucleus of spinal cord dorsal horn astrocytes in *Aldh1l1* mice. (A) Injected construct to express nuclear localised Ca^{2+} indicator. **(B)** Immunohistochemistry staining of fixed slices expressing indicator (GFP in green) and stained against GFAP for astrocytes (red). Picture shows overlay expression of GFAP positive and indicator expressing cells (white arrow heads). **(C)** Immunohistochemistry staining of fixed slices expressing indicator (GFP in green) and stained against NeuN to label neurons (red). No overlay was detected. **(D)** Representative response behaviour for 20 Hz (1 s) stimulation with intensities from 0.5 – 1 mA. In grey bars represented the time point of stimulation. **(E)** Stimulation response showed as peak amplitude as fraction of 2x SD for 100 Hz Aβ-, 20 Hz Aδ- and 4 Hz C-fibre stimulation. n = 7 slices (3 mice). # = one-sample t-test for suprathreshold significance for a hypothetical value of 1. Scale bar = 50 µm

To investigate this problem and to verify the previous results, the astrocytic specific CRE-mouse line Aldh1l1 was now used to express EF1:GCaMP3.3xNLS.myc in a floxed tamoxifen injection dependent manner (Fig. 11 A). The procedure with these mice was the same as for mice from previous experiments. Only the mice were not induced with any pain protocols as we just wanted to verify the evoked Ca^{2+} signalling behaviour of different fibre stimulation, without focusing on the difference of pain versus non-pain conditions. The stimulation protocol was as just described in the previous sections. Stained slices and observation of the spinal dorsal horn from those injected mice showed an overlay with GFAP positive stained astrocytic cell structures, meaning that GFAP structures (red) surrounded the nuclear GFP (green) signal from the expressed indicator (white arrow heads Fig. 11 B). When stained with NeuN, the GFP signal showed no overlay at all with the NeuN signal (red) (Fig. 11 C). This means that no Ca^{2+} indicator was expressed in neurons in this mice-type.

The response traces from the stimulation were similar to traces from wild-type mice that were injected with rAAV induced Ca^{2+} indicators under the GFAP promoter (Fig. 11 D). Furthermore, responses were evoked by all the different fibres, resembling the evoked responses in mice with nuclear localised Ca^{2+} indicator under GFAP promoter control (Fig. 11 E). Thus, the previous experiments were reliable in respect to astrocytic evoked Ca^{2+} responses in the different cell compartments, even when a small amount of indicator was expressed in neurons.

3.1.1.5 Multiphasic evoked Ca^{2+} responses in dorsal horn cells

During the recordings of especially astrocytic Ca^{2+} signalling behaviour, we observed that sometimes the cells responded to one stimulation with not only one single peak amplitude, but with a second mostly smaller peak (Fig. A). This multiphasic evoked Ca^{2+} response was not detected in all analysed slices. Also not for all stimulation intensities, this second peak occurred. Mainly for stimulation intensities between 0.2 and 1 mA the second response peak would develop. Therefore, it was detected under all stimulated fibre classes (Fig. B). From the total amount, the most second peaks were detected at 0.8 mA stimulation intensity for all the tested fibre classes. The presented data did not distinguish between pain protocols or their appropriate controls. All detected second peaks were plotted in groups of the stimulated fibre class (Aβ-, Aδ- and C-fibre) from all used Ca^{2+} indicator type (GCaMP5 or GCaMP3.NLS) and the pain model (chronic inflammatory pain or neuropathic pain).

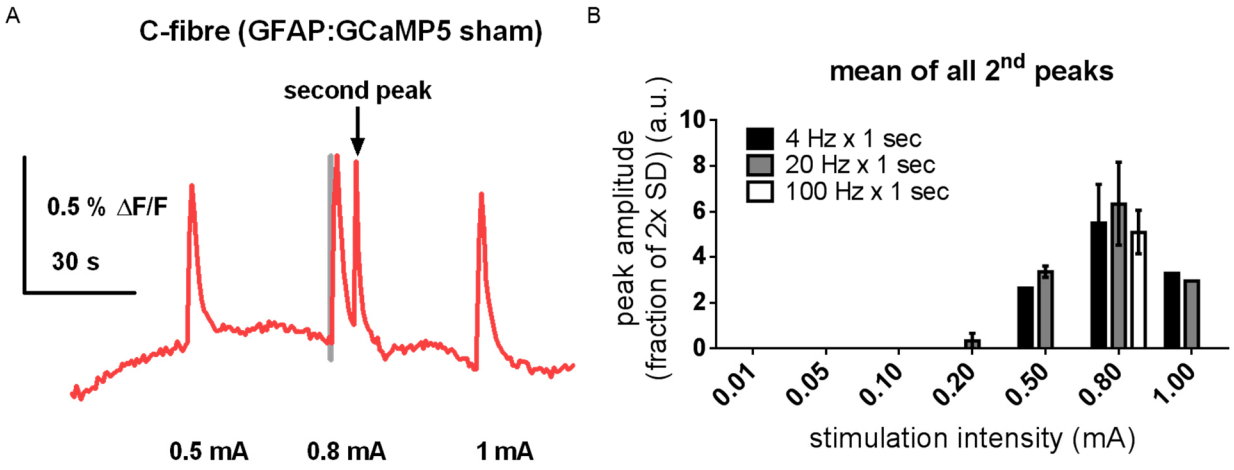

Figure 12: Multiphasic evoked Ca^{2+} responses. (A) Representative example of second peak after first evoked response through DR stimulation. Presented example for 4 Hz stimulation with intensities between 0.5 and 1 mA of an GFAP:GCaMP5 expressing acute slice after sham surgery. **(B)** Graph shows distribution of second peak occurrence as peak amplitude as fraction of 2x SD from all analysed slices with Ca^{2+} indicator expression in astrocytes. Groups divided into stimulated fibre classes: 4 Hz for C-fibre (black), 20 Hz for Aδ- (grey) and 100 Hz for Aβ-fibre (white). n = mean ± SEM.

3.1.1.6 Longer lasting Aδ-fibre stimulation

In order to mimic a more physiological stimulation, we introduced a stimulation of 20 Hz squared pulsed but instead of only stimulating for 1 s, the dorsal root was

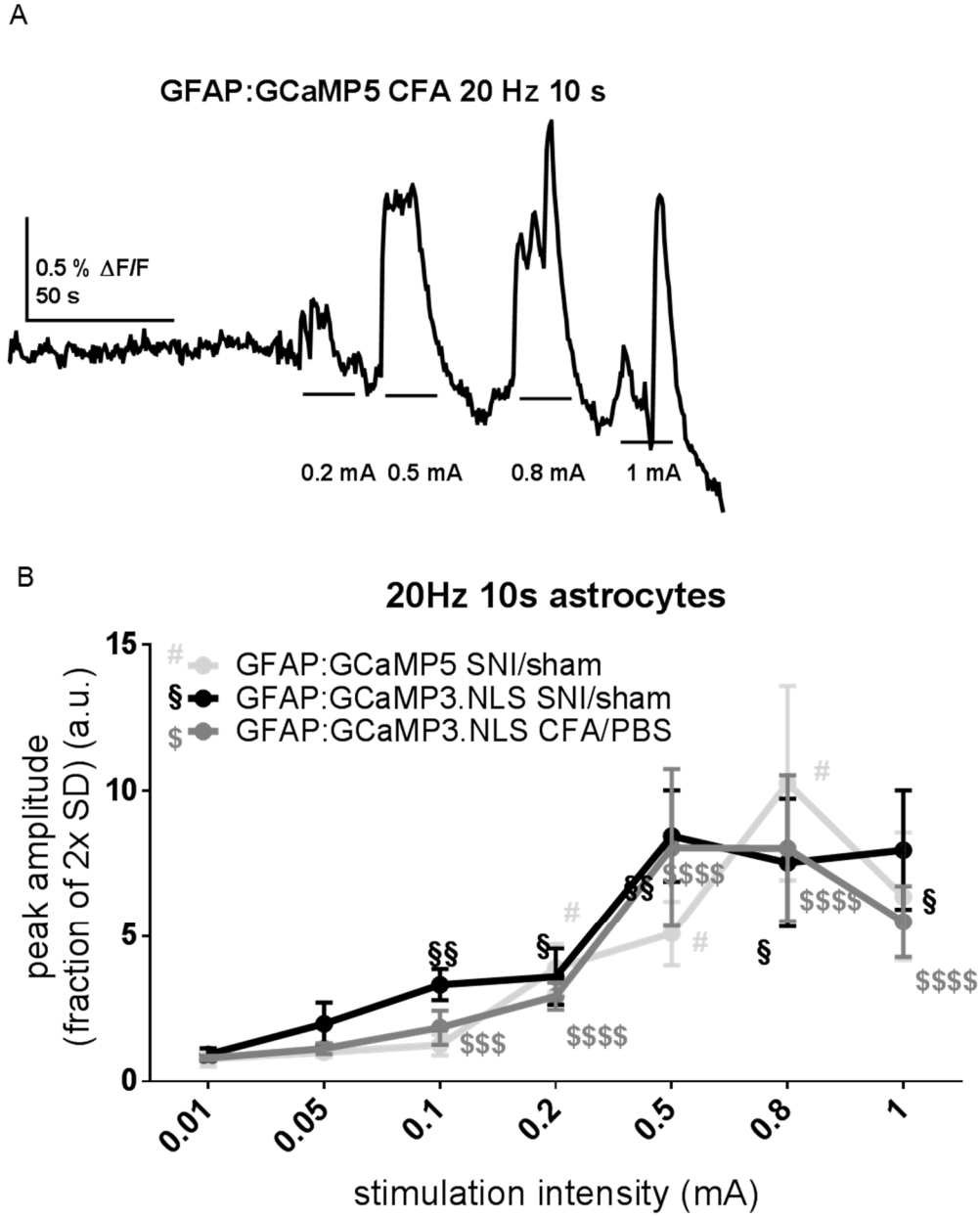

Figure 13: Long lasting Aδ-fibre stimulation. (A) Representative example of Ca^{2+} response on 20 Hz stimulation for 10 s for each intensity (black horizontal bar). Presented is a GFAP:GCaMP5 acute slice stimulation with visible response as % of ΔF/F for intensities from 0.2 – 1 mA. **(B)** Graph shows peak amplitude as fraction of 2x SD for the 20 Hz 10 s stimulation responses for the three groups: GFAP:GCaMP5 SNI/sham (light grey), GFAP:GCaMP3.NLS SNI/sham (black) and GFAP:GCaMP3.NLS CFA/PBS (grey). n = 6 for each group. Mean ± SEM. ns > 0.05, # < 0.05, ## < 0.005, ### <0.0005, #### < 0.0001; #, § and $ = one-sample t-test for suprathreshold significance for a hypothetical value of 1.

stimulated at the end of each stimulation protocol for 10 s with this frequency with all the before used stimulation intensities. The idea was that a normal stimulation input to the body would normally last longer than 1 s. Here, we observed an interesting phenomenon. The Ca^{2+} response and peak amplitude were much higher than for the 20 Hz 1 s stimulation (normal Aδ-fibre stimulation) for all the tested indicators (cytoplasm and nucleus) (Fig. 13 A). One example trace showed how the amplitude seemed to build up and increased over time of stimulation to reach a peak or sometimes a plateau. We also observed “drops” in the recorded responses (data not shown) where the recorded Ca^{2+} signal decreased below 0 during the whole

stimulation and went back to its baseline after stimulation. These data were excluded from measurements. The remaining measurements were pooled together into three groups: GFAP:GCaMP5 (SNI and sham together), GFAP:GCaMP3.NLS (SNI and sham together) and GFAP:GCaMP3.NLS (CFA and PBS together) (Fig. 13 B). Except for the Ca^{2+} indicator localised in the cytoplasm, all other groups reached a significant suprathreshold from 0.1 mA stimulation intensity on. GFAP:GCaMP5 reached the first significant suprathreshold at 0.2 mA. The curve increased and reached its maximum for the two groups with Ca^{2+} indicator localised in the nucleus at 0.5 mA. The indicator, expressed in the cytosol, reached its maximum at 0.8 mA.

3.1.2 Ca^{2+} signalling in parvalbumin-positive neurons

3.1.2.1 Cytoplasmic Ca^{2+} signalling in parvalbumin positive cells under chronic inflammatory pain conditions

As excitatory neurons showed increased Ca^{2+} signalling under chronic inflammatory pain conditions (Simonetti et al. 2013) and as we observed interesting Ca^{2+} signalling behaviour in astrocytes, it was of a high interest to investigate a group of inhibitory neurons in the spinal dorsal horn for their fibre evoked Ca^{2+} signalling under chronic pain conditions. In addition, it has already been shown that under certain chronic pain conditions inhibitory neurons in the CNS are impaired in their function and total number of cells (Basbaum). This made the investigation of inhibitory neurons even more interesting. For the purpose to study this open question, a subtype of inhibitory neurons, a parvalbumin (pv) Cre-mouse line, kindly provided by the collaborating group from Prof. Dr. Rohini Kuner (Pharmakologisches Institut, Heidelberg Universität, Germany) was used. The mice were injected with a rAAV-construct in a Cre

recombinase-dependent manner under control of the human EF1α promoter in order to express a cytoplasmic Ca^{2+} indicator inside pv-positive cells (Fig. 14 A), including a nucleus export signal (NES) to keep the indicator in the cytosol only. In the fluorescent pictures, the expression of the GCaMP3.NES was visible in the spinal dorsal horn (Fig. 14 B). As for the dorsal root stimulation, all stimulated fibre types, Aβ-, Aδ- and C-fibres, evoked Ca^{2+} signalling in the spinal dorsal horn pv-neurons inside the cytoplasm (Fig. 14 C). The peak amplitude, presented as the fraction of 2x SD,

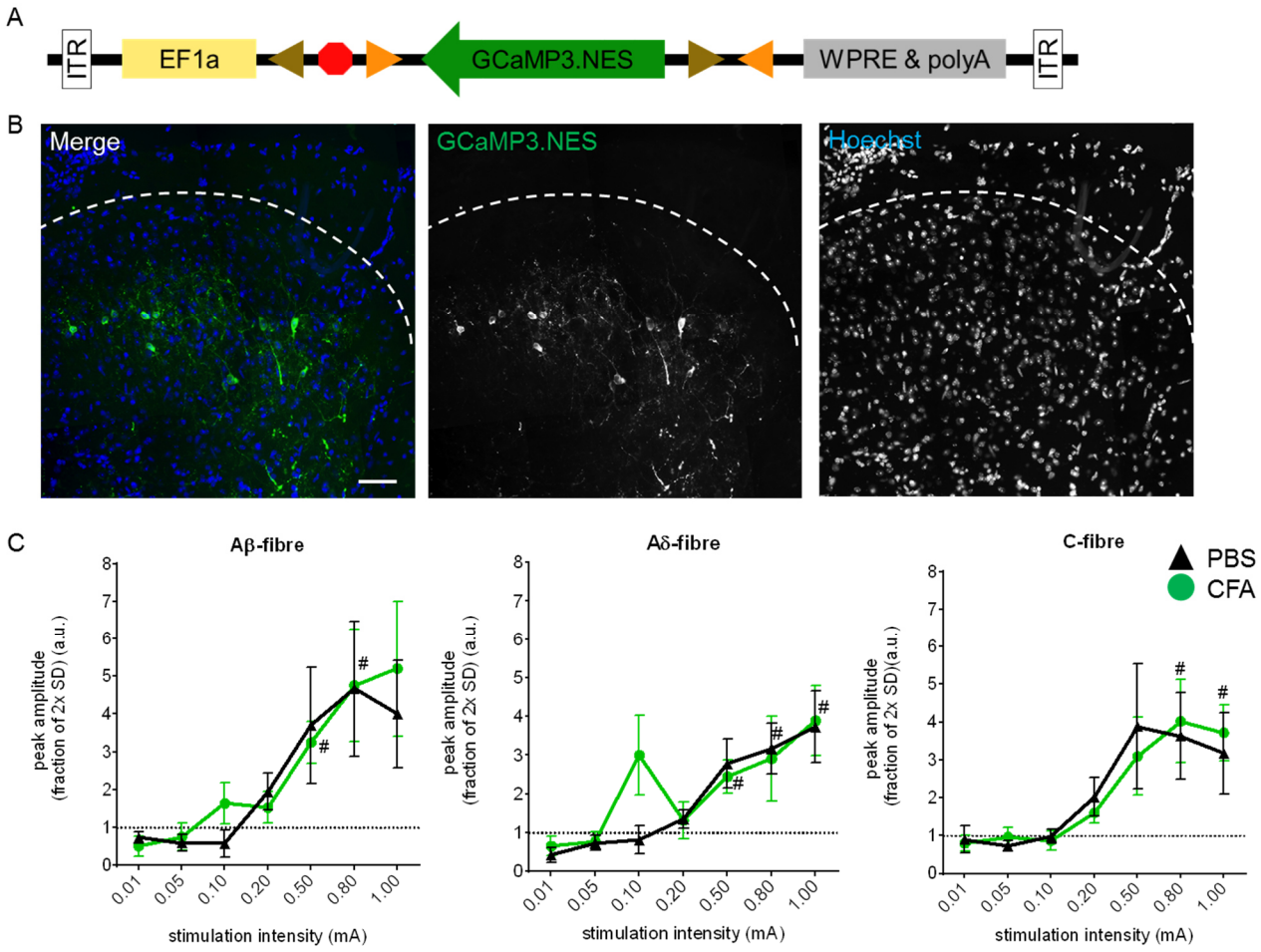

Figure 14: Ca^{2+} signalling changes in the cytoplasm of spinal cord dorsal horn pv-positive inhibitory neurons mice. (A) Injected construct to express cytosolic localised Ca^{2+} indicator with nuclear export signal (NES). **(B)** Image of fixed slices expressing indicator (GFP in green) in spinal dorsal horn. Dotted line indicating border of dorsal horn. **(C)** Stimulation response showed as peak amplitude as fraction of 2x SD for 100 Hz Aβ-, 20 Hz Aδ- and 4 Hz C-fibre stimulation. There was no detectable difference between the chronic inflammatory group, injected with CFA (green) and the PBS injected control group (black). n = 7 slices (5 mice) for CFA and n = 4 slices (4 mice) for PBS; ns > 0.05. # = one-sample t-test for suprathreshold significance for a hypothetical value of 1. Scale bar = 50 µm

increased the higher the stimulation intensity was. Under PBS conditions there was no suprathreshold detectable for none of the tested fibres. Under CFA (chronic inflammatory pain) conditions suprathresholds were measured. For Aβ-fibres stimulation, the suprathreshold of the CFA treated group was significant for 0.5 and 0.8 mA stimulation intensity. Aδ-fibres stimulation led to suprathreshold for intensities between 0.5 – 1 mA for acute slices from CFA treated mice. Also for C-fibre stimulation, the CFA injected group showed suprathreshold for 0.8 and 1 mA stimulation intensity.

The tested pain model was the one for chronic inflammatory pain, injection of CFA into the hind paw. There was no difference in any of the stimulated fibres between the CFA group and the PBS injected control group. That was similar to the tested chronic inflammatory pain in astrocytes.

Further experiments showed that neuropathic pain seems to have more influence onto the Ca^{2+} signalling behaviour of pv-cells, but this will be discussed in a later section (3.2.1 Npas4 expression under chronic inflammatory and neuropathic pain).

3.1.2.2 Spontaneous Ca^{2+} signals in parvalbumin-positive neurons

In addition to the evoked signals that were presented above, we observed spontaneous activity of pv-positive cells in the spinal cord dorsal horn. This spontaneous activity was different in many cells. The pattern, as well as the duration of the Ca^{2+} signal was highly diverse. The spontaneous activity was more prominent at the beginning of the recording procedure and lost its frequent activity during the stimulation protocol. Examples of Ca^{2+} imaging from cells with spontaneous activity are represented in Fig. 15. An example slices included a PV-positive neuron with very regular spontaneous Ca^{2+} signals that held its high Ca^{2+} level for 15 – 20 s and then decreased back to its Ca^{2+} baseline level. In the presented time window of 200 s, the cell (Fig. 15 A, red) had seven Ca^{2+} signals. A second cell of the same slice (blue) had no spontaneous activity during the first 100 s and then showed five peaks of Ca^{2+} signals in 50 s. These signals looked in their dynamics (duration of the signal) very different from the cell that is represented in red.

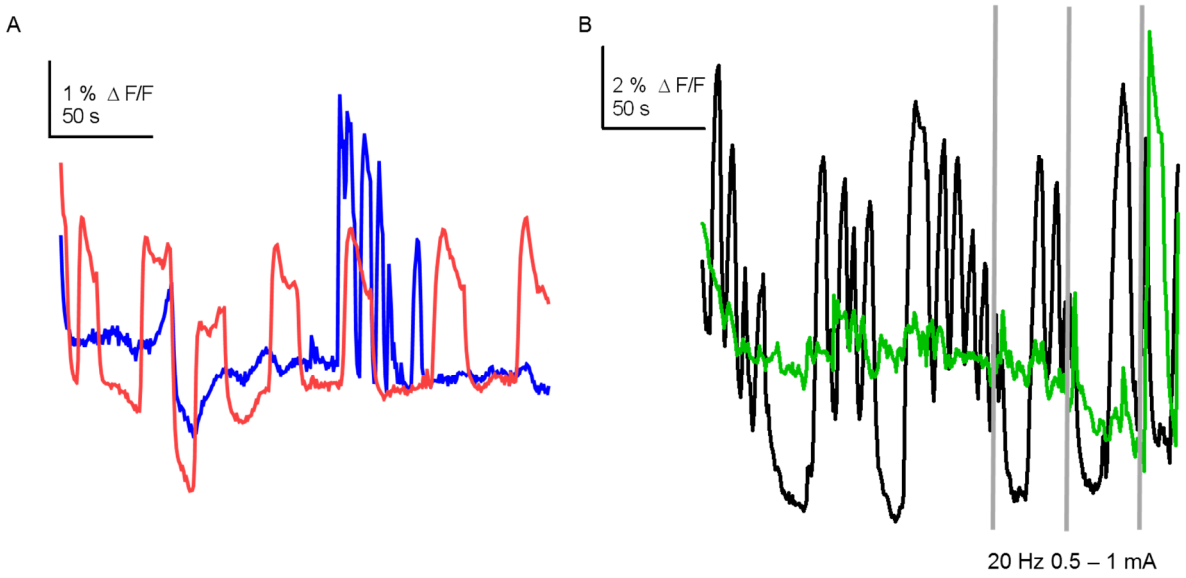

Figure 15: Spontaneous Ca^{2+} signalling in the cytoplasm of spinal cord dorsal horn pv-positive inhibitory neurons of mice. Displayed are two example slices with recorded spontaneous Ca^{2+} signalling before and during dorsal root stimulation. Every colour indicates a single cell. **(A)** Presented are two cells from an acute slice with one cell (red) which had regular and long lasting Ca^{2+} signals between 15 – 20 s. Second cell (blue) showed a sudden spiking of Ca^{2+} signals of 5 peaks in 50 s. **(B)** One cell (black) showed multiple spiking of Ca^{2+} signals with silencing in between. Peak number varied from 3 – 6 peaks for each of the 5 presented activity periods in the presented time window. Second cell (green) showed no spontaneous activity but evoked responses for 20 Hz stimulation with intensities of 0.5 – 1 mA (grey bars). Y-axes indicates Ca^{2+} signals as amplitude ΔF/F in % and X-axes indicates time in s.

A second example slice from a different mouse showed a PV-positive neuron (Fig. 15 B, black) with again regular spontaneous activity but instead of holding a high Ca^{2+} level during main activity periods, the cell had five main activities in the displayed time window of 200 s which showed decreases in the peak amplitude during each main activity that resulted in three to six peaks during these activities where the signal decreased but not completely to baseline level. After each main activity the Ca^{2+} level decreased back to baseline. A second cell from the slice (green) did not show

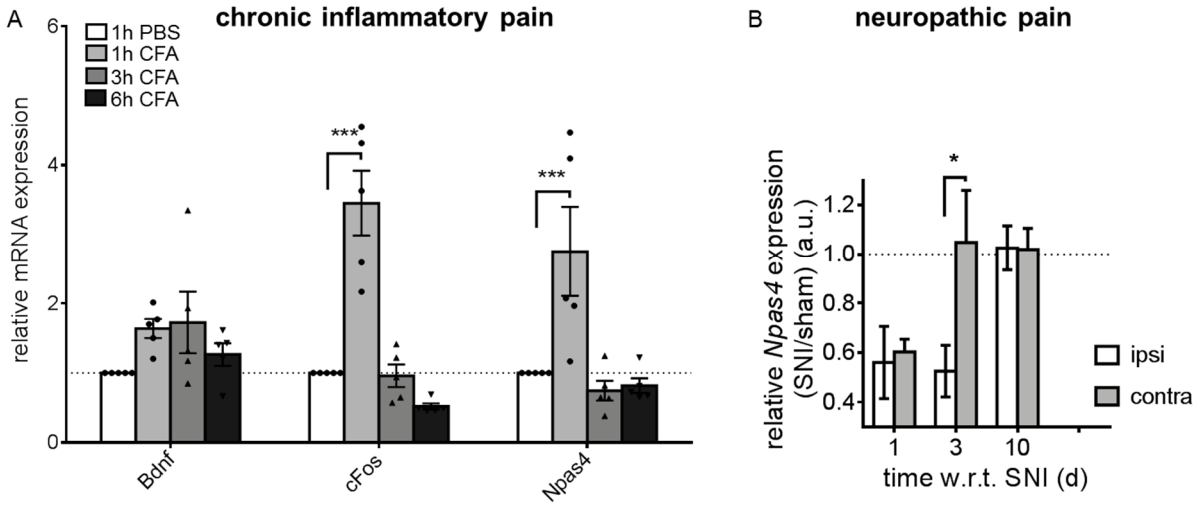

Figure 16: *Npas4* expression changes during chronic inflammatory and neuropathic pain. Dorsal horn tissue from lumbar area L3-L5 from the spinal cord was analyzed after the indicated pain protocols by qRT-PCR at the mentioned time points. **(A)** Graph represents relative mRNA expression of CFA treated mice over PBS (1 h after injection) at different time points in different grey scales (1 h, 3 h and 6 h after CFA injection) for the expression of *Npas4*, *Bdnf* and *cFos*. Dotted line represents the baseline level (defined by 1 h PBS injection). **(B)** Graph represents relative *Npas4* expression (SNI over sham group) from the ipsi lateral side (white) at different time points after surgery, compared to the *Npas4* expression of the contra lateral side (grey). A: n = 5 (CFA/PBS) or B: n = 4 (SNI/sham); mean ±SEM; two-way ANOVA Bonferonni's multiple comparison post-hoc test for differences between the two tested condition groups, ns > 0.05; * < 0.05; *** < 0.0005.

spontaneous activity but evoked responses for stimulation of 20 Hz and only for the intensities of 0.5 – 1 mA.

3.2 Consequences of Ca^{2+} signalling in spinal dorsal horn neurons

3.2.1 *Npas4* expression under chronic inflammatory and neuropathic pain

It was shown that inhibitory neurons in the spinal cord dorsal horn are impaired regarding their synaptic activity and their amount under neuropathic pain (Basbaum et al. 2009). Inhibitory neurons showed a decreased number of synapses and decreased total number of cells under neuropathic pain. As presented in the previous section (3.1.2 3.1.2 Ca^{2+} signalling in parvalbumin-positive neurons), Ca^{2+} signals in pv-positive cells in the spinal cord dorsal horn were evoked by dorsal root stimulation. This might indicate that there is a direct input from the periphery to inhibitory neurons in the spinal dorsal horn, which are then part of the pain circuit system. These stimulations from the periphery induced cytoplasmic Ca^{2+} increases in pv-positive cells. Cytoplasmic Ca^{2+} signalling leads to nuclear Ca^{2+} signalling, as the Ca^{2+}/calmodulin complex can freely travel through the nuclear pore complexes. The nuclear Ca2+ signalling leads to gene expression respectively (Eder and Bading 2007).

This strongly suggests that peripheral activity such as signal transmission through fibres like Aβ-, Aδ- and C-fibres caused neuronal activation of inhibitory neurons in the spinal dorsal horn. What role do these neurons play in terms of their Ca^{2+} signalling induced gene transcription under chronic pain? To investigate alterations of gene expression in cells that drive inhibitory balance in the neuronal circuit of the dorsal horn under chronic pain conditions, wild-type mice were either treated with the SNI or sham surgery for neuropathic and a different group of animals with either CFA or PBS injection to elicit chronic inflammatory pain. The mice spinal cord dorsal horn from lumbar section L3-L5 were collected at different time points after treatment.

Npas4 expression is responsible for inhibitory balance of the neuronal circuit after neuronal activity only (Sun and Lin 2016). It increases the amount of excitatory synapses onto inhibitory neurons and increases the amount of inhibitory synapses onto excitatory neurons. Thus, *Npas4* regulates the homeostatic balance of inhibition in the CNS. In our experiment, focus was put onto the expression of *Npas4* in the collected tissue. *Npas4* expression is not only dependent from neuronal activity but specifically from Ca^{2+} signalling (Zhang et al. 2009). As presented above, cytoplasmic Ca^{2+} in inhibitory neurons can be evoked through dorsal root stimulation, mimicking

peripheral inputs to the CNS. Thus, the Ca^{2+} signalling would cause nuclear Ca^{2+} rises and finally gene transcription activity. The role of *Npas4* in the neuronal circuit in the spinal cord dorsal horn was therefore of great interest, particularly under different pain models.

The qPCR results from the collected spinal cord tissue from mice that were treated with CFA injections showed a significant increase of *Npas4* mRNA already 1 h after injection in comparison to the PBS injected mice at the same time point (Fig. 16 A). This result is in agreement with other publications showing that, *Npas4* is an IEG already expressed ~ 5 min after neuronal activity (Maya-Vetencourt 2013). After 3 h, the relative expression of *Npas4* returned to baseline levels. *Bdnf* was not significantly induced. *cFos* was highly significantly induced after 1 h and returned to baseline after 3 h.

Interestingly, in the neuropathic pain model, where spinal cord tissue was collected after different time points after SNI or sham surgery, *Npas4* expression was reduced for both the treated (ipsilateral) and not treated (contralateral) at day 1 after surgery. While the ipsilateral side remained reduced at day 3 after surgery, the not treated side returned to baseline levels (Fig. 16 B) and stayed at that level up to day 10 after surgery. At day 10, the relative *Npas4* expression of both the ipsilateral side and the non-treated contralateral side was equally at baseline levels. These results were generated with Dr. Anna Hertle.

3.2.2 Manipulation of expression of *Npas4 in vitro*

The findings from the previous section, that *Npas4* expression was impaired under neuropathic pain in the early phase of pain development, indicated an important role of Ca^{2+} signalling induced *Npas4* in the spinal dorsal horn functional circuit. To further investigate the role of NPAS4 in the context of chronic pain, we developed a rAAV-sh*Npas4*, a dominant-negative NPAS4 construct and a *Npas4* over-expression rAAV, together with their equivalent controls. First, we tested the constructs for their function in hippocampal and later in spinal cord cell culture.

First, the sh*Npas4* construct was tested. The sh-sequence was expressed under an U6 promoter. For visualisation, added to the construct was a GFP sequence under the control of a CMV promoter (Fig. 17 A).

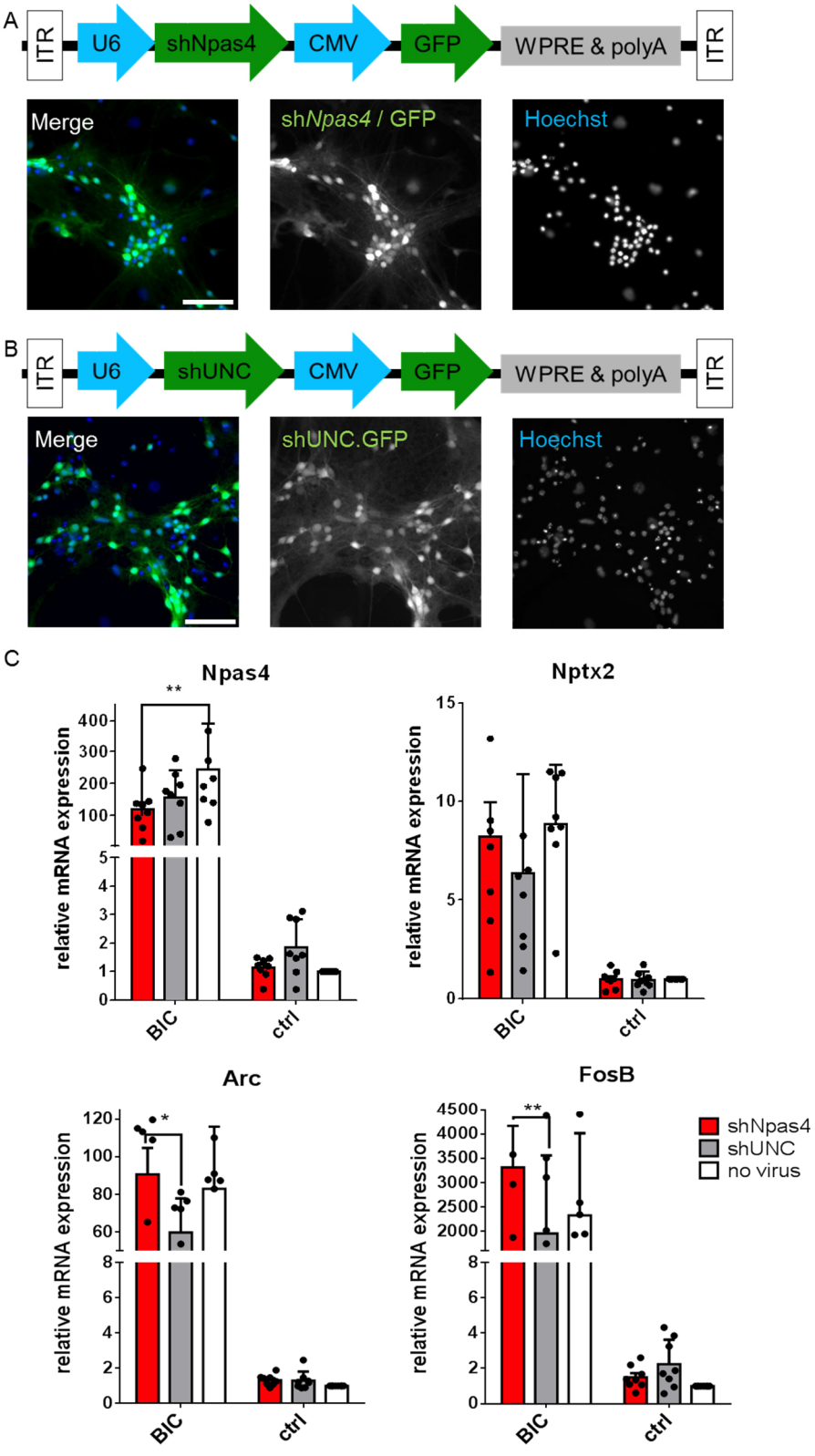

Figure 17: Relative expression levels after rAAV shNpas4 treatment *in vitro*. (A) sh*Npas4* construct with GFP sequence for visual labeling. Pictures show example expression of construct in hippocampal primary neuron culture. **(B)** shUNC construct with GFP sequence for visual labeling. Pictures show example expression of construct in hippocampal primary neuron culture. **(C)** Relative gene expression of *Npas4*, *Nptx2*, *Arc* and *FosB* from primary hippocampal neuron culture that had sh*Npas4* (red), shUNC (grey) or no rAAV (white). Graphs show relative gene expression with or without 2 h BIC treatment. n = 8 for all groups; mean ±SEM; two-way ANOVA Bonferonni's multiple comparison post-hoc test for differences between the two tested condition groups, ns > 0.05, * < 0.05, ** < 0.005. scale bar = 100 µm.

The control construct consisted of the same promoters and fluorescent protein, with a scrambled version of the sh-sequence (Fig. 17 B), established in our lab and not targeting any mRNA, thus not having an effect on any other gene expression. The expression levels of the rAAV constructs, the sh*Npas4* as well as its control construct, were visible in primary hippocampal mouse cell cultures (Fig. 17 A, B). In order to test the function of the constructs, cells were transfected with rAAV constructs (DIV 3) and

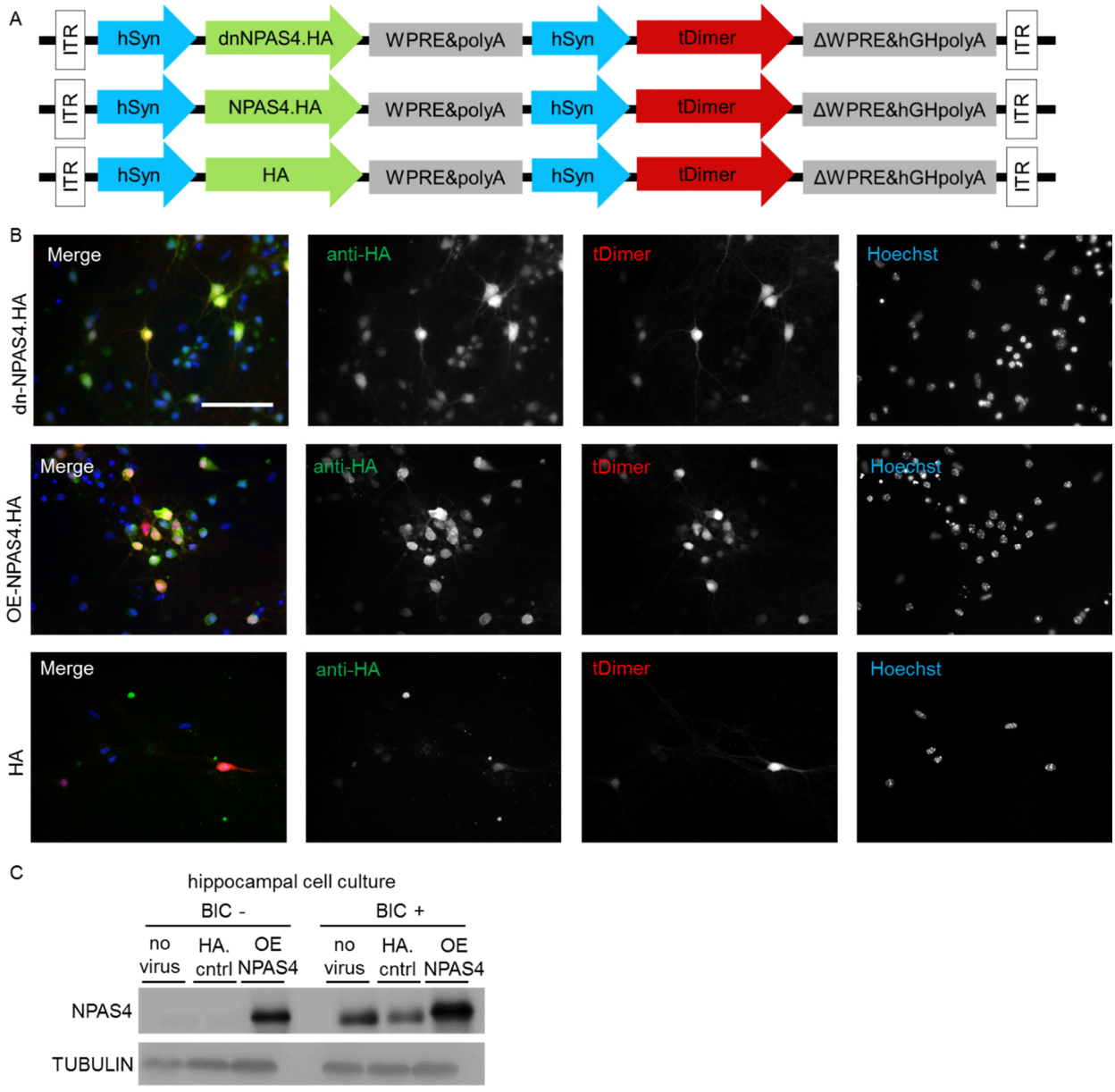

Figure 18: *in vitro* manipulation of NPAS4. (A) rAAV constructs for NPAS4 manipulation. **(B)** Immunohistochemistry pictures from primary hippocampal cells expressing rAAV constructs from (A) and stained against HA. **(C)** Protein levels of primary hippocampal cell culture for NPAS4 and TUBULIN when treated with no virus, OE-NPAS4 or control construct and ± BIC treatment. n = 2; scale bar = 100 µm.

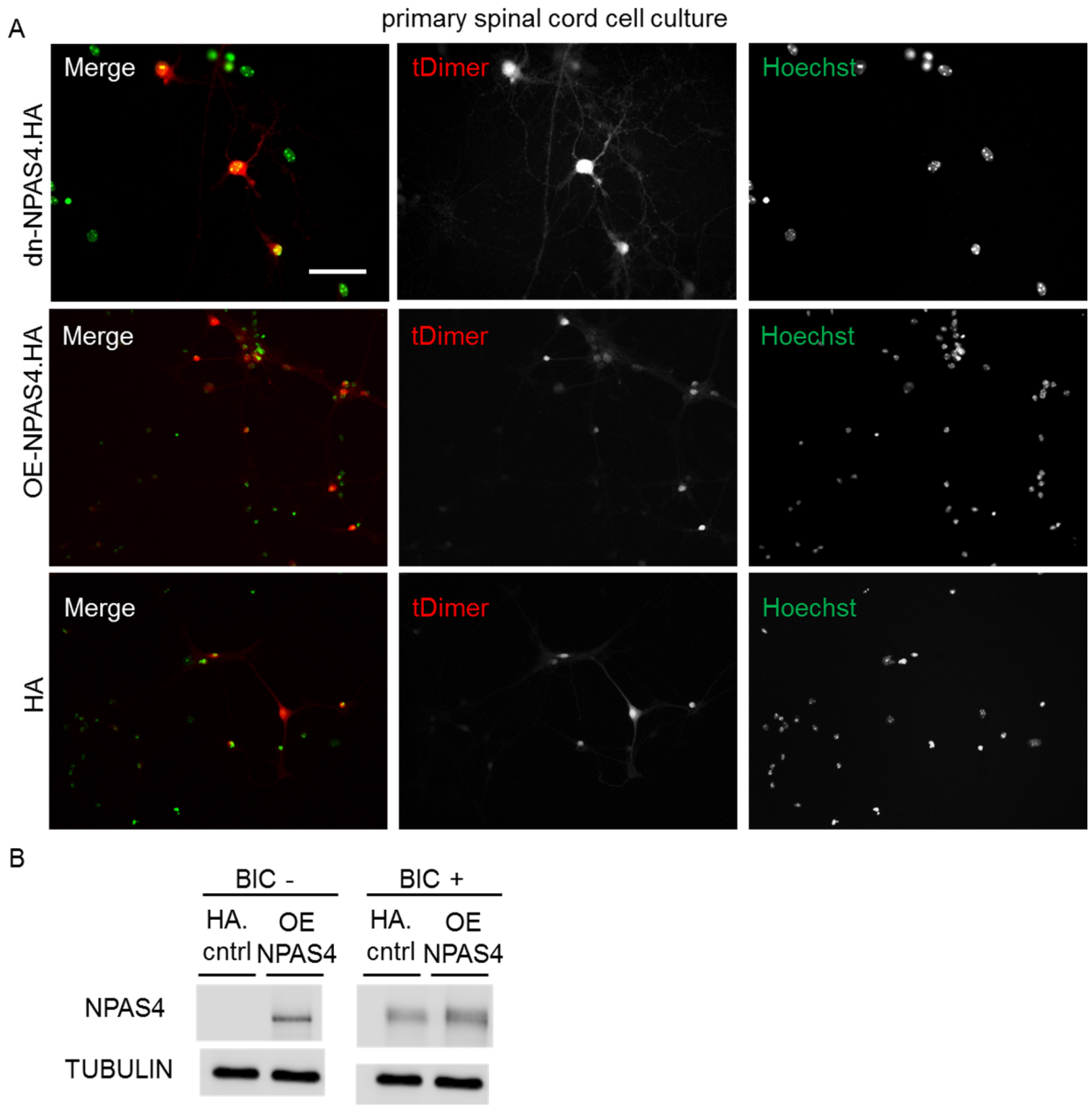

Figure 19: *in vitro* manipulation of NPAS4 in primary spinal cord culture. (A) Fluorescent pictures from rAAV constructs expressing in primary spinal cord cell culture. **(B)** Protein level of NPAS4 (~ 130 kDa) and TUBULIN (~ 55 kDa) of primary hippocampal cell culture when transfected with HA-control rAAV or OE-NPAS4 rAAV and treated with ± BIC. n = 2; scale bar = 100 µm.

treated for 2 h with bicuculline (BIC) at DIV 10 to induce more excitatory neuronal activation and thus neuronal depolarisation through inhibition of GABA receptors. The result showed that the relative expression of the tested genes in hippocampal cell culture did not change for *Npas4* expression (Fig. 17 C). The sh*Npas4* construct did not significantly decreased the relative mRNA expression of *Npas4* compared to its proper control: shUNC. We detected a significant decrease of the relative *Npas4* expression under sh*Npas4* influence compared to the cultures that were not treated

with rAAVs. Also other Npas4-dependent genes such as *Nptx2* were not significantly decreased compared to the controls when treated with shNpas4. The only significant difference between sh*Npas4* and shUNC treated cells was detected for *Arc* and *FosB* expression. In both cases the sh*Npas4* treated cultures showed increased levels of those tested genes.

In conclusion, the sh*Npas4* construct resulted unsuitable for further experiments as the control.

That led to a development of a dominant-negative (dn) Npas4 construct. The dominant-negative construct was made of a sequence to act antagonistically on the wild-type expressed NPAS4 protein and would like this make it not functional acting anymore. The construct was set behind a human synapsin (hSyn) promoter to be expressed in any kind of neuron, inhibitory as well as excitatory. In addition the dn-NPAS4 had an HA-tag and afterwards, also under hSyn control, a tDimer, for visually detectable red expression (Fig. 18 A – B).

To not only block NPAS4 functionality but also to try to rescue the decreased phenotype from under the neuropathic pain conditions, we developed an over-expression construct in order to have an increased amount of NPAS4 protein compared to the baseline expression. The over-expression virus (OE-Npas4) was placed under a hSyn and in addition, it was coupled to an HA-tag. In the end the construct had, as well under the hSyn promoter, a tDimer, for red visualisation of the expression in cells later on. The control construct consisted of only an HA-tag under hSyn promoter and a tDimer, also under hSyn control. Like this it functioned as control construct for the dn-NPAS4 rAAV as well as for the OE-NPAS4 (Fig. 18 A – B).

The function of the constructs were tested for their expression and function in primary hippocampal mouse cell culture. Fig. 18 B shows the expression level of the tDimer from the different constructs in the neurons. There was an overlay of the tDimer expression and a staining against the HA.tag. In addition, the protein levels of NPAS4 were tested. In primary hippocampal cell culture basal level of NPAS4 under conditions of no virus transfection, transfection with the control or the dn-construct

were not elevated but the OE-NPAS4 construct showed a strong band positive for NPAS4-antibody. Under BIC treatment, which led to neuronal activation, the NPAS4 expression was visible for all tested constructs, proving again that NPAS4 expression is dependent on neuronal activity.

The same tests were performed in primary spinal cord culture. The expression levels of the different constructs was visible in the cells and also the protein levels were similar to the expression levels that were already detected under BIC or without BIC treatment in primary hippocampal cultures (Fig. 19).

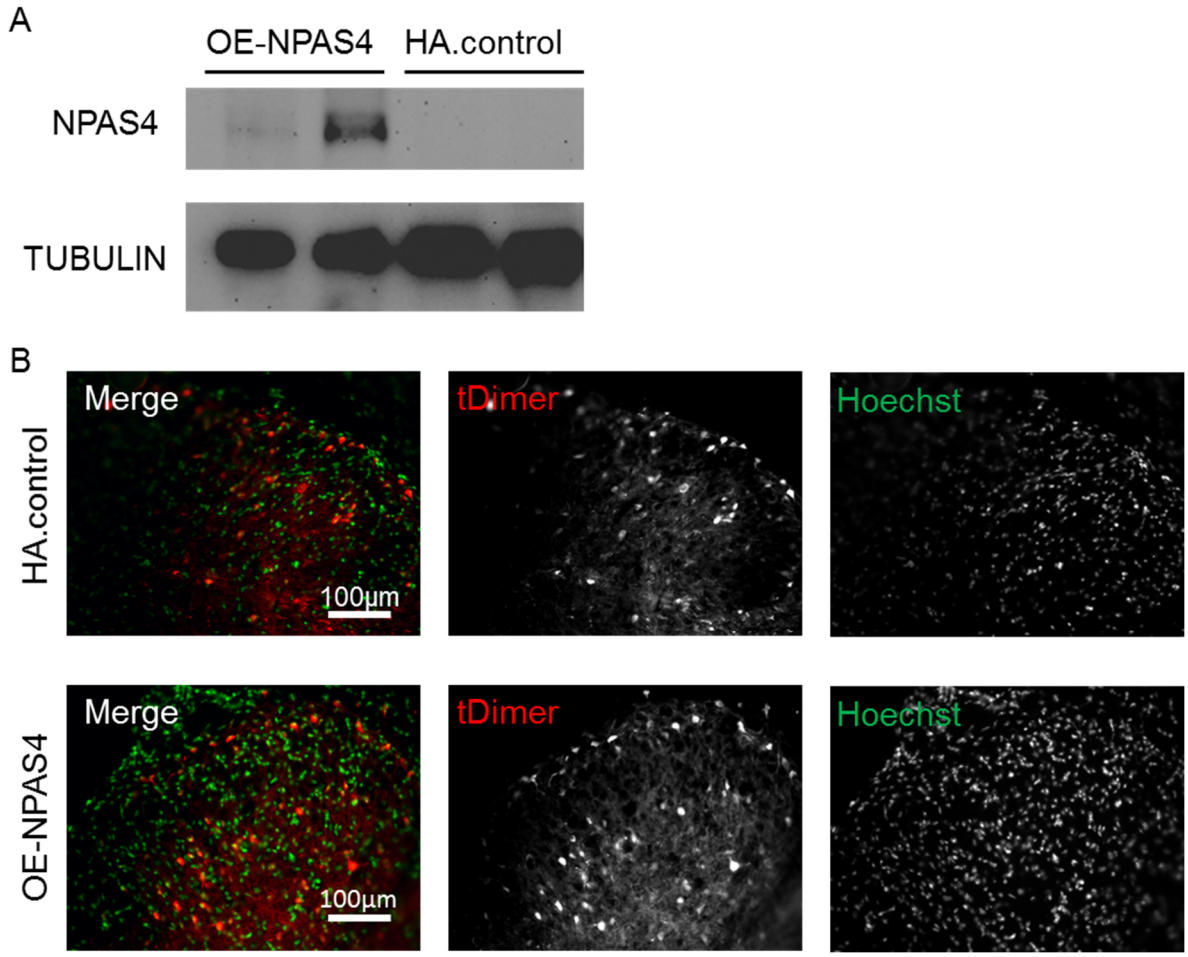

Figure 20: NPAS4 changes in spinal dorsal horn under different rAAV constructs. Dorsal horn tissue from lumbar area L3-L5 from the spinal cord was analyzed after the injection of rAAV constructs for over expressing NPAS4, rAAV with a control plasmid and a dominant-negative Npas4 construct. **(A)** Graph represents two mice for each construct and their levels of NPAS4 proteins (~ 130 kDa). For control expression, TUBULIN expression (~ 55 kDa) was tested. **(B)** Pictures show representative expression of OE-NPAS4 construct and control construct in the spinal dorsal horn of mice that were used for behavioural experiments. Visible are tDimer expression from injected constructs and Hoechst from staining. Scale bar 100 µm.

3.2.3 *Npas4* manipulation *in vivo*

The control construct and the OE-NPAS4 construct were tested for their effect *in vivo*. *In vivo* the constructs were injected with rAAVs into the spinal cord of two WT mice each and after three weeks of expression time the mice were perfused and the spinal dorsal horn was collected for protein level analysis. The results showed that the OE-NPAS4 construct successfully induced higher levels of baseline NPAS4 compared to the control construct and the dn-Npas4 construct (Fig. 20 A).

The basal level of NPAS4 is too low to be visible on a western blot. As control for protein expression, tubulin was used and detectable in all constructs.

The expression of the constructs was also shown in fluorescent pictures that were made after behavioural experiments. Fig. 20 B shows the tDimer expression of the HA.control construct and the OE-NPAS4 construct. Under both constructs, expression was visible in many cells of the mouse spinal dorsal horn in superficial as well as in deeper dorsal horn laminae.

3.2.4 *Npas4* over expression *in vivo* under neuropathic pain conditions

In section 3.2.1 it was presented that *Npas4* expression is altered under early phases of neuropathic pain conditions. For that reason, the *Npas4* influence under neuropathic pain was tested. The hypothesis was to increase the protein level of NPAS4 in spinal dorsal horn cells, introduced by the rAAV construct which was injected into the spinal cord dorsal horn of WT mice just as described in the previous sections, related to Ca^{2+} signalling, in order to rescue neuropathic pain, induced through SNI surgery. The theory was, that through the increase of NPAS4 in the spinal dorsal horn, it would lead to an increase of the inhibitory balance and thus would buffer the normally alteration of the inhibitory system under neuropathic pain, as described in the introduction. As a control, another group of WT mice would be injected with the control construct but handled the same way, and would also receive SNI surgery. Mice were tested for mobility behaviour through catwalk testing previous to spinal cord injection and previous to SNI but after injection of the rAAV constructs. Also at day 4 after SNI surgery the mobility behaviour was tested on the catwalk (Fig. 21). In addition,

mechanical pain threshold was tested with von Frey filaments as well as the thermal pain threshold through cold plate as baseline before and after injection to rule out any effect of the rAAV injection into the spinal dorsal horn. Both pain behaviour tests are known to be increased in their mechanical threshold or thermal hypersensitivity after neuropathic pain induction. To investigate the effect of *Npas4* over expression on neuropathic pain conditions, the previous developed and tested tools, the rAAV constructs of OE-NPAS4 and HA.control, were injected into the left side lumbar part L3-L5 of WT mice spinal cord dorsal horn. 10 days after injection, baseline behaviour for the indicated behavioural tests (catwalk, von Frey filaments and cold plate) (Fig. 21 B) were tested. At day 15 after spinal cord injection, a day were the expression level of the rAAV constructs would already be at a high level, SNI surgery was introduced to the injected mice. Mechanical pain threshold through von Frey filaments and thermal pain threshold through cold plate were tested at day 2, 3, 5, 7 and 10 after

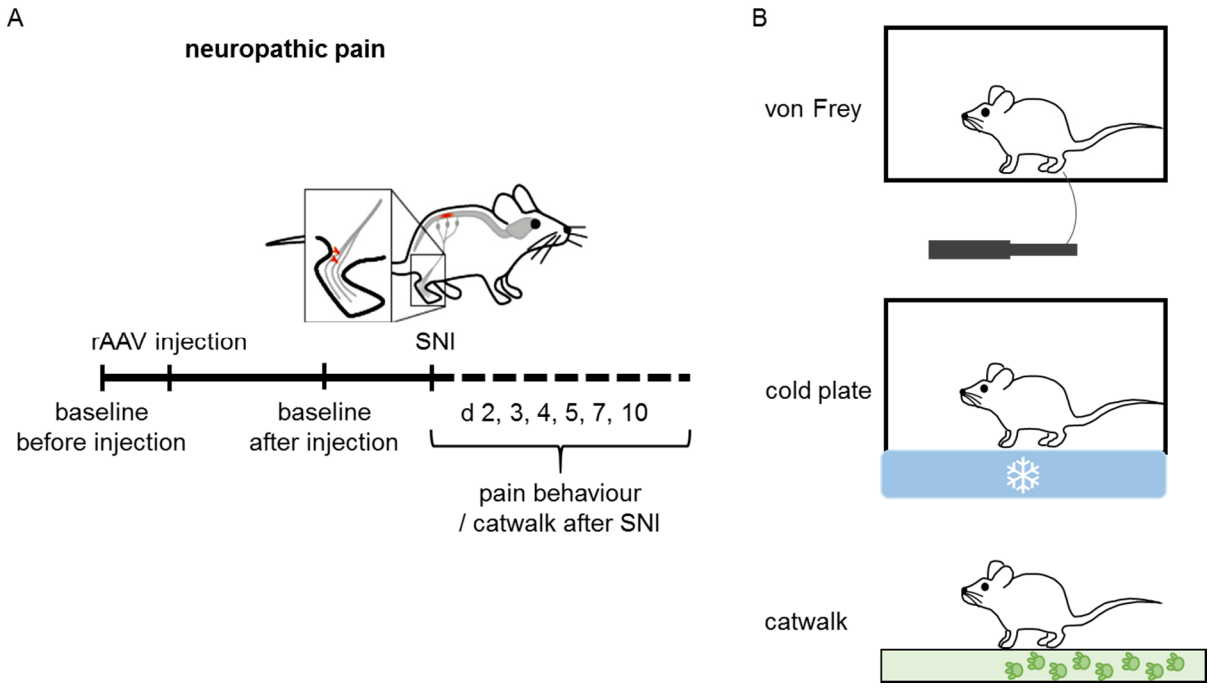

Figure 21: Experimental procedure of OE-NPAS4 injection and pain behaviour. (A) For the neuropathic pain model, baseline behaviour was measured before and after injection to rule out any effect of the rAAV injection itself. Injected were OE-NPAS4 construct or HA.control construct. Two weeks after injection, SNI surgery was performed to induce neuropathic pain to all the mice. Pain behaviour was measured at day 2, 3, 4, 5, 7 and 10 after SNI surgery. **(B)** The tested pain behaviours were von Frey for mechanical sensitivity, cold plate for thermal sensitivity and catwalk for motoric impairment and behaviour.

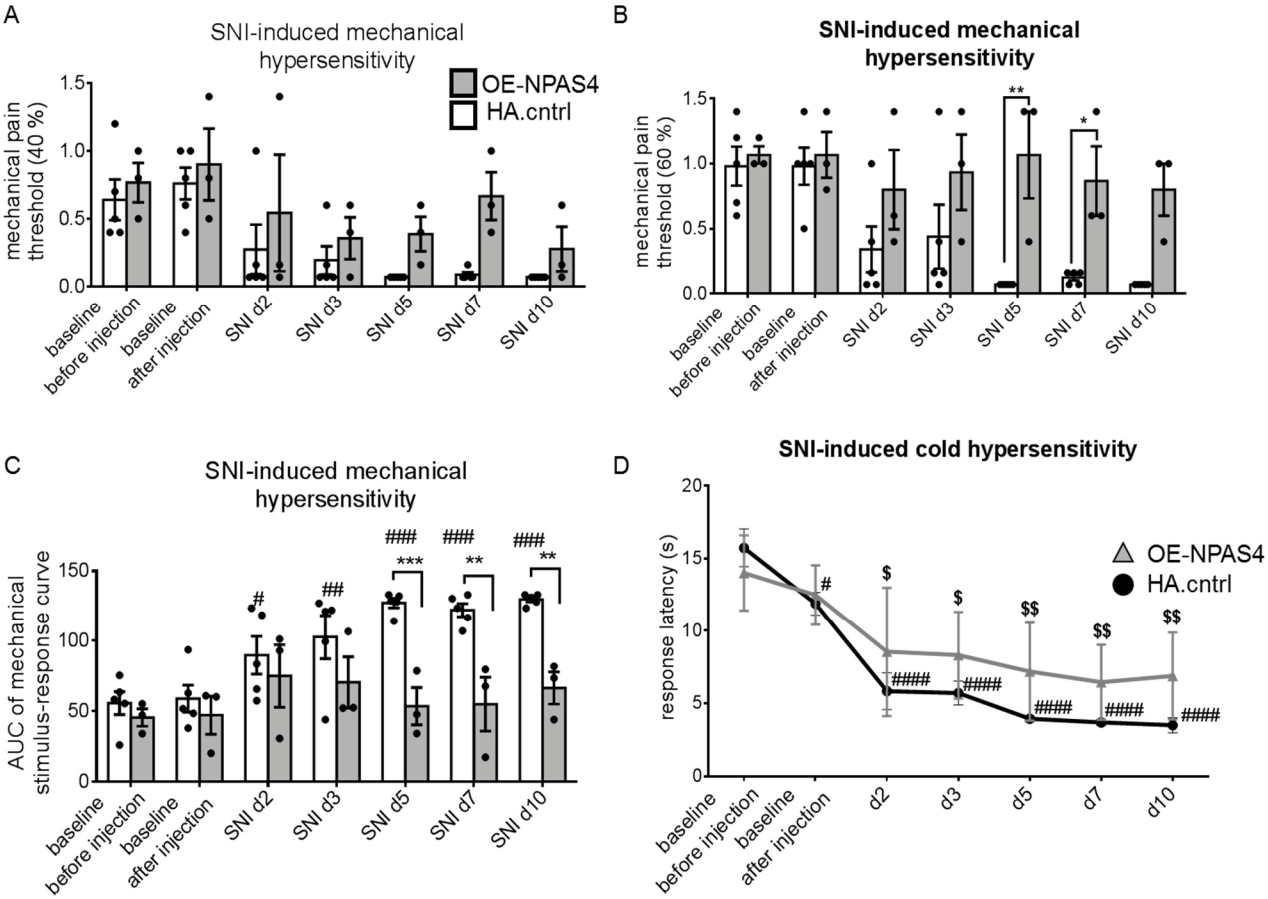

Figure 22: Pain behaviour under von Frey and cold plate tests. (A) Measured mechanical pain threshold of 40 % for different fibre strengths at different time point: baseline before rAAV injection, baseline after rAAV injection and measurements at day 2, 3, 5, 7 and 10 after SNI surgery. Two groups are displayed: OE-NPAS4 (grey) expressing animals or HA.control (white) expressing animals. No significant differences detectable. **(B)** Measured mechanical pain threshold of 60 % for different fibre strengths at different time point: baseline before rAAV injection, baseline after rAAV injection and measurements at day 2, 3, 5, 7 and 10 after SNI surgery. No significant differences if not indicated otherwise. **(C)** Area under the curve of mechanical stimulus-response at different indicated time points. Not significant if not indicated otherwise. **(D)** Tested thermal hypersensitivity was measured as response latency in s at the indicated time points. No significant differences. n = 3 (OE-NPAS4 group) and n = 5 (control group), ± SEM; significance compared to the own baseline before injection of a group was tested with two-way ANOVA Bonferonni's multiple comparison post-hoc test: ns > 0.05, # < 0.05, ## < 0.005, ### <0.0005, #### < 0.0001 for control group and same p-values for OENpas4 group with indicated symbol: $; significance compared between the two animal groups: two-way ANOVA Bonferonni's multiple comparison post-hoc test for differences between the two tested condition groups: ns > 0.05, * < 0.05, ** < 0.005, *** <0.005.

SNI surgery. Fig. 22 A showed no significant increase of the mechanical pain hypersensitivity at a threshold of 40 % tested for the different strengths of von Frey filaments. There is a visible decrease of the control group after SNI surgery compared to the basal levels. For the mechanical pain hypersensitivity at a threshold of 60 % tested for the different strengths of von Frey filaments there was a detectable decrease of the threshold from the control group compared to the OE-NPAS4 injected group for days 5 and 7 after SNI surgery and a trend of decrease for day 10 after surgery (Fig. 22 B). The area under the curve of the mechanical stimulus-response showed even better the effect of the OE-NPAS4 construct on the mechanical pain behaviour. There was no difference between the groups and the two measured baselines. But already at day 2 after SNI surgery, the control group showed significant increased mechanical hypersensitivity (Fig. 22 C). This hypersensitivity increased over the following days. The OE-NPAS4 injected group showed on the other hand no significant increase of hypersensitivity compared to the baseline levels at any days after surgery. At day 5 – 10 after surgery the control group showed increased hypersensitivity not only compared to the baseline levels but also compared to the OE-NPAS4 group.

The tested thermal hypersensitivity showed no difference between the two different animal groups. The animals of the control group showed significant difference compared to the baseline measurements, when tested at the different time points after SNI surgery. So thermal hypersensitivity was increased by measured response latency of paw withdraw when placed onto the 4°C cold plate (Fig. 22 D).

The catwalk showed no impairment of run duration or run average between the groups or the tested time points (Fig. 23 A and B). For the other tested parameters (print area, swing speed, step cycle and single stance) (Fig. 23 C – F) there was a significant decrease between the two baseline time points and day 4 after SNI surgery for both groups of animal. That showed that the left hind paw, that underwent SNI surgery, was impaired in its motor function, represented through the swing speed, the step cycle and the single stance (Fig. 23 D – F). The print area is an indicator for the intensity of usage of the paw. The hind paw of both groups showed significant decreased print areas for both groups compared to the baseline (Fig. 23 C). Examples of the visualisation of the catwalk video as well as the print area and the print intensity can be found in Appendix Figure 2.

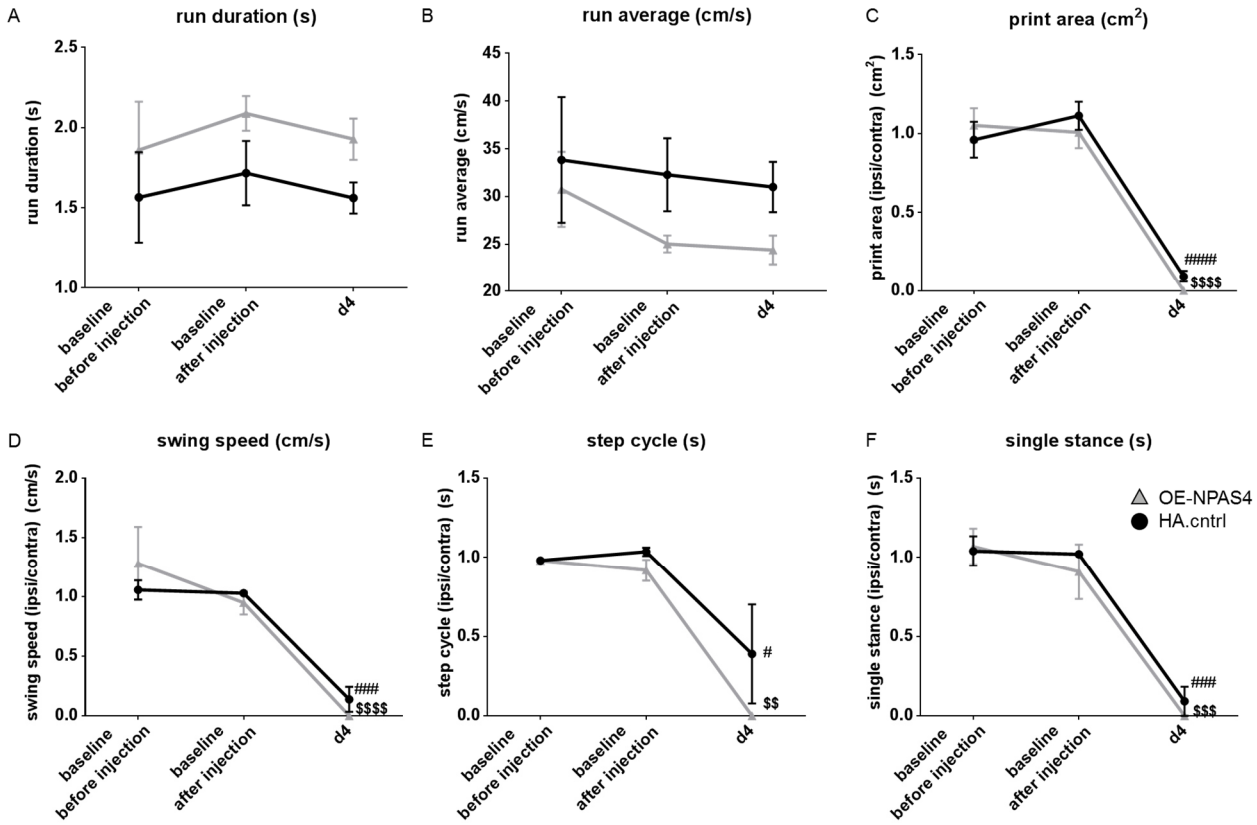

Figure 23: Catwalk behaviour. Mice were tested on the catwalk before rAAV injection, 10 days after rAAV injection and 4 days after SNI surgery (d4). Mice were represented in the two groups: OE-NPAS4 injected mice (grey) and control construct injected mice (black). **(A)** Run duration in s for the indicated time points. **(B)** Run average in cm/s. **(C)** Print area of the hind paws calculated as the ipsi lateral side (rAAV injected and SNI surgery side) over the contra lateral side as cm^2. **(D)** Swing speed of the hind paws calculated as the ipsi lateral side (rAAV injected and SNI surgery side) over the contra lateral side as cm/s. **(E)** Step cycle of the hind paws calculated as the ipsi lateral side (rAAV injected and SNI surgery side) over the contra lateral side in s. **(F)** Single stance of the hind paws calculated as the ipsi lateral side (rAAV injected and SNI surgery side) over the contra lateral side in s. No significant differences between OE-NPAS4 and control group in all the tested parameters. n = 3 (OE-NPAS4) and n = 5 (control), ± SEM; significance compared to the own baseline before injection of a group was tested with two-way ANOVA Bonferonni's multiple comparison post-hoc test: ns > 0.05, # < 0.05, ## < 0.005, ### <0.0005, #### < 0.0001 for control group and same p-values for OE-NPAS4 group with indicated symbol: $; significance compared between the two animal groups: two-way ANOVA Bonferonni's multiple comparison post-hoc test for differences between the two tested condition groups: ns > 0.05.

4. Discussion

The experiments presented in this thesis gave an insight into the circuit mechanisms of the development and maintenance of different chronic pain models. We investigated the Ca^{2+} signals of astrocytes and PV-positive neurons in the spinal dorsal horn. We showed that fibre stimulation of different fibre classes can evoke Ca^{2+} signals in astrocytic cytosol and nucleus. Furthermore, we detected decreased Ca^{2+} signalling in the cytoplasm of astrocytes under neuropathic pain conditions when stimulated with frequencies mainly recruiting Aβ-fibres and Aδ-fibres concerning nuclear Ca^{2+} signalling. For chronic inflammatory pain conditions, we didn't find any impairment in Ca^{2+} signalling in astrocytes as well as in PV-neurons.

Still, NPAS4, a protein, expressed specifically after Ca^{2+} signalling in neurons and responsible for a homeostatic balance in favour of inhibition, was decreased under neuropathic pain conditions. Further investigation on NPAS4 showed that over expressing NPAS4 in the spinal dorsal horn of mice rescued mechanical hypersensitivity but not thermal hypersensitivity or motoric impairment after neuropathic pain induction.

4.1 Challenges during experiments

Injections into the spinal dorsal horn of mice are a challenging procedure. Due to respiration movements and the difficulty to fix the mice back like it is done for brain injections, a precise depth cannot be assured for all injections, compromising the quality of the procedure. In addition, touching the dorsal horn with an injection needle can lead to sudden movements of the mice even under deep anaesthesia because of a mechanical stimulation of the neurons. These mechanical stimulations might activate neurons that are connected via interneurons with deeper motor neurons in the ventral part of the spinal cord, which then leads to a sudden movement (possibly a reflex). Nevertheless, we confirmed out method by injecting the Ca^{2+} indicators and labelling C-fibre endings with Isolectin B4 (Fig. 6). These results approved our methods for all coming experiments.

Also during imaging of Ca^{2+} some unexpected difficulties occurred. Unfortunately due to the set-up and the fact that the software control of the stimulator was not directly connected to the imaging recording set-up, it was difficult to determine an accurate

time point of stimulation and its relation to the evoked Ca^{2+} response. The response time can be set to ~ 1 – 3 s after stimulation. Still as it is under debate how fast astrocytic Ca^{2+} signals can occur, it would have been very interesting to determine a specific time point of Ca^{2+} signal after stimulation.

During live imaging of acute slices with indicators that were expressed in the cytosol or at the astrocytic membrane, it turned out to be difficult to make out single cells or fine processes. In contrast, expressing cells appeared cloudy during imaging if at all as the baseline level of Ca^{2+} in astrocytes is very low. With the used wide-field microscope resolution it was impossible to make out single or fine processes, as focusing on fine processes in the relatively thick slices is not possible with the set-up we used. A confocal microscope with high recording frequency would be more suitable to investigate Ca^{2+} in fine processes and astrocytic endfeet.

Another problem was the neuronal expression of our used indicators under the GFAP promoter. Even when further experiments with the Aldh1l1 cre-mouse line showed that the evoked Ca^{2+} behaviour was similar in both mice, WT mice with injected indicator under GFAP promoter and Aldh1l1-mice with injected indicator in a floxed manner, for further experiments it is necessary to use Aldh1l1-mice preferably as the possible contamination of neuronal effects under the GFAP promoter cannot be excluded.

During stimulation with 20 Hz for 10 s we observed in some acute slices a drop instead of an increase in the evoked Ca^{2+} signal. We believe that the strong stimulation led to a heat up of the electrode which then formed air bubbles at the tip of the stimulation pipette and thus pressed down the tissue during the recording which was detected as a decrease below 0. After this stimulation we often observed bubbles at the tip of the electrode even when the DR was still well attached to the spinal cord slice as well as to the stimulation electrode. Furthermore, for this stimulation it is possible that through such a high and long, thus intense stimulation, not only Aδ-fibres but also other fibre classes like Aβ- and C-fibres were recruited during the stimulation. Thus, it is not clear which fibre class evoked this strong Ca^{2+} response. It is possible that of one fibre class over a longer stimulation time more fibres are recruited and that this would as an addition increase the detected signal or if all fibre classes are recruited over the stimulation time and would result in such a high evoked Ca^{2+} response. This problem could be addressed by specifically blocking different fibre classes and investigating

the Ca^{2+} signalling behaviour for only one active fibre class. The long stimulation protocol should also be performed independently of the other stimulation protocols in order to directly stimulate a “naïve” acute slice, which was not stressed through previous stimulations. This could prevent the occasionally bubble formation at the tip of the electrode pipette.

It is also possible that the strong stimulation and the long and stressful stimulation protocol impaired the quality of the cells and the whole acute slice tissue.

4.2 Ca^{2+} signalling in astrocytes

4.2.1 Ca^{2+} signals in astrocytes induced through fibre stimulation

Astrocytes are known to not only support but also communicate with neurons through Ca^{2+} signals or the release of gliotransmitters initiated by Ca^{2+} elevations in astrocytes. Still it is under debate if they play a crucial role in for example learning and memory contexts (Agulhon, Fiacco, and McCarthy 2010). When it comes to chronic pain and the role of astrocytes in this context, there are even more questions unresolved. It was shown that astrocytes respond with astrogliosis and increased Ca^{2+} signalling and transmitter release under inflammatory pain conditions in the brain (Hansson 2010) and in the cortex under neuropathic pain (Kim et al. 2016). Also slight plasticity changes in the spinal cord dorsal horn (Ikeda, Kiritoshi, and Murase 2012) were shown under inflammatory and neuropathic pain conditions. Still, especially in the spinal cord, there is not much known about the role of Ca^{2+} signalling in astrocytes in the context of chronic pain. This thesis offers a new perspective and new insight into that matter.

The stimulation of the DR from acute slices showed for all the different preferable fibre classes, Aβ-, Aδ- and C-fibre, evoked Ca^{2+} signals in the cytoplasm of astrocytes. The membrane bound indicator was not suitable for our investigation and set-up as it would need a confocal microscope to focus on labelled processes in order to distinguish them from deeper layers signal. Still, our data on Ca^{2+} indicators expressed in the cytoplasm of astrocytes gave us insight into the Ca^{2+} signalling behaviour evoked by peripheral fibres of different types. All fibre classes that were tested by stimulation showed to have at least a Ca^{2+} signalling increasing effect on astrocytes. We detected a suprathreshold for all tested fibre classes in astrocytes from 0.5 mA stimulation intensity on. Furthermore, our data showed that there was an impairment of astrocytic

Ca^{2+} signalling under neuropathic pain conditions in Aβ- and Aδ-fibre stimulation. This indicates that astrocytes from the spinal dorsal horn are involved in circuits of sensation of touch fibres and nociceptors as they reacted on neuronal activity from the periphery. Probably glutamate and ATP from pre-synapses, evoking action potentials in post-synaptic excitatory neurons also evoked Ca^{2+} signalling in astrocytes that were in close proximity of those synaptic clefts. The consequence of the initiation of Ca^{2+} signals in astrocytes through neuronal activity, induced by peripheral signal transmission into the spinal dorsal horn, might be recruitment of astrocytes for supporting the neurons by increased metabolism of glycogenesis, by increased gliotransmitter release and thus influencing the signal cascade in the dorsal horn and induction of plasticity changes of astrocytes to probably adjust to the neuronal surrounding which probably also changed in its plasticity (concerning excitatory and inhibitory neurons, which will be discussed in a later section).

As we showed Ca^{2+} signals in the cytoplasm of astrocytes, the next step was to investigate the possibility of those signals entering the nucleus. In this thesis I have also shown, to my knowledge for the first time, evoked nuclear Ca^{2+} signals in astrocytes. With electrical stimulation of the dorsal roots, I was able to evoke those Ca^{2+} signals in spinal cord dorsal horn astrocytes robustly. All stimulated preferred fibres were shown to be responsible for downstream stimulation of nuclear Ca^{2+} signals in astrocytes. The lack of research on the topic of nuclear Ca^{2+} signalling in astrocytes is striking. As it is established by now that nuclear Ca^{2+} signals in neurons cause gene transcription and influence the plasticity of neurons, what might be the role of nuclear Ca^{2+} signals in astrocytes? It has been mentioned in a few publications already, that the key players of the nuclear Ca^{2+} pathway in neurons are also represented in astrocytes. For example (Liu, Dong, et al. 2017) showed that through Ca^{2+} signals CaMKIV is increased in order to regulate the expression of BDNF in astrocytes. This indicates already a potential role of nuclear Ca^{2+} signals in astrocytes similar to its role in neurons: gene transcription. This opens a whole new field of research: is it possible that stimulation evoked nuclear Ca^{2+} signals in astrocytes lead to gene transcription? And if so, would it mean a similar outcome as in neurons: change of plasticity for example? Thus, is nuclear Ca^{2+} signalling in astrocytes causing a plasticity change of astrocytes such as growth of endfeet? To investigate this matter

in more detail, gene expression levels specifically from astrocytes from the spinal dorsal horn under fibre stimulation have to be analysed.

Considering the purpose of astrocytes, the support of neurons and its metabolism on glycolysis to provide lactate for neuronal consumption (Magistretti 2006; Morita et al. 2019) it is possible that this mechanism is regulated by nuclear Ca^{2+} signalling. The activity from the fibres would evoke neuronal activity in the spinal dorsal horn, which would require an increased amount of energy. So in parallel, this activity would induce astrocytic nuclear Ca^{2+} signalling in order to start a process of increased metabolism for plasticity changes of astrocytes as well as of neurons so that further energy support would be facilitated. Taking into account that synaptic activity, which is definitely caused evoked through DR stimulation, also requires glucose utilisation as energy provider (neurometabolic coupling) (Magistretti 2006) and the fact that astrocytes play a major role in the providence of this energy source through glycolysis, it makes sense that astrocytes respond with Ca^{2+} signalling to also neuronal activity. To explain this further: the synaptic activity from neurons leads to glutamate and ATP release from neurons and astrocytes would react with Ca^{2+} signalling which would then induce mechanism that would lead to increased glycolysis to provide neurons as an answer to their increased activity. Furthermore, the nuclear Ca^{2+} signalling could also lead to gene induction to change plasticity structures in order to adapt to the new environment of neuronal circuits to ensure the frequent “assistance” to neurons in the spinal dorsal horn.

4.2.2 Ca^{2+} signals in astrocytes under neuropathic pain conditions

As we tested in this study the Ca^{2+} signalling at the time points where the defined chronic pain status, 24 h for chronic inflammatory pain and 7 d for neuropathic pain, already reached its peak of an established state of pain, it would further be of interest to test the Ca^{2+} signal changes in the development phase of chronic pain. As we see no difference in the Ca^{2+} signalling under chronic inflammatory pain in astrocytes, it might well be possible that the changes are required in the development and not in the maintenance of chronic inflammatory pain. The required plasticity changes might already been completed and not in need of increased Ca^{2+} signalling in astrocytes.

Also the changes of neuropathic pain in astrocytes in earlier phases, for example 24 h or 48 h after SNI surgery, when the first mechanical hypersensitivity is measured in mice, would be of great interest. Would it show the same signalling behaviour as at later time points such as detected at seven days or would the development signalling differ from the established state?

The data represented in this thesis indicate an important role of nuclear Ca^{2+} signalling in astrocytes in the context of neuropathic pain. The data show that there is a decrease of nuclear Ca^{2+} signalling especially for the stimulation of Aβ- and Aδ-fibres seven days after SNI surgery. That might indicate that astrocytes play a minor role in later phases of neuropathic pain in the context of gene transcription and plasticity changes and thus possible metabolism changes. These data have to be enforced by further experiments that would concentrate on the analysis of Ca^{2+} signals evoked by DR stimulation at different time points before and after 7 days after SNI surgery. As SNI means that nerves are cut and thus fewer signals reach the dorsal horn, it might explain the reduction of astrocytic Ca^{2+} signalling. Still, other time points have to be investigated as at some point excitatory neurons develop a hypersensitivity under neuropathic pain and the role of astrocytes in this context would be of high interest. In addition, the gene expression has to be analysed of astrocytes that were stimulated under neuropathic pain conditions. These data would give new interesting insights into the active role of astrocytes during neuropathic pain in the circuit of spinal dorsal horn cells driven and regulated by Ca^{2+} signalling.

4.2.3 Ca^{2+} signalling in astrocytes under chronic inflammatory pain

Under chronic inflammatory pain conditions there were no differences detected in the Ca^{2+} signalling behaviour between the CFA group and the PBS group of astrocytes. But this doesn't mean, that there is no involvement of astrocytes in the development of chronic inflammatory pain. As mentioned above, other groups showed slight increase of morphological changes in form of astrogliosis under inflammatory pain conditions. The presented data just suggests that there is no role of Ca^{2+} signalling in the maintenance of chronic inflammatory pain in astrocytes when measured at a time point of 24 h after CFA injection, a time point when the chronic state of inflammatory pain is established. But at earlier time points, the development of this pain condition,

the Ca^{2+} signalling behaviour might still be different compared to its control group. Here more investigations have to be done. The Ca^{2+} signalling in astrocytes can be investigated at much earlier time points and the Ca^{2+} signalling dependent gene expression levels have to be identified at different time points after CFA injection and compared to PBS injected conditions. This would give even more insight into the possible role of Ca^{2+} signalling in astrocytes under chronic inflammatory pain conditions.

Other approaches could concentrate on the sources of Ca^{2+} signalling induction. This could be investigated through blocking of different channels that are already known to be involved in astrocytic Ca^{2+} signalling, such as IP3 receptors to provide Ca^{2+} from the ER. Others might be ATP receptors, TRP channels and glutamate receptors. This could provide information about the driving force of DR evoked Ca^{2+} signalling in spinal dorsal horn astrocytes. This investigation could then also be extended to approach the occurrence of multiphasic Ca^{2+} responses. As we saw in our experiments, there were multiphasic responses after the initially evoked Ca^{2+} response in Ca^{2+} indicator expressing astrocytes. But we do not know the source of those multiphasic responses, nor do we know why they occur only occasionally. We were only able to describe them in a stimulation intensity dependent manner. We observed, that the multiphasic responses often occurred at a stimulation intensity of 0.5 – 1 mA in all stimulated fibre classes. In the end, this topic has to be explored in more detail. How can astrocytes react with more than one response onto fibre stimulation? Probably because they receive signals from other neurons from the dorsal horn as well. Ca^{2+} imaging with Ca^{2+} indicators, expressed in different cell types, could possibly give some insight into signal behaviour, concerning proximity of different neurons and astrocytes as well as their time dynamics. This could lead to conclusions about the influence of neuronal activity in excitatory and inhibitory neurons onto the Ca^{2+} signalling in astrocytes.

4.2.4 Ca^{2+} signalling in Aldh1l1 mice

During our work, we found that the used GFAP promoter for indicator expression in astrocytes is not as specific as we thought. Our data showed that the indicator under the GFAP promoter is also expressed in cells that were positive for NeuN labelling, suggesting that our recorded Ca^{2+} signals from previous experiments might have been

contaminated with neuronal Ca^{2+} signals. Even when the neurons that expressed the indicator had a weak GFP signal compared to astrocytes, which had much stronger labelling of the GFP expressing indicators, the possibility of neuronal Ca^{2+} signal contamination had to be taken serious. Our data from the Ca^{2+} imaging showed that the Ca^{2+} indicators in Aldh1l1 mice expressed in astrocytes only and not in neurons. The imaging further showed that the evoked signals resembled the signals from the WT mice where we used the expression of the indicators under the GFAP promoter. The data from the Aldh1l1 mouse-line support the detected dynamics of Ca^{2+} signals in astrocytes evoked by DR stimulation in the experiments from WT mice.

In addition we showed that there is a possibility for more immediate Ca^{2+} signals than so far believed (Winship, Plaa, and Murphy 2007; Cali et al. 2008). More and more studies present the fast dynamics of Ca^{2+} signals in astrocytes endfeet and processes. This matter has to be investigated in greater detail by Ca^{2+} imaging using Ca^{2+} indicators in astrocytes tagged to the membrane in order to analyse the Ca^{2+} signals in the processes evoked by DR stimulation. For this study it is important to record with a high resolution set-up and recording with high frequencies, as the signals might be low and not reaching the astrocytic soma. Moreover, the resolution has to be as high as possible to exclude contamination of signals from astrocytes from deeper layers of the acute slice.

4.3 Ca^{2+} signalling in parvalbumin-positive neurons under chronic inflammatory pain

Excitatory neurons of the spinal cord dorsal horn exhibit enhanced Ca^{2+} signals in chronic inflammatory pain conditions (Simonetti et al. 2013). In addition, inhibitory neurons are impaired in their function and plasticity under chronic pain conditions (Basbaum et al. 2009). Only a few studies concentrated on the role of inhibitory neurons in the spinal dorsal horn under chronic inflammatory pain, suggesting that also under inflammatory pain there might be a disinhibition of inhibitory neurons (Lu et al. 2011). The evidence situation here is very thin, not many studies can be found on that topic. These facts led to the investigation of PV-positive cells in the spinal dorsal horn.

Our data showed that Ca^{2+} indicators expressed in pv-positivie cells, responded to DR stimulation to all the tested fibre types. Not only did they show evoked signals but they also showed spontaneous activity in different patterns and dynamics. We were not able to analyse the data of spontaneous activity as they were highly variable in their occurrence and dynamics. In addition, it might well be, that these different spontaneous activities represented artefact behaviour from the procedure of the acute slicing. Due to many different factors that might influence this spontaneous activity, for example stress, like the cutting procedure, the transportation from storage chambers to the set-up and quality of the tissue, it was not possible to analyse for a difference between CFA treated and PBS treated groups as the spontaneous activity also changed during stimulation.

Under chronic inflammatory pain conditions the Ca^{2+} signals did not show any differences in PV-positive cells. Concerning the evoked signals, it can be, just as it was possible for the astrocytes Ca^{2+} signals, that the time point of the imaging is important to detect possible changes of Ca^{2+} signalling. Of course it can also not be excluded that under chronic inflammatory pain there are simply no changes in the Ca^{2+} signalling in PV-positive cells. In the end, there were no changes in the Ca^{2+} signalling 24 h after chronic inflammatory pain induction in our experiments concerning PV-positive neurons.

Despite that, it is important to investigate in further detail the dynamics and characteristics of Ca^{2+} signals in PV-positive cells under chronic inflammatory pain at different time points after CFA injections as well as their gene expression levels, evoked by DR stimulation and driven by Ca^{2+} signalling. As already mentioned there are only a few studies on this topic and the role of inhibitory neurons under chronic inflammatory pain in the spinal dorsal horn needs to be more characterised in order to understand the mechanism of chronic inflammatory pain development and maintenance so that treatments can be developed.

4.4 The role of Npas4 in chronic pain conditions

Npas4 is an IEG which is induced by neuronal activity, to be more specific, by Ca^{2+} signalling. It is responsible for a homeostatic balance in favour of inhibition in the CNS. As we saw Ca^{2+} signals in PV-neurons induced through DR stimulation, we

investigated *Npas4* in more detail, considering the special role of inhibitory neurons in the context of chronic pain. The analysis of *Npas4* expression in the spinal dorsal horn of mice treated with CFA, we saw an immediate increase in the *Npas4* expression at 1 h after CFA injection. This level decreased back to baseline after 3 h. This indicates an immediate but not persistent requirement of *Npas4* in the spinal dorsal horn under chronic inflammatory pain.

In contrast, the analysis of *Npas4* expression from spinal dorsal horn tissue under neuropathic pain induced through SNI surgery, showed a decrease compared to the contralateral side (not treated leg) at day 3 after surgery. This finding of decreased *Npas4* levels makes sense as the fibres are cut from the periphery, so there would be no input to the CNS, thus no neuronal activity and no induction of *Npas4*. This showed that there is not such an immediate induction of *Npas4* after SNI surgery compared to CFA injection. At day 10 after surgery, the *Npas4* level is increased back to baseline level in the ipsilateral side. The question now would be, if the reduction of *Npas4* in the early phase of neuropathic pain development plays an important role in the development of the persistent pain. Could a strong induction of *Npas4* rescue the neuropathic pain development?

It is clear, that inhibitory neurons play a crucial role in the neuropathic pain conditions. It has already been shown that inhibitory neurons are impaired in their function and their morphology under neuropathic pain models. As NPAS4 represents an important protein which controls through neuronal activity the plasticity changes that increase inhibitory control in the CNS, it is possible that chronic pain conditions involve impaired NPAS4 levels. This idea is supported by the fact that disinhibition is an important part of chronic pain formation (Petitjean et al. 2015) and combined with the fact that *Npas4* regulates the homeostatic balance in favour of inhibition. To investigate the exact role of NPAS4 in neuropathic pain conditions, NPAS4 levels were increased via an overexpression construct which was injected into the spinal cord dorsal horn of wild type mice. This construct induced increased protein levels of *Npas4 in vitro* and *in vivo*. Two weeks after the injection of this construct or its control construct, the mice got SNI surgery to induce neuropathic pain. The results showed that already 5 days after surgery the mice that were injected with the Npas4 overexpression construct showed a significant decrease of mechanical hypersensitivity compared to the group

that was injected with the control construct (Fig. 23 C). These findings show that *Npas4* indeed plays an important role in the development of neuropathic pain. My hypothesis is, that increased levels of *Npas4* in the spinal dorsal horn prevent the development of disinhibition in the spinal cord circuits which would normally lead to chronic pain formation. Through the permanent high expression of *Npas4* the neuronal inhibitory system can “counteract” against the increased excitability caused by the SNI surgery.

Further experiments would concentrate on the role of *Npas4* in chronic inflammatory pain. Here it would be possible to inject the dn-NPAS4 construct, which was already tested *in vitro*, into the spinal cord dorsal horn of wild type mice and induce CFA driven chronic inflammatory pain. As the relative gene expression in the first experiments (Fig. 16 A) showed that under CFA conditions *Npas4* is increased, 1 h after injection. So here increased NPAS4 would maybe induce the chronic pain development. The suggested experiment would give some insight about the role of NPAS4 under chronic inflammatory pain conditions. The hypothesis would be that due to impaired function of NPAS4 through the dn-NPAS4 construct, there would be no induction of plasticity changes that are NPAS4 dependent.

As the Ca^{2+} signalling of inhibitory neurons in the spinal dorsal horn showed no changes under chronic inflammatory pain, it is possible, that inhibitory neurons only are induced at the beginning of the CFA injection, at early time points, if at all. The relative gene expression levels of Npas4 after CFA injection doesn’t allow us unfortunately a differentiation between Npas4 levels in excitatory or inhibitory neurons. We were only able to make statements about the overall expression, independent from the cell type. Due to fibre activation, also inhibitory neurons are activated in the spinal dorsal horn, but there is no detectable difference between the CFA and the control group. But they seem to play no important role in the maintenance of chronic inflammatory pain.

It seems that the Ca^{2+} regulation and thus the Npas4 expression is important especially for the Aβ-fibres, the touch sensory fibres. This is shown through the decreased Npas4 expression under neuropathic pain but also that the OENpas4 only rescued the mechanical but not the thermal hypersensitivity. This is also emphasised by the fact that Aβ-fibres mainly build synapses in lamina III where also many interneurons are placed to regulate the cell circuit in the dorsal horn.

Further approaches would be the testing of dn-Npas4 in acute inflammatory pain models, like formalin-induced acute inflammatory pain. The results would give information about possible differences of the role of Npas4 in acute and chronic pain conditions. In addition both pain models, the acute and the chronic inflammatory pain model, could also be tested with the OE-Npas4 construct. Permanent increased Npas4 level could possibly suppress the chronic pain development by strong inhibitory control of the CNS.

4.5 Final conclusion and outlook

Taken together, the results may lead to the suggestion that not C-fibres are responsible for chronic pain formation or maintenance, as they seem to not change their Ca^{2+} signalling and activity behaviour. It is very likely that the chronic and thus maladaptive pain formation occurs due to changes from the Aβ-fibres. All our data show that Aβ-fibres where in one way or another involved in pain formation or maintenance in different cell types. They changed their Ca^{2+} signalling behaviour during DR stimulation under chronic pain conditions. Under neuropathic pain conditions, they showed decreased Ca^{2+} signalling in astrocytes, in the cytosol as well as in the nucleus.

In neurons, it was shown in our data that Ca^{2+} induced *Npas4* expression was reduced under neuropathic pain conditions. This might indicate an impaired Ca^{2+} signalling in spinal dorsal horn neurons under neuropathic pain. The involvement of Aβ-fibres was shown in this context in the mechanical hypersensitivity under neuropathic pain, which means, that normally non-noxious touch stimuli were sensed by the mice as painful. NPAS4 overexpression rescued that phenotype as the pain threshold with OE-NPAS4 injected mice was similar to the pre-SNI baseline.

When we hurt ourselves, we tend to rub the injured place or mothers blow on a wound of children, to relieve their pain. This touch-sensory stimulation normally suppresses the pain sensation. Here might be the key to chronic pain formation. Taken the two pieces together, the “silencing” effect of Aβ (“touch”) fibres under chronic pain conditions to the spinal dorsal horn neurons seems to be disturbed as well as the regulation of inhibition through NPAS4.

Ideas for therapeutic treatment could be to support of Aβ-fibres in their normal function as touch fibres and to ensure the function of NPAS4 in the dorsal horn circuits.

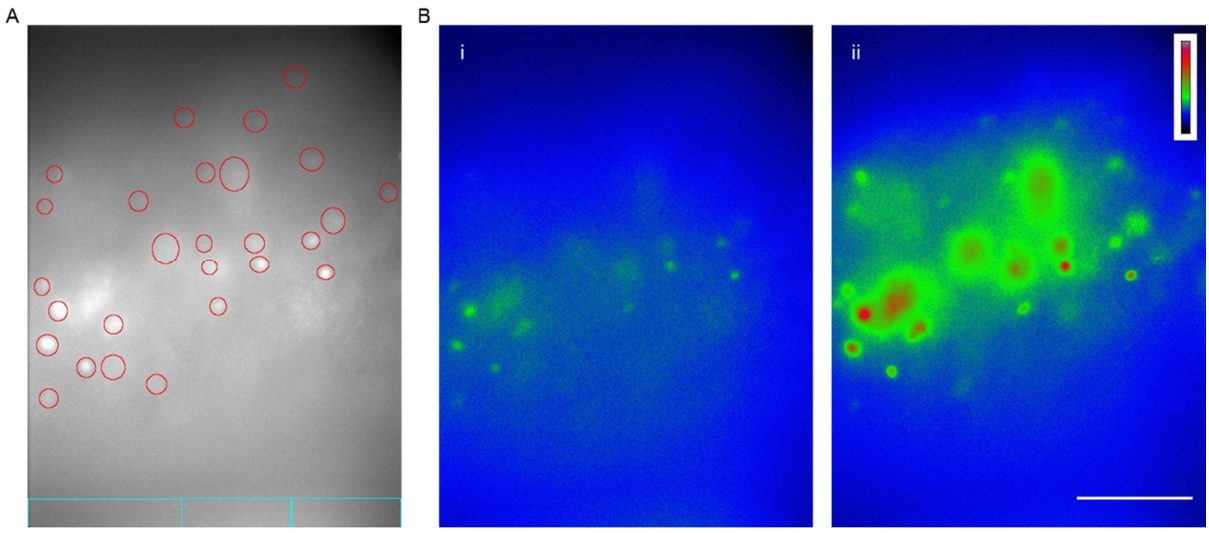

Appendix Figure 1: Visualisation of Ca^{2+} imaging. (A) Example of live picture of acute slice while expressing GFP signal from Ca^{2+} indicators (here GFAP:GCaMP5) at basal level. Round ROIs indicate cells that showed signals during stimulation procedure. Rectangular ROIs indicate background. **(B)** Representative example picture of expressed indicator (GFAP:GCaMP3.NLS.myc) in spinal dorsal horn during imaging before (i) and at stimulation (ii). Blue indicates low and red high intensity. Orientation of pictures: dorsal side up and ventral side down. Scale bar = 50 µm

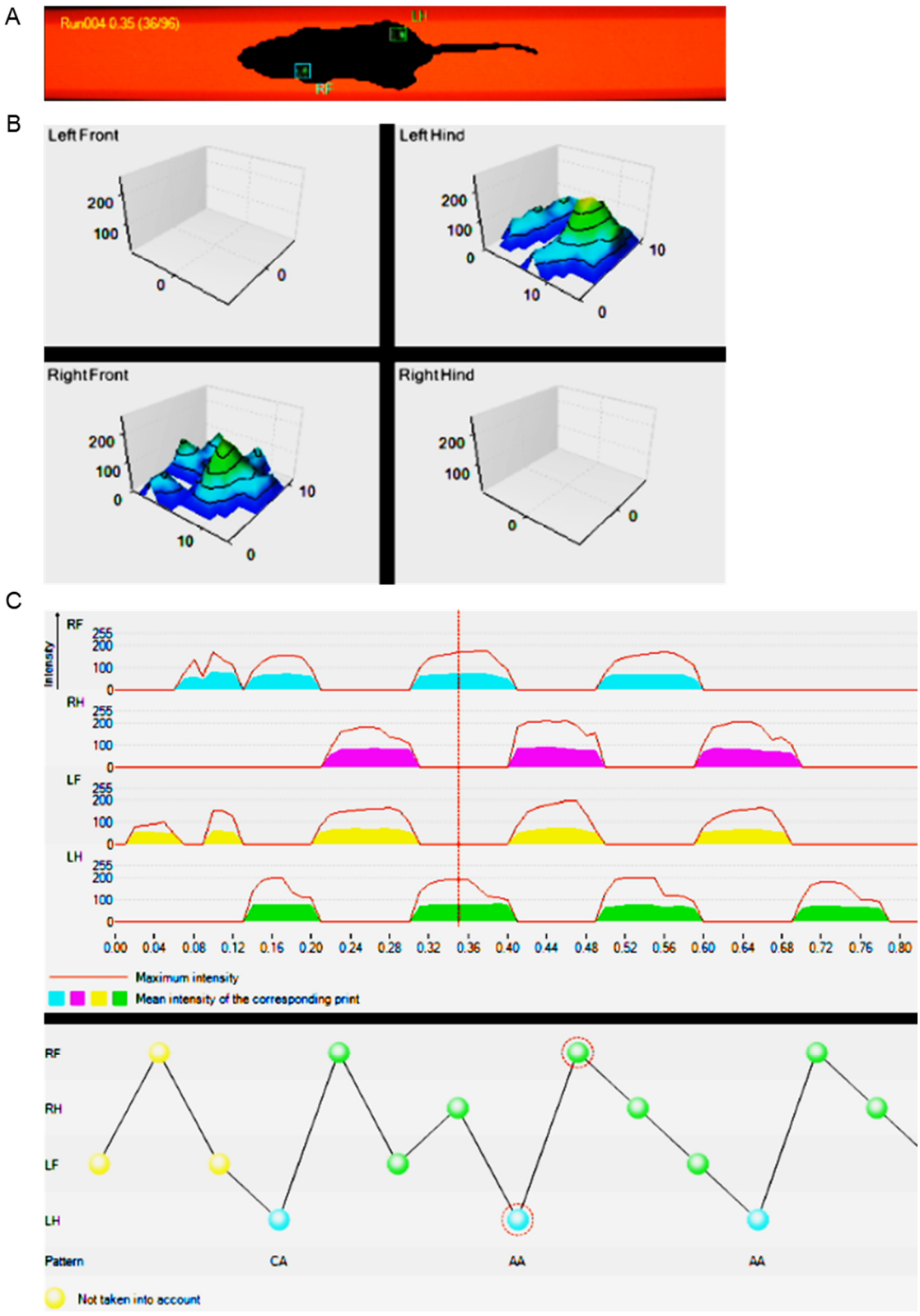

Appendix Figure 2: Visualisation of catwalk. (A) Representative screenshot of a run way with mouse and the detected paws touching the surface. **(B)** Representative example graph showing the print surface of each paw touching the run way surface. **(C)** Representative graph showing the step intensity of each paw over time (s) of the mouse running along the run way. LF = left front paw, LH = left hind paw, RF = right front paw, RH = right hind paw.

5. References

Abdallah, C. G., and P. Geha. 2017. 'Chronic Pain and Chronic Stress: Two Sides of the Same Coin?', *Chronic Stress (Thousand Oaks)*, 1.

Agulhon, C., T. A. Fiacco, and K. D. McCarthy. 2010. 'Hippocampal short- and long-term plasticity are not modulated by astrocyte Ca2+ signaling', *Science*, 327: 1250-4.

Agulhon, C., J. Petravicz, A. B. McMullen, E. J. Sweger, S. K. Minton, S. R. Taves, K. B. Casper, T. A. Fiacco, and K. D. McCarthy. 2008. 'What is the role of astrocyte calcium in neurophysiology?', *Neuron*, 59: 932-46.

Anderson, C. M., and M. Nedergaard. 2003. 'Astrocyte-mediated control of cerebral microcirculation', *Trends Neurosci*, 26: 340-4; author reply 44-5.

Antal, M., T. F. Freund, and E. Polgar. 1990. 'Calcium-binding proteins, parvalbumin- and calbindin-D 28k-immunoreactive neurons in the rat spinal cord and dorsal root ganglia: a light and electron microscopic study', *J Comp Neurol*, 295: 467-84.

Araque, A., R. P. Sanzgiri, V. Parpura, and P. G. Haydon. 1999. 'Astrocyte-induced modulation of synaptic transmission', *Can J Physiol Pharmacol*, 77: 699-706.

Bading, H. 2013. 'Nuclear calcium signalling in the regulation of brain function', *Nat Rev Neurosci*, 14: 593-608.

Basbaum, A. I., D. M. Bautista, G. Scherrer, and D. Julius. 2009. 'Cellular and molecular mechanisms of pain', *Cell*, 139: 267-84.

Basbaum, A. I., and J. M. Braz. 2010. 'Transgenic Mouse Models for the Tracing of "Pain" Pathways.' in L. Kruger and A. R. Light (eds.), *Translational Pain Research: From Mouse to Man* (Boca Raton, FL).

———. 2016. 'Cell transplants to treat the "disease" of neuropathic pain and itch', *Pain*, 157 Suppl 1: S42-7.

Basbaum, A. I., and C. J. Woolf. 1999. 'Pain', *Curr Biol*, 9: R429-31.

Bengtson, C. P., H. E. Freitag, J. M. Weislogel, and H. Bading. 2010. 'Nuclear calcium sensors reveal that repetition of trains of synaptic stimuli boosts nuclear calcium signaling in CA1 pyramidal neurons', *Biophys J*, 99: 4066-77.

Berridge, M. J. 1998. 'Neuronal calcium signaling', *Neuron*, 21: 13-26.

Bloodgood, B. L., N. Sharma, H. A. Browne, A. Z. Trepman, and M. E. Greenberg. 2013. 'The activity-dependent transcription factor NPAS4 regulates domain-specific inhibition', *Nature*, 503: 121-5.

Boersma, K., M. Sodermark, H. Hesser, I. K. Flink, B. Gerdle, and S. J. Linton. 2019. 'Efficacy of a transdiagnostic emotion-focused exposure treatment for chronic pain patients with comorbid anxiety and depression: a randomized controlled trial', *Pain*, 160: 1708-18.

Brenner, M., W. C. Kisseberth, Y. Su, F. Besnard, and A. Messing. 1994. 'GFAP promoter directs astrocyte-specific expression in transgenic mice', *J Neurosci*, 14: 1030-7.

Cali, C., J. Marchaland, R. Regazzi, and P. Bezzi. 2008. 'SDF 1-alpha (CXCL12) triggers glutamate exocytosis from astrocytes on a millisecond time scale: imaging analysis at the single-vesicle level with TIRF microscopy', *J Neuroimmunol*, 198: 82-91.

Chessell, I. P., J. P. Hatcher, C. Bountra, A. D. Michel, J. P. Hughes, P. Green, J. Egerton, M. Murfin, J. Richardson, W. L. Peck, C. B. Grahames, M. A. Casula, Y. Yiangou, R. Birch, P. Anand, and G. N. Buell. 2005. 'Disruption of the P2X7 purinoceptor gene abolishes chronic inflammatory and neuropathic pain', *Pain*, 114: 386-96.

Christensen, R. K., R. Delgado-Lezama, R. E. Russo, B. L. Lind, E. L. Alcocer, M. F. Rath, G. Fabbiani, N. Schmitt, M. Lauritzen, A. V. Petersen, E. M. Carlsen, and J. F. Perrier. 2018. 'Spinal dorsal horn astrocytes release GABA in response to synaptic activation', *J Physiol*, 596: 4983-94.

Clapham, D. E. 2007. 'Calcium signaling', *Cell*, 131: 1047-58.
Daniele, C. A., and A. B. MacDermott. 2009. 'Low-threshold primary afferent drive onto GABAergic interneurons in the superficial dorsal horn of the mouse', *J Neurosci*, 29: 686-95.
De Vincenti, A. P., A. S. Rios, G. Paratcha, and F. Ledda. 2019. 'Mechanisms That Modulate and Diversify BDNF Functions: Implications for Hippocampal Synaptic Plasticity', *Front Cell Neurosci*, 13: 135.
Decosterd, I., and C. J. Woolf. 2000. 'Spared nerve injury: an animal model of persistent peripheral neuropathic pain', *Pain*, 87: 149-58.
Drdla, R., and J. Sandkuhler. 2008. 'Long-term potentiation at C-fibre synapses by low-level presynaptic activity in vivo', *Mol Pain*, 4: 18.
Duan, B., L. Cheng, S. Bourane, O. Britz, C. Padilla, L. Garcia-Campmany, M. Krashes, W. Knowlton, T. Velasquez, X. Ren, S. Ross, B. B. Lowell, Y. Wang, M. Goulding, and Q. Ma. 2014. 'Identification of spinal circuits transmitting and gating mechanical pain', *Cell*, 159: 1417-32.
Echeverry, S., M. J. Rodriguez, and Y. P. Torres. 2016. 'Transient Receptor Potential Channels in Microglia: Roles in Physiology and Disease', *Neurotox Res*, 30: 467-78.
Eder, A., and H. Bading. 2007. 'Calcium signals can freely cross the nuclear envelope in hippocampal neurons: somatic calcium increases generate nuclear calcium transients', *BMC Neurosci*, 8: 57.
Eng, L. F., R. S. Ghirnikar, and Y. L. Lee. 2000. 'Glial fibrillary acidic protein: GFAP-thirty-one years (1969-2000)', *Neurochem Res*, 25: 1439-51.
Fiacco, T. A., C. Agulhon, S. R. Taves, J. Petravicz, K. B. Casper, X. Dong, J. Chen, and K. D. McCarthy. 2007. 'Selective stimulation of astrocyte calcium in situ does not affect neuronal excitatory synaptic activity', *Neuron*, 54: 611-26.
Gangadharan, V., and R. Kuner. 2013. 'Pain hypersensitivity mechanisms at a glance', *Dis Model Mech*, 6: 889-95.
———. 2015. 'Unravelling Spinal Circuits of Pain and Mechanical Allodynia', *Neuron*, 87: 673-5.
Gangadharan, V., R. Wang, B. Ulzhofer, C. Luo, R. Bardoni, K. K. Bali, N. Agarwal, I. Tegeder, U. Hildebrandt, G. G. Nagy, A. J. Todd, A. Ghirri, A. Haussler, R. Sprengel, P. H. Seeburg, A. B. MacDermott, G. R. Lewin, and R. Kuner. 2011. 'Peripheral calcium-permeable AMPA receptors regulate chronic inflammatory pain in mice', *J Clin Invest*, 121: 1608-23.
Gaskin, D. J., and P. Richard. 2012. 'The economic costs of pain in the United States', *J Pain*, 13: 715-24.
Gassner, M., J. Leitner, D. Gruber-Schoffnegger, L. Forsthuber, and J. Sandkuhler. 2013. 'Properties of spinal lamina III GABAergic neurons in naive and in neuropathic mice', *Eur J Pain*, 17: 1168-79.
Gosselin, R. D., M. R. Suter, R. R. Ji, and I. Decosterd. 2010. 'Glial cells and chronic pain', *Neuroscientist*, 16: 519-31.
Hagenston, A. M., and H. Bading. 2011. 'Calcium signaling in synapse-to-nucleus communication', *Cold Spring Harb Perspect Biol*, 3: a004564.
Hansson, E. 2010. 'Long-term pain, neuroinflammation and glial activation', *Scand J Pain*, 1: 67-72.
Hartzell, A. L., K. M. Martyniuk, G. S. Brigidi, D. A. Heinz, N. A. Djaja, A. Payne, and B. L. Bloodgood. 2018. 'NPAS4 recruits CCK basket cell synapses and enhances cannabinoid-sensitive inhibition in the mouse hippocampus', *Elife*, 7.
Haydon, P. G., and G. Carmignoto. 2006. 'Astrocyte control of synaptic transmission and neurovascular coupling', *Physiol Rev*, 86: 1009-31.
Hyman, S. E., R. C. Malenka, and E. J. Nestler. 2006. 'Neural mechanisms of addiction: the role of reward-related learning and memory', *Annu Rev Neurosci*, 29: 565-98.
Ikeda, H., T. Kiritoshi, and K. Murase. 2012. 'Contribution of microglia and astrocytes to the central sensitization, inflammatory and neuropathic pain in the juvenile rat', *Mol Pain*, 8: 43.
Ji, R. R., T. Kohno, K. A. Moore, and C. J. Woolf. 2003. 'Central sensitization and LTP: do pain and memory share similar mechanisms?', *Trends Neurosci*, 26: 696-705.

Ji, R. R., and G. Strichartz. 2004. 'Cell signaling and the genesis of neuropathic pain', *Sci STKE*, 2004: reE14.

Ji, Ru-Rong, Temugin Berta, and Maiken Nedergaard. 2013. 'Glia and pain: Is chronic pain a gliopathy?', *Pain*.

Jonas, R., B. Namer, L. Stockinger, K. Chisholm, M. Schnakenberg, G. Landmann, M. Kucharczyk, C. Konrad, R. Schmidt, R. Carr, S. McMahon, M. Schmelz, and R. Rukwied. 2018. 'Tuning in C-nociceptors to reveal mechanisms in chronic neuropathic pain', *Ann Neurol*, 83: 945-57.

Kang, H., L. D. Sun, C. M. Atkins, T. R. Soderling, M. A. Wilson, and S. Tonegawa. 2001. 'An important role of neural activity-dependent CaMKIV signaling in the consolidation of long-term memory', *Cell*, 106: 771-83.

Kim, S. K., H. Hayashi, T. Ishikawa, K. Shibata, E. Shigetomi, Y. Shinozaki, H. Inada, S. E. Roh, S. J. Kim, G. Lee, H. Bae, A. J. Moorhouse, K. Mikoshiba, Y. Fukazawa, S. Koizumi, and J. Nabekura. 2016. 'Cortical astrocytes rewire somatosensory cortical circuits for peripheral neuropathic pain', *J Clin Invest*, 126: 1983-97.

Lee, T. W., V. W. Tsang, and N. P. Birch. 2008. 'Synaptic plasticity-associated proteases and protease inhibitors in the brain linked to the processing of extracellular matrix and cell adhesion molecules', *Neuron Glia Biol*, 4: 223-34.

Limback-Stokin, K., E. Korzus, R. Nagaoka-Yasuda, and M. Mayford. 2004. 'Nuclear calcium/calmodulin regulates memory consolidation', *J Neurosci*, 24: 10858-67.

Liu, D., M. Zhang, X. Rong, J. Li, and X. Wang. 2017. 'Potassium 2-(1-hydroxypentyl)-benzoate attenuates neuronal apoptosis in neuron-astrocyte co-culture system through neurotrophy and neuroinflammation pathway', *Acta Pharm Sin B*, 7: 554-63.

Liu, X. J., J. R. Gingrich, M. Vargas-Caballero, Y. N. Dong, A. Sengar, S. Beggs, S. H. Wang, H. K. Ding, P. W. Frankland, and M. W. Salter. 2008. 'Treatment of inflammatory and neuropathic pain by uncoupling Src from the NMDA receptor complex', *Nat Med*, 14: 1325-32.

Liu, Y. Q., J. N. Dong, Q. X. Meng, P. Sun, and J. Zhang. 2017. 'Ultrasound for postoperative surveillance after mastectomy in patients with breast cancer: A retrospective study', *Medicine (Baltimore)*, 96: e9244.

Lu, J., T. Katano, D. Uta, H. Furue, and S. Ito. 2011. 'Rapid S-nitrosylation of actin by NO-generating donors and in inflammatory pain model mice', *Mol Pain*, 7: 101.

Magistretti, P. J. 2006. 'Neuron-glia metabolic coupling and plasticity', *J Exp Biol*, 209: 2304-11.

Marchi, S., S. Patergnani, S. Missiroli, G. Morciano, A. Rimessi, M. R. Wieckowski, C. Giorgi, and P. Pinton. 2018. 'Mitochondrial and endoplasmic reticulum calcium homeostasis and cell death', *Cell Calcium*, 69: 62-72.

Mauceri, D., H. E. Freitag, A. M. Oliveira, C. P. Bengtson, and H. Bading. 2011. 'Nuclear calcium-VEGFD signaling controls maintenance of dendrite arborization necessary for memory formation', *Neuron*, 71: 117-30.

Maya-Vetencourt, J. F. 2013. 'Activity-dependent NPAS4 expression and the regulation of gene programs underlying plasticity in the central nervous system', *Neural Plast*, 2013: 683909.

Melzack, R., and P. D. Wall. 1965. 'Pain mechanisms: a new theory', *Science*, 150: 971-9.

Merskey, H. 1994. 'Logic, truth and language in concepts of pain', *Qual Life Res*, 3 Suppl 1: S69-76.

Morita, M., H. Ikeshima-Kataoka, M. Kreft, N. Vardjan, R. Zorec, and M. Noda. 2019. 'Metabolic Plasticity of Astrocytes and Aging of the Brain', *Int J Mol Sci*, 20.

Nestler, E. J., M. B. Kelz, and J. Chen. 1999. 'DeltaFosB: a molecular mediator of long-term neural and behavioral plasticity', *Brain Res*, 835: 10-7.

Panatier, A., J. Vallee, M. Haber, K. K. Murai, J. C. Lacaille, and R. Robitaille. 2011. 'Astrocytes are endogenous regulators of basal transmission at central synapses', *Cell*, 146: 785-98.

Papadia, S., P. Stevenson, N. R. Hardingham, H. Bading, and G. E. Hardingham. 2005. 'Nuclear Ca2+ and the cAMP response element-binding protein family mediate a late phase of activity-dependent neuroprotection', *J Neurosci*, 25: 4279-87.

Peirs, C., S. P. Williams, X. Zhao, C. E. Walsh, J. Y. Gedeon, N. E. Cagle, A. C. Goldring, H. Hioki, Z. Liu, P. S. Marell, and R. P. Seal. 2015. 'Dorsal Horn Circuits for Persistent Mechanical Pain', *Neuron*, 87: 797-812.

Petitjean, H., S. A. Pawlowski, S. L. Fraine, B. Sharif, D. Hamad, T. Fatima, J. Berg, C. M. Brown, L. Y. Jan, A. Ribeiro-da-Silva, J. M. Braz, A. I. Basbaum, and R. Sharif-Naeini. 2015. 'Dorsal Horn Parvalbumin Neurons Are Gate-Keepers of Touch-Evoked Pain after Nerve Injury', *Cell Rep*, 13: 1246-57.

Ramamoorthi, K., R. Fropf, G. M. Belfort, H. L. Fitzmaurice, R. M. McKinney, R. L. Neve, T. Otto, and Y. Lin. 2011. 'Npas4 regulates a transcriptional program in CA3 required for contextual memory formation', *Science*, 334: 1669-75.

Ren, K., and M. A. Ruda. 1994. 'A comparative study of the calcium-binding proteins calbindin-D28K, calretinin, calmodulin and parvalbumin in the rat spinal cord', *Brain Res Brain Res Rev*, 19: 163-79.

Sandkuhler, J. 2009. 'Models and mechanisms of hyperalgesia and allodynia', *Physiol Rev*, 89: 707-58.

Sandkuhler, J., J. G. Chen, G. Cheng, and M. Randic. 1997. 'Low-frequency stimulation of afferent Adelta-fibers induces long-term depression at primary afferent synapses with substantia gelatinosa neurons in the rat', *J Neurosci*, 17: 6483-91.

Semyanov, A. 2019. 'Spatiotemporal pattern of calcium activity in astrocytic network', *Cell Calcium*, 78: 15-25.

Shepard, R., K. Heslin, P. Hagerdorn, and L. Coutellier. 2019. 'Downregulation of Npas4 in parvalbumin interneurons and cognitive deficits after neonatal NMDA receptor blockade: relevance for schizophrenia', *Transl Psychiatry*, 9: 99.

Simonetti, M., A. M. Hagenston, D. Vardeh, H. E. Freitag, D. Mauceri, J. Lu, V. P. Satagopam, R. Schneider, M. Costigan, H. Bading, and R. Kuner. 2013. 'Nuclear calcium signaling in spinal neurons drives a genomic program required for persistent inflammatory pain', *Neuron*, 77: 43-57.

Sofroniew, M. V. 2009. 'Molecular dissection of reactive astrogliosis and glial scar formation', *Trends Neurosci*, 32: 638-47.

Spiegel, I., A. R. Mardinly, H. W. Gabel, J. E. Bazinet, C. H. Couch, C. P. Tzeng, D. A. Harmin, and M. E. Greenberg. 2014. 'Npas4 regulates excitatory-inhibitory balance within neural circuits through cell-type-specific gene programs', *Cell*, 157: 1216-29.

Srinivasan, R., B. S. Huang, S. Venugopal, A. D. Johnston, H. Chai, H. Zeng, P. Golshani, and B. S. Khakh. 2015. 'Ca(2+) signaling in astrocytes from Ip3r2(-/-) mice in brain slices and during startle responses in vivo', *Nat Neurosci*, 18: 708-17.

Sun, X., and Y. Lin. 2016. 'Npas4: Linking Neuronal Activity to Memory', *Trends Neurosci*, 39: 264-75.

Szokol, K., K. Heuser, W. Tang, V. Jensen, R. Enger, P. Bedner, C. Steinhauser, E. Tauboll, O. P. Ottersen, and E. A. Nagelhus. 2015. 'Augmentation of Ca(2+) signaling in astrocytic endfeet in the latent phase of temporal lobe epilepsy', *Front Cell Neurosci*, 9: 49.

Takazawa, T., and A. B. MacDermott. 2010a. 'Glycinergic and GABAergic tonic inhibition fine tune inhibitory control in regionally distinct subpopulations of dorsal horn neurons', *J Physiol*, 588: 2571-87.

———. 2010b. 'Synaptic pathways and inhibitory gates in the spinal cord dorsal horn', *Ann N Y Acad Sci*, 1198: 153-8.

Tang, W., K. Szokol, V. Jensen, R. Enger, C. A. Trivedi, O. Hvalby, P. J. Helm, L. L. Looger, R. Sprengel, and E. A. Nagelhus. 2015. 'Stimulation-evoked Ca2+ signals in astrocytic processes at hippocampal CA3-CA1 synapses of adult mice are modulated by glutamate and ATP', *J Neurosci*, 35: 3016-21.

Tawfik, V. L., N. Nutile-McMenemy, M. L. LaCroix-Fralish, and J. A. DeLeo. 2007. 'Reprint of "efficacy of propentofylline, a glial modulating agent, on existing mechanical allodynia following peripheral nerve injury" [Brain Behav. Immun. 21 (2007) 238-246]', *Brain Behav Immun*, 21: 677-85.

Todd, A. J. 2010. 'Neuronal circuitry for pain processing in the dorsal horn', *Nat Rev Neurosci*, 11: 823-36.

———. 2017. 'Identifying functional populations among the interneurons in laminae I-III of the spinal dorsal horn', *Mol Pain*, 13: 1744806917693003.

Treede, R. D., W. Rief, A. Barke, Q. Aziz, M. I. Bennett, R. Benoliel, M. Cohen, S. Evers, N. B. Finnerup, M. B. First, M. A. Giamberardino, S. Kaasa, E. Kosek, P. Lavand'homme, M. Nicholas, S. Perrot, J. Scholz, S. Schug, B. H. Smith, P. Svensson, J. W. Vlaeyen, and S. J. Wang. 2015. 'A classification of chronic pain for ICD-11', *Pain*, 156: 1003-7.

Tsuda, M. 2016. 'Microglia in the spinal cord and neuropathic pain', *J Diabetes Investig*, 7: 17-26.

Ung, D. C., G. Iacono, H. Meziane, E. Blanchard, M. A. Papon, M. Selten, J. R. van Rhijn, R. Montjean, J. Rucci, S. Martin, A. Fleet, M. C. Birling, S. Marouillat, R. Roepman, M. Selloum, A. Lux, R. A. Thepault, P. Hamel, K. Mittal, J. B. Vincent, O. Dorseuil, H. G. Stunnenberg, P. Billuart, N. Nadif Kasri, Y. Herault, and F. Laumonnier. 2018. 'Ptchd1 deficiency induces excitatory synaptic and cognitive dysfunctions in mouse', *Mol Psychiatry*, 23: 1356-67.

Volterra, A., N. Liaudet, and I. Savtchouk. 2014. 'Astrocyte Ca(2)(+) signalling: an unexpected complexity', *Nat Rev Neurosci*, 15: 327-35.

Wang, X. M., G. F. Zhang, M. Jia, Z. M. Xie, J. J. Yang, J. C. Shen, and Z. Q. Zhou. 2019. 'Environmental enrichment improves pain sensitivity, depression-like phenotype, and memory deficit in mice with neuropathic pain: role of NPAS4', *Psychopharmacology (Berl)*, 236: 1999-2014.

Watanabe, S., M. Hong, N. Lasser-Ross, and W. N. Ross. 2006. 'Modulation of calcium wave propagation in the dendrites and to the soma of rat hippocampal pyramidal neurons', *J Physiol*, 575: 455-68.

Winship, I. R., N. Plaa, and T. H. Murphy. 2007. 'Rapid astrocyte calcium signals correlate with neuronal activity and onset of the hemodynamic response in vivo', *J Neurosci*, 27: 6268-72.

Woolf, C. J. 1983. 'Evidence for a central component of post-injury pain hypersensitivity', *Nature*, 306: 686-8.

Woolf, C. J., and M. W. Salter. 2000. 'Neuronal plasticity: increasing the gain in pain', *Science*, 288: 1765-9.

Wu, H., Y. Huang, X. Tian, Z. Zhang, Y. Zhang, Y. Mao, C. Wang, S. Yang, Y. Liu, W. Zhang, and Z. Ma. 2019. 'Preoperative anxiety-induced glucocorticoid signaling reduces GABAergic markers in spinal cord and promotes postoperative hyperalgesia by affecting neuronal PAS domain protein 4', *Mol Pain*, 15: 1744806919850383.

Yamamoto, T., P. A. Carr, K. G. Baimbridge, and J. I. Nagy. 1989. 'Parvalbumin- and calbindin D28k-immunoreactive neurons in the superficial layers of the spinal cord dorsal horn of rat', *Brain Res Bull*, 23: 493-508.

Zacharova, G., and J. Palecek. 2009. 'Parvalbumin and TRPV1 receptor expression in dorsal root ganglion neurons after acute peripheral inflammation', *Physiol Res*, 58: 305-9.

Zacharova, G., D. Sojka, and J. Palecek. 2009. 'Changes of parvalbumin expression in the spinal cord after peripheral inflammation', *Physiol Res*, 58: 435-42.

Zhang, S. J., M. Zou, L. Lu, D. Lau, D. A. Ditzel, C. Delucinge-Vivier, Y. Aso, P. Descombes, and H. Bading. 2009. 'Nuclear calcium signaling controls expression of a large gene pool: identification of a gene program for acquired neuroprotection induced by synaptic activity', *PLoS Genet*, 5: e1000604.

Zhang, Z. J., B. C. Jiang, and Y. J. Gao. 2017. 'Chemokines in neuron-glial cell interaction and pathogenesis of neuropathic pain', *Cell Mol Life Sci*, 74: 3275-91.

Zhao, L., and R. D. Brinton. 2003. 'Vasopressin-induced cytoplasmic and nuclear calcium signaling in embryonic cortical astrocytes: dynamics of calcium and calcium-dependent kinase translocation', *J Neurosci*, 23: 4228-39.